Unraveling the mechanism of multicopper oxidases : from ensemble to single molecule

Gupta, A.

Unraveling the Mechanism of Multicopper Oxidases: From Ensemble to Single Molecule

Ankur Gupta

Unraveling the Mechanism of Multicopper Oxidases: From Ensemble to Single Molecule

Proefschrift

ter verkrijging van
de graad van Doctor aan de Universiteit Leiden,
op gezag van Rector Magnificus prof. mr. C.J.J.M. Stolker,
volgens besluit van het College voor Promoties
te verdedigen op dinsdag 29 april 2014
klokke 10.00 uur

door

Ankur Gupta
geboren te Agra, India
in 1983

Promotiecommisie:

Promotoren:	Prof. dr. G. W. Canters (Universiteit Leiden)
	Prof. dr. T. J. Aartsma (Universiteit Leiden)
Overige Leden:	Prof. dr. E. R. Eliel (Universiteit Leiden)
	Prof. dr. E. J. J. Groenen (Universiteit Leiden)
	Prof. dr. O. Farver (University of Copenhagen)
	Prof. dr. N. S. Scrutton (University of Manchester)

The research described in this thesis was financially supported by a TOP-grant from the Netherlands Research Council for the Chemical Sciences (NWO-CW).

Casimir PhD series, Delft-Leiden 2014-7
ISBN: 978-90-8593-182-9

Preface

Natural processes rely heavily on proper functioning of nature's tiny machineries called proteins and enzymes. They are not only supposed to perform their tasks in isolation but also in collaboration with all other colleagues in a synergistic manner. Any imbalance imposes severe penalties not only to the immediate surroundings but often to the organism as a whole. It turns on feedback mechanisms calling for an emergency. Maybe we don't realize it but it is this synergy and functioning of these tiny machineries that keeps us alive and allows us to enjoy the beauty that nature has to offer us. While it is always fascinating to explore nature with our eyes and other senses, some of us derive great pleasure in "getting a feeling" about how does it all work at the molecular level. It is beyond the scope of this thesis to understand the "synergy" in multicomponent systems but an effort has been made to understand the functioning of a protein in isolation.

The protein studied is derived from *Streptomyces coelicolor*, called small laccase (SLAC). It utilizes four copper ions to catalyze the oxidation of substrate molecules concomitant with the reduction of oxygen to water. The catalytic cycle of this enzyme is studied using a variety of spectroscopic and kinetic methods in an attempt to improve our understanding of the internal operations which are critical to its functioning. The new results obtained are presented in this thesis.

Ankur Gupta

Contents

Preface		5
1	Introduction	9
2	Involvement of Tyr108 in the Enzyme Mechanism of the Small Laccase from *Streptomyces coeliocor*	25
3	Small laccase from *S. coelicolor* can turnover without Type 2 Cu but not without its Coordinating Histidine	51
4	One at a Time: Intramolecular Electron–Transfer Kinetics in Small Laccase observed during turnover	67
5	Conclusions and Outlook	93
Summary		97
Samenvatting		101
List of Publications		107
Curriculum Vitae		109
Acknowledgements		111

Chapter 1

Introduction

Ever since the structural data of biological macromolecules became available, there has been consistent struggle to relate this new information to the existing spectroscopy, activity and theoretical descriptions of these proteins and to understand the evolution and/or to predict the role of yet uncharacterized gene products in this light. This Chapter serves to provide basic background and introduction to this thesis that primarily deals with understanding the structure–function relationship of a newly discovered blue copper protein from *Streptomyces coelicolor*. Scope and outline of each chapter has also been presented.

1.1 Motivation

The evolution of life on earth has been intimately linked to the great oxidation event that occurred around 2.7 billion years ago.[1,2] At this time, the cyanobacteria started to poison the environment by releasing a toxic gas during photosynthesis which we know today as O_2.[2] There were only two ways for the existing life forms to cope up: either to avoid it altogether or to adapt their machinery to live with it. Some followed the former path and could still survive under deep oceans which remained anoxic. However, for others, it soon emerged that the advantages of this toxin were far more than the disadvantages involved. This is because oxygenic respiration could provide a lot more energy per reaction step than fermentation or other respiratory pathways. The toxicity of O_2 is related to the reactive oxygen species (ROS)[2] which are produced during respiration and by partial reduction of O_2 by organic matter. Thus, a tight control on the production of ROS was essential for survival. Transition metals like Cu, Fe and others were incorporated into the existing machineries for these purposes which have existed and further evolved since. The research presented in this thesis focuses on understanding the mechanism of O_2 metabolism by the small laccase (SLAC), a multicopper protein, from *Streptomyces coelicolor*.

1.2 (Multi)copper Proteins

Copper is an essential dietary element owing to its crucial role in biological redox processes.[3] Cu proteins are involved in oxygen transport (hemocyanin), electron transfer (azurin), respiration (cytochrome–c oxidase), metal homeostasis (ceruloplasmin) to name but a few examples. The latter two processes involve controlled reduction of O_2 to H_2O. Cytochrome–c oxidase (CcO), a membrane bound protein in the mitochondria, utilizes NADPH as a reductant and ceruloplasmin (Cp) which is found in human sera, uses Fe(II) to do so. In addition to Cu ions, CcO also contains heme prosthetic groups which are involved in catalysis, but Cp utilizes only Cu ions to accomplish the same task. Cp belongs to the category of oxidoreductases (enzymes which catalyze redox reactions) termed as multicopper oxidases (MCO).[4] Other well–known enzymes which fall into this category are the laccases (Lc) and ascorbate oxidase (AO). All

MCO's catalyze the reduction of O_2 to H_2O without the release of ROS to solution, while oxidizing one or more molecules of co–substrate, which acts as a sacrificial electron donor. Most MCO's are blue in color and contain four Cu ions which are important for catalysis (Figure 1).

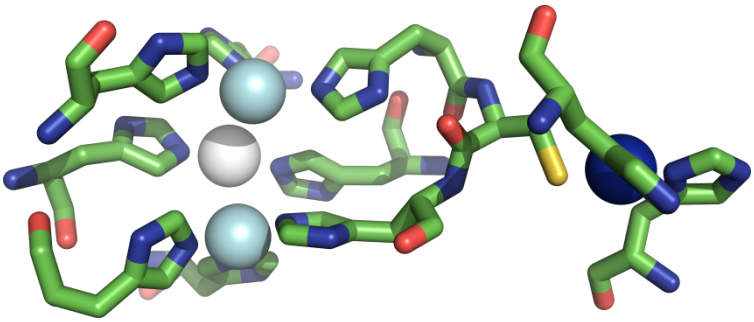

Figure 1: Active site of the MCO SLAC from *S. coelicolor* (pdb: 3CG8). Cu ions are shown as spheres (blue: T1 Cu; cyan: T3 Cu's; gray: T2 Cu). The coordinating residues are shown as sticks.

The blue color of MCO's is due to the presence of a Cu(II) ion (called type 1 (T1) Cu) with its unique coordination sphere. The T1 Cu is coordinated by two His and one Cys residue while the fourth ligand varies among different proteins. T1 Cu is characterized by its intense, $S_{Cys} \rightarrow Cu(II)$ charge transfer transition in the visible spectrum at ~600 nm and a narrow hyperfine splitting ($A_{\parallel}$ = (40–100) x 10^{-4} cm^{-1}) in the electron paramagnetic resonance (EPR) spectrum (Figure 2). This type of Cu is found in electron transfer (ET) proteins like azurin. It has a similar role in MCO's where the T1 Cu accepts electrons from reducing substrates, one at a time, and transfers them across a conserved HisCysHis pathway to the so called trinuclear Cu cluster (TNC) (Figure 1). The TNC is composed of the remaining three Cu(II) ions one of which is called type 2 (T2) Cu. T2 Cu does not contribute significantly to the absorption spectrum of the protein but has a large hyperfine splitting ($A_{\parallel}$ = (160–200) x 10^{-4} cm^{-1}) in the EPR spectrum (Figure 2). The other two Cu(II) ions at the TNC form a binuclear type 3 (T3) Cu pair bridged by a hydroxide anion. T3 Cu pair shows a band in the UV–region of the absorption spectrum around 330 nm (Figure 2). The two Cu's of the T3 Cu site are antiferromagnetically coupled and thus do

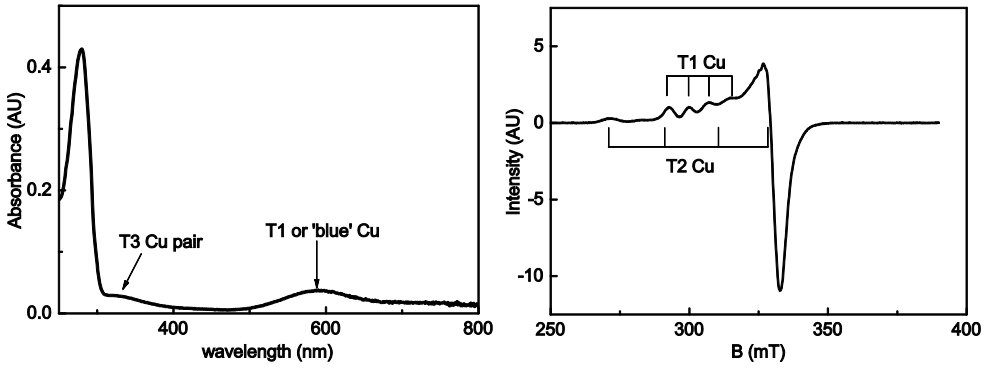

Figure 2: Typical (a) absorption spectrum and (b) EPR spectrum of the MCO SLAC from *S. coelicolor*.

not give rise to an EPR signal. This type of Cu pair is found in O_2 transport and O_2 activating proteins like hemocyanins and tyrosinases. In MCO's O_2 binds at the TNC, possibly at the T3 Cu site, and gets reduced to H_2O. The mechanism of O_2 binding and reduction to H_2O at the TNC has been subject of a long standing debate, which is discussed further in the forthcoming chapters.

1.3 Small Laccase

MCO's generally consist of three cupredoxin domains (3dMCO) which are arranged in three dimensional space such that the domains 1 and 3 fold back on each other where domain 3 contains the T1 Cu and the TNC is located at the interface of these two domains (Figure 3).[5–8] However, some exceptions do exist. Cp, for instance, consists of six, instead of three, cupredoxin domains where the TNC is located at the interface of domain 1 and domain 6 (Figure 3).[9] Domains 2, 4 and 6 contain three T1 Cu sites of which the one in domain 6, next to the TNC, is considered crucial for the enzyme activity.

Some years back, on the basis of a genome analysis, a new kind of MCO was identified and subsequently isolated from the culture of *Streptomyces coelicolor* which was different in shape and size from the MCO's known earlier.[10] The DNA sequence of this protein consisted of 1029 bases which accounts for 343 amino acids in the protein and an estimated molecular weight of 36.8 kDa. The protein was given the name 'small laccase' (SLAC), possessed the spectroscopic

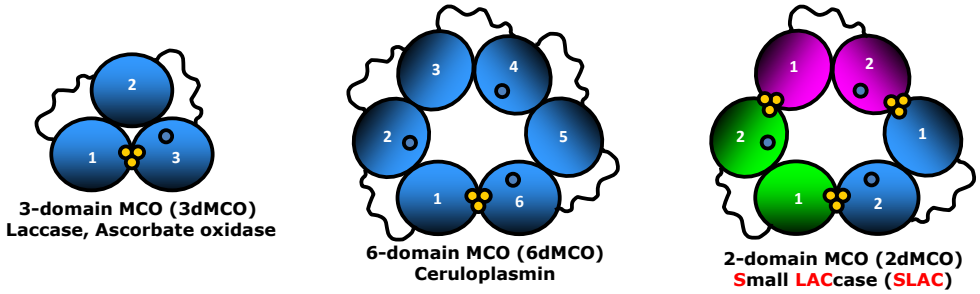

Figure 3: Cartoon representation of MCO's with different domain organization. The cupredoxin domains of same color belong to the same peptide chain and are also connected with a short loop. The Cu ions are shown as small spheres (blue: T1 Cu; yellow: TNC) within these domains.

features characteristic of MCO's and was found to be active as a trimer. Later the 3D structure of the protein revealed that SLAC is a homotrimer where each monomer consists of two cupredoxin domains.[11] The overall geometry appears very similar to Cp except that SLAC contains three T1 Cu's and three TNC's, and the six domains, two from each monomer, are not covalently linked (Figure 3). Moreover the TNC is situated between the N– and C–terminus of adjacent monomers unlike the 3dMCO's where the TNC is located between the N– and C–terminus of the same peptide chain. It was interesting to note that sequences similar to that of SLAC were identified in the genomes of many other organisms indicating the presence of such 2DMCO's in the *Streptomyces* genus. Phylogenetic analysis and evolutionary relationships of the blue copper proteins suggest that such two–domain multicopper blue proteins might have appeared earlier in the evolution of the conventional 3dMCO's like Lc's, AO and the six–domain Cp.[12–14] The research presented in this thesis was undertaken to understand the fundamental structure–function relationship of this new protein that may throw new light on the evolution of its family members.

1.4 Scope and outline of the work

Laccases are one of the well–studied members of the MCO family. Owing to their capability to oxidize a wide variety of substrates, they find use in the industry for textile dye finishing, waste treatment, food applications, biosensors and medicinal and asymmetric organic synthesis.[15] However, one of the major

upcoming applications of Lc's is in their capability to act as a cathode in a (bio)fuel cell where O_2 acts as the ultimate electron acceptor. SLAC is well suited for this application since there exists a recombinant expression system that can produce large quantities of protein which are easy to purify, and preliminary studies seem to suggest its superior performance over conventional Lc's.[16] Thus, it is important to understand the mechanism of O_2 reduction by SLAC and compare it to that of the well–studied Lc's.

The reaction of O_2 may take place with the four–electron reduced form of the protein.[17–19] This will prevent the formation of long lived ROS since the O_2 bound at the TNC can be completely reduced by $4e^-$ equivalents. However, the possibility of O_2 reacting with a two– or three–electron reduced form of the protein under turnover conditions cannot be excluded. Direct four–electron reduction of O_2 is unlikely. Instead, it is expected to occur in multiple steps (Figure 4).[17–19] There exists considerable evidence that the first step in this process is $2e^-$ reduction of O_2 to form peroxide intermediate (PI).[18,19] Since this intermediate is highly oxidizing, it may rapidly accept two more electrons to complete the four–electron reduction of O_2 while the enzyme is oxidized back to what is called as the native intermediate (NI). It is not clear whether the conversion of PI to NI takes place in two $1e^-$ transfer steps or a single $2e^-$ transfer step (see below). The NI is different from the resting form of enzyme in the way OH^- is bound at the TNC.[20] The multi–step process of O_2 reduction is fast, at least at room temperature, and it is very difficult to characterize the intermediates steps with conventional pre–steady–state kinetics techniques like stopped–flow. However, X–ray diffraction measurements of the crystals of multiple MCO's, often performed at cryogenic temperatures, have provided a snapshot of the O_2/ROS bound at the TNC.[21,22] Still, there is no clear evidence to support the idea that such intermediates exist during steady–state turnover. Therefore, to dissect the mechanism of O_2 reduction, enzyme forms have been prepared where the T1 Cu site is absent (T1D)[23] or has been replaced with a redox inert Hg(II) (T1Hg).[24] When fully reduced T1D or T1Hg Lc reacts with O_2, the reaction is stalled at the first $2e^-$ reduction stage, when a PI is formed, since there are not sufficient electrons (fully reduced protein has only 3 Cu's and thus can load a maximum of three electrons) to carry out complete reduction of O_2. It is

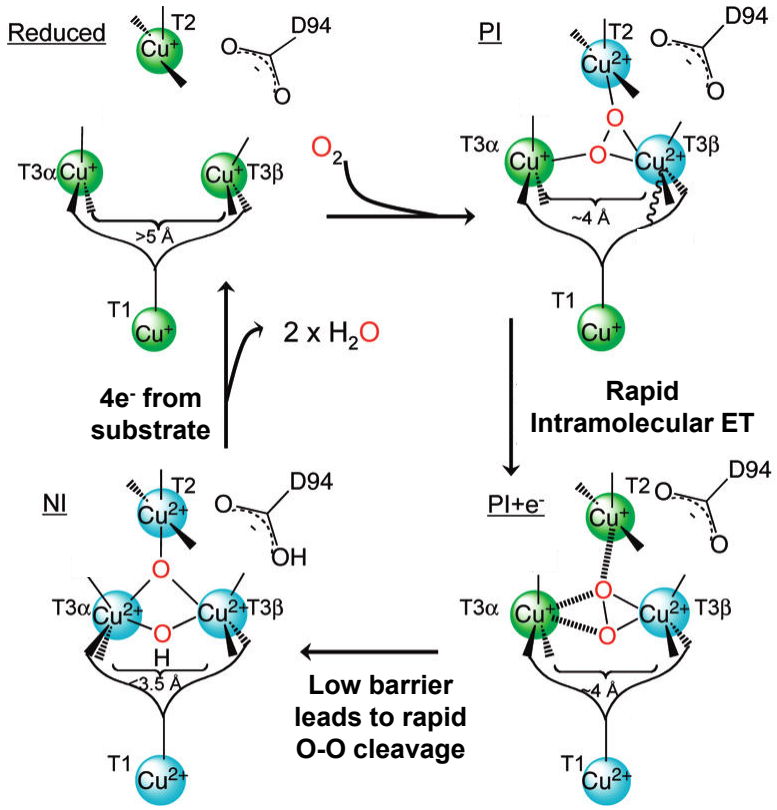

Figure 4: Possible mechanism of O_2 reduction by Fet3p, an MCO from *Saccharomyces cerevisiae*, as proposed by Solomon and coworkers. Reduced Cu's are depicted in green and oxidized Cu's in cyan. The T3 Cu's are inequivalent and are marked as T3α and T3β. The proposed mechanism may require further revisions and is not necessarily applicable to all other members of the MCO family. For more details, see the text. The figure is adapted from ref 28.

noteworthy that in spite of the protein having three–electrons, the reduction of O_2 doesn't go beyond the peroxide stage. There are some preliminary evidences in the literature which indicate that further one–electron reduction of PI may yield a molecule of water and an oxygen based radical (possibly hydroxyl) bound at the TNC.[25–27] However, there is a strong debate about the nature of the peroxide binding and the redox states of the different Cu ions in the PI. On multiple occasions, X–ray diffraction measurements have indicated a symmetric binding of the peroxide between the Cu ions of the T3 Cu pair but when

applying this technique as the only method of investigation, discrete assignment of the redox states of different Cu ions cannot be made.[21,22] On the other hand, mutagenesis experiments, spectroscopy and theoretical arguments indicate that the peroxide may also be coordinated to the T2 Cu.[28,29] The discrepancy could possibly arise because the above conclusions are each specific to a particular protein and, therefore, can't be generalized to all MCO's. Another possibility is that while the measurements on crystals are performed at cryogenic temperatures where natural movements of protein side chains are restricted, the measurements in solution are performed at ambient temperature allowing more motional freedom on atomic scale. It is beyond the scope of this thesis to review all possible mechanisms which have been proposed so far leading to the four–electron reduction of O_2. The interested reader is referred to the relevant literature.[17–19] However, because of its 3D–structural similarity with SLAC, it is appropriate to present here the mechanism proposed for ferrous oxidase (Fet3p) from *Saccharomyces cerevisiae*, which has been constructed on the basis of a variety of spectroscopic and kinetics measurements and theoretical considerations (Figure 4).[28] In the light of results obtained for other MCO's, the mechanism or the nature of intermediates presented in Figure 4 shall not be taken as a generalization for the entire 3dMCO family. In particular, it will be shown in Chapter 4 that some of the findings of our single molecule experiments may necessitate a revision of particular aspects of the scheme presented in Figure 4.

While the reaction of O_2 with fully reduced T1D Lc yields the PI, the similar reaction of T1D SLAC gives rise to a different kind of intermediate, a biradical intermediate, as demonstrated from the absorption and EPR spectroscopy.[30] **Chapter 2** of this thesis provides clear evidence about the nature of this intermediate and its possible role in the reduction of O_2 by SLAC. It appears that Tyr108 is a redox non–innocent residue which gets oxidized to form a radical when the TNC falls short of electrons, for example when the T1 Cu site is absent. Thus, the enzyme seems to adopt a rescue mechanism to prevent ROS formation and survive under conditions where there is an imbalance in the reducing and oxidizing co–substrates. Interestingly, this tyrosine residue is conserved across all the sequences of the purported 2dMCO's of this family and also in Cp.

For AO and many Lc's, it was also discovered that all four Cu ions are essential for the activity of the protein.[31] T2 Cu, for example, is coordinated by only two His residues and can be easily removed by using strong copper chelators and/or mild denaturing conditions.[31–34] Such a protein devoid of T2 Cu (T2D) does not possess any activity and neither can the fully reduced protein react with O_2 like the wt– or T1D forms of the protein. These findings together with a series of site–directed mutagenesis, kinetics and computational studies suggest that O_2 binds to the T2 Cu and one of the T3 Cu, referred to as T3Cuβ (Figure 4), instead of binding symmetrically to the two T3 Cu's as in hemocyanin.[28] This is because the coordination spheres of the two Cu's of the T3 site are slightly different leading to an asymmetry at the TNC. **Chapter 3** of this thesis aims to demonstrate another singularity of SLAC within the mechanism of O_2 reduction by this protein. The T2D form of SLAC only loses its activity partially, indicating that this copper is not a necessary requirement for the protein to function. Thus O_2 must bind to the T3 Cu pair, at least in SLAC. Interestingly, mutation of His102, one of the two histidine residues that coordinate to T2 Cu, abolishes enzyme activity almost completely, i.e. by 2–3 orders of magnitude, indicating the importance of this residue in the enzyme catalysis. However, it is still unclear how the protein containing only three equivalents of Cu's per monomer is capable of carrying out the four electron reduction of O_2 to H_2O.

Although the redox potentials of the Cu's at the TNC are very similar to that of T1 Cu, the TNC Cu's cannot be reduced directly by the substrate. T1 Cu, on the other hand, is directly reduced but doesn't interact or coordinate to O_2. This is why the protein lacking the T1 Cu site is inactive. Thus, the electrons which are accepted at the T1 Cu site must be transferred to the TNC, one at a time, before the TNC can react with O_2. This ET process must be fast and efficient so as to prevent formation of long lived ROS at the TNC which might pose a threat to the protein.

The vast majority of oxidoreductases, including the MCO's, uncouple the reduction and oxidation half reactions by using separate sites for them. The protein matrix takes care of ET and communication between the two sites. There has been extensive research on understanding the theory and mechanism of ET

kinetics and the role of the surrounding environment in this process. The interested reader is referred to the appropriate reviews to obtain an overview of ET mechanisms.[35,36] Conventional routes to follow the fast ET processes are to study pre–steady–state kinetics using rapid–mixing, flash quench/photolysis and pulse radiolysis. Usually when the ET rate is to be measured between two proteins (intermolecular ET) diffusing freely in solution, rapid–mixing techniques like stopped–flow, rapid–freeze–quench, chemical–quench are useful. To study the kinetics of intramolecular ET or ET between confined redox partners, the techniques that come handy are electrochemistry, flash quench/photolysis and pulse radiolysis.[37] However, there is a common limitation of all these techniques in that the ET process under investigation is measured under the pre–steady–state conditions. While such measurements continue to provide a wealth of information about the spectroscopy and nature of possible intermediates, not always does trapping of the intermediates under such conditions represent the series of events that occur in the turning over enzyme during steady–state. Electrochemistry is an exception here which sometimes allows investigation of steady–state kinetics of proteins immobilized on conducting electrodes, but the communication of protein with the electrode is rarely efficient and thus limits the study of the ET steps in question.[38]

Study of proteins at single molecule level has opened doors to investigate salient features of enzyme kinetics, including ET kinetics, that were inaccessible or very difficult to measure in bulk.[39–43] Recently, a Förster Resonance Energy Transfer (FRET) based approach was introduced, which provides fluorescence readout of the redox state of the protein or its specific cofactors.[44] Thus, the analyses of dwell times of a time trajectory of a single molecule provides information about the lifetimes of the respective 'on' and 'off' states which correspond to the rate of inter–conversion of two or more redox states involved in the process. The advantages of this approach are at least two–fold. First, it allows the real–time observation of individual ET events as the molecule is turning over under steady–state, and secondly, it allows studying the kinetics of individual molecules and unraveling the heterogeneity that exists across many molecules which is otherwise averaged out in an ensemble measurement. **Chapter 4** of this thesis makes use of the above approach to study kinetics of ET between the T1 and

TNC sites of SLAC. SLAC variants were prepared for site–specific labeling and immobilization on transparent supports to minimize the heterogeneity in sample preparation. It has been argued that the distribution of ET rates across many molecules corresponds to a disorder of activation energy in the ensemble. It remains to be seen whether this disorder is truly a random phenomenon or a systematic control that nature imposes over the active site to address different requirements in different environments by one and the same gene product.

1.5 References

[1] Bekker, A.; Holland, H. D.; Wang, P. L.; Rumble, D., 3rd; Stein, H. J.; Hannah, J. L.; Coetzee, L. L.; Beukes, N. J. *Nature* **2004**, *427*, 117.

[2] Halliwell, B.; Gutteridge, J. *Free Radicals in Biology and Medicine*; OUP Oxford, 2007.

[3] Karlin, K. D.; Tyeklár, Z. *Bioinorganic chemistry of copper*; Chapman & Hall, 1993.

[4] Messerschmidt, A. *Multi-copper Oxidases*; World Scientific, 1997.

[5] Messerschmidt, A.; Ladenstein, R.; Huber, R.; Bolognesi, M.; Avigliano, L.; Petruzzelli, R.; Rossi, A.; Finazzi-Agro, A. *J. Mol. Biol.* **1992**, *224*, 179.

[6] Taylor, A. B.; Stoj, C. S.; Ziegler, L.; Kosman, D. J.; Hart, P. J. *Proc. Natl. Acad. Sci. U. S. A.* **2005**, *102*, 15459.

[7] Roberts, S. A.; Weichsel, A.; Grass, G.; Thakali, K.; Hazzard, J. T.; Tollin, G.; Rensing, C.; Montfort, W. R. *Proc. Natl. Acad. Sci. U. S. A.* **2002**, *99*, 2766.

[8] Hakulinen, N.; Kiiskinen, L. L.; Kruus, K.; Saloheimo, M.; Paananen, A.; Koivula, A.; Rouvinen, J. *Nat. Struct. Biol.* **2002**, *9*, 601.

[9] Bento, I.; Peixoto, C.; Zaitsev, V. N.; Lindley, P. F. *Acta Crystallogr., Sect. D: Biol. Crystallogr.* **2007**, *63*, 240.

[10] Machczynski, M. C.; Vijgenboom, E.; Samyn, B.; Canters, G. W. *Protein Sci.* **2004**, *13*, 2388.

[11] Skalova, T.; Dohnalek, J.; Ostergaard, L. H.; Ostergaard, P. R.; Kolenko, P.; Duskova, J.; Stepankova, A.; Hasek, J. *J. Mol. Biol.* **2009**, *385*, 1165.

[12] Dwulet, F. E.; Putnam, F. W. *Proceedings of the National Academy of Sciences of the United States of America-Biological Sciences* **1981**, *78*, 2805.

[13] Nakamura, K.; Go, N. *Cell. Mol. Life Sci.* **2005**, *62*, 2050.

[14] Murphy, M. E. P.; Lindley, P. F.; Adman, E. T. *Protein Sci.* **1997**, *6*, 761.

[15] Xu, F.; Damhus, T.; Danielsen, S.; Østergaard, L. H. In *Modern Biooxidation*; Wiley–VCH Verlag GmbH & Co. KGaA: 2007, p 43.

[16] Wheeldon, I. R.; Gallaway, J. W.; Barton, S. C.; Banta, S. *Proc. Natl. Acad. Sci. U. S. A.* **2008**, *105*, 15275.

[17] Solomon, E. I.; Sundaram, U. M.; Machonkin, T. E. *Chem. Rev.* **1996**, *96*, 2563.

[18] Solomon, E. I.; Augustine, A. J.; Yoon, J. *Dalton Trans.* **2008**, 3921.

[19] Wherland, S.; Farver, O.; Pecht, I. *J. Biol. Inorg. Chem.* **2014**.

[20] Heppner, D. E.; Kjaergaard, C. H.; Solomon, E. I. *J. Am. Chem. Soc.* **2013**.

[21] Messerschmidt, A.; Luecke, H.; Huber, R. *J. Mol. Biol.* **1993**, *230*, 997.

[22] Ferraroni, M.; Matera, I.; Chernykh, A.; Kolomytseva, M.; Golovleva, L. A.; Scozzafava, A.; Briganti, F. *J. Inorg. Biochem.* **2012**, *111*, 203.

[23] Palmer, A. E.; Quintanar, L.; Severance, S.; Wang, T. P.; Kosman, D. J.; Solomon, E. I. *Biochemistry* **2002**, *41*, 6438.

[24] Cole, J. L.; Ballou, D. P.; Solomon, E. I. *J. Am. Chem. Soc.* **1991**, *113*, 8544.

[25] Andréasson, L. E.; Brändén, R.; Malsmtröm, B. G.; Vänngård, T. *FEBS Lett.* **1973**, *32*, 187.

[26] Aasa, R.; Brändén, R.; Deinum, J.; Malmström, B. G.; Reinhammar, B.; Vänngård, T. *FEBS Lett.* **1976**, *61*, 115.

[27] Branden, R.; Deinum, J. *Biochim. Biophys. Acta* **1978**, *524*, 297.

[28] Augustine, A. J.; Kjaergaard, C.; Qayyum, M.; Ziegler, L.; Kosman, D. J.; Hodgson, K. O.; Hedman, B.; Solomon, E. I. *J. Am. Chem. Soc.* **2010**, *132*, 6057.

[29] Solomon, E. I.; Ginsbach, J. W.; Heppner, D. E.; Kieber–Emmons, M. T.; Kjaergaard, C. H.; Smeets, P. J.; Tian, L.; Woertink, J. S. *Faraday Discuss.* **2011**, *148*, 11.

[30] Tepper, A. W. J. W.; Milikisyants, S.; Sottini, S.; Vijgenboom, E.; Groenen, E. J. J.; Canters, G. W. *J. Am. Chem. Soc.* **2009**, *131*, 11680.

[31] Malkin, R.; Malmstrom, B. G.; Vanngard, T. *Eur. J. Biochem.* **1969**, *7*, 253.

[32] Graziani, M. T.; Morpurgo, L.; Rotilio, G.; Mondovi, B. *FEBS Lett.* **1976**, *70*, 87.

[33] Avigliano, L.; Desideri, A.; Urbanelli, S.; Mondovi, B.; Marchesini, A. *FEBS Lett.* **1979**, *100*, 318.

[34] Morpurgo, L.; Savini, I.; Mondovi, B.; Avigliano, L. *J. Inorg. Biochem.* **1987**, *29*, 25.

[35] Marcus, R. A.; Sutin, N. *Biochim. Biophys. Acta* **1985**, *811*, 265.

[36] Gray, H. B.; Winkler, J. R. *Q. Rev. Biophys.* **2003**, *36*, 341.

[37] Farver, O.; Pecht, I. *Coord. Chem. Rev.* **2011**, *255*, 757.

[38] Heering, H.; Canters, G. *Engineering the Bioelectronic Interface: Applications to Analyte Biosensing and Protein Detection; Davis, JJ, Ed* **2010**, 120.

[39] Lu, H. P.; Xun, L.; Xie, X. S. *Science* **1998**, *282*, 1877.

[40] English, B. P.; Min, W.; van Oijen, A. M.; Lee, K. T.; Luo, G.; Sun, H.; Cherayil, B. J.; Kou, S. C.; Xie, X. S. *Nat. Chem. Biol.* **2006**, *2*, 87.

[41] Kuznetsova, S.; Zauner, G.; Aartsma, T. J.; Engelkamp, H.; Hatzakis, N.; Rowan, A. E.; Nolte, R. J.; Christianen, P. C.; Canters, G. W. *Proc. Natl. Acad. Sci. U. S. A.* **2008**, *105*, 3250.

[42] Goldsmith, R. H.; Tabares, L. C.; Kostrz, D.; Dennison, C.; Aartsma, T. J.; Canters, G. W.; Moerner, W. E. *Proc. Natl. Acad. Sci. U. S. A.* **2011**, *108*, 17269.

[43] Tabares, L. C.; Kostrz, D.; Elmalk, A.; Andreoni, A.; Dennison, C.; Aartsma, T. J.; Canters, G. W. *Chem. Eur. J.* **2011**, *17*, 12015.

[44] Kuznetsova, S.; Zauner, G.; Schmauder, R.; Mayboroda, O. A.; Deelder, A. M.; Aartsma, T. J.; Canters, G. W. *Anal. Biochem.* **2006**, *350*, 52.

Chapter 2

Involvement of Tyr108 in the Enzyme Mechanism of the Small Laccase from *Streptomyces coelicolor**

Abstract:

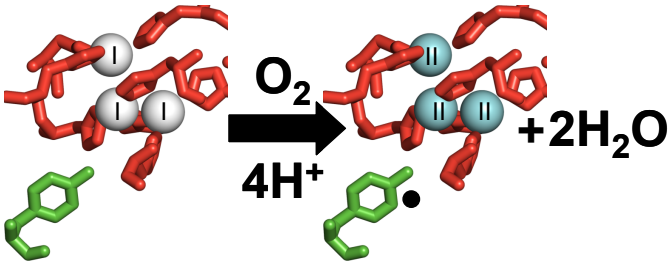

The enzyme mechanism of the multicopper oxidase (MCO) SLAC from *Streptomyces coelicolor* was investigated by structural (XRD), spectroscopic (optical, EPR) and kinetics (stopped-flow) experiments on variants in which residue Tyr108 had been replaced by Phe or Ala through site-directed mutagenesis. Contrary to the more common three-domain MCOs, a tyrosine in the two-domain SLAC is found to participate in the enzyme mechanism by providing an electron during oxygen reduction, giving rise to the temporary appearance of a tyrosyl radical. The relatively low k_{cat}/K_M of SLAC and the involvement of Y108 in the enzyme mechanism may reflect an adaptation to a milieu in which there is an imbalance between the available reducing and oxidizing co-substrates. The purported evolutionary relationship between the two-domain MCO's and human ceruloplasmin appears to extend not only to the 3D structure and the mode of binding of the Cu's in the trinuclear center, as noted before, but also to the enzyme mechanism.

*Adapted from: Gupta, A.; Nederlof, I.; Sottini, S.; Tepper, A.W.J.W.;Groenen, E.J.J; Thomassen, E.A.J.; Canters, G.W. *J. Am. Chem. Soc.* **2012**, *134*, 18213.

2.1 Introduction

Multicopper oxidases (MCOs) catalyze the oxidation of a wide variety of substrates while reducing molecular oxygen to water. To achieve this, they utilize four copper atoms: a type 1 (T1) Cu which accepts reducing equivalents from the substrates and a trinuclear Cu cluster (TNC) where oxygen binds and gets converted to water. The TNC consists of a normal or type 2 (T2) Cu and a binuclear type 3 (T3) Cu pair. The mechanism of O_2 reduction at the TNC has been extensively studied by a variety of techniques.[1,2] It has been proposed that O_2 first binds at the TNC and then gets reduced in two $2e^-$ steps while others have argued for (left open) a first two–electron reduction step and subsequently two consecutive one–electron transfer steps.[2-5] The conserved residues between T1 Cu and TNC form a covalent link and promote rapid electron transfer from T1 Cu to the TNC.[6] However, views about O_2 binding and the mechanism of reduction have changed over time and still remain a topic of debate.[2,7-9] A brief account is presented in Chapter 1.

Analysis of the genome of *Streptomyces coelicolor* revealed the presence of a gene possibly encoding an MCO,[10] "small laccase" (SLAC), which owes its name to its smaller molecular weight as compared to the other well–known MCOs such as ascorbate oxidase, laccase, Fet3p and CueO. SLAC was found to be active as a homotrimer unlike most other MCOs described until now, which are monomeric proteins in solution.[11-14] It has been suggested that the three–domain ascorbate oxidase, the three–domain laccases and the six–domain ceruloplasmins have evolved via formation of a trimer of two–domain cupredoxins.[15] The recent crystal structure of SLAC clearly shows that the enzyme has such a trimeric form with a canocical TNC.[16,17] The structure together with structures of other 2–domain MCOs has been used in an attempt to fill in the gaps in the proposed evolution of MCOs.[16,18,19] Thus, it was of interest to study SLAC not only from a fundamental point of view to understand the structure–function relationship of this new enzyme, but also to seek footprints of the proposed ancestor that may have been carried over or discarded by the generations that followed after. Apart from that, SLAC holds potential for its applications in industry and its use as a cathode in biofuel cells to cater for the demands of green energy.[20,21]

SLAC was found to be excreted in the growth media of *S. coelicolor* cultures and, thus, was identified as an extracellular enzyme. The physiological roles of most extracellular enzymes, including SLAC, are unclear, researchers have mixed views,[22] but it is well known that members of the *Streptomycetes* genus produce dozens of antibiotics as secondary metabolites using such secreted enzymes.[23] For ease of expression and purification in higher yields, the gene encoding SLAC was isolated and recombinantly expressed in *E. coli*. Following the preliminary characterization, it was recently reported that reduced, type 1 depleted (T1D) SLAC, upon reaction with oxygen, forms an unusual biradical intermediate which has not been reported for the more common laccases.[24] Spectroscopic signatures, when compared with those of other enzymes and model systems, led to the hypothesis that a ferromagnetically coupled triplet state arises in SLAC due to exchange coupling of two unpaired spins, one residing on T2 Cu and the other on a tyrosyl radical ~5Å away. Similar spectroscopic features were also observed during turnover of the native enzyme, and a role of the radical in catalytic turnover was implicated (see also ref 21[25]). The present study attempts to identify the position of the radical and its role in enzyme catalysis. The preliminary results indicate that Tyr108 is the site carrying the unpaired spin. Its absence in site–directed mutants affects the enzyme kinetics. To the best of our knowledge, this is the first example where direct involvement of a tyrosyl radical in MCO catalysis has been demonstrated.

2.2 Results and Discussion

The crystal structure of wild–type (*wt)* SLAC (PDB: 3CG8)[16] shows the presence of a tyrosine residue (Y108) ~5Å away from the T2 Cu, as predicted from electron paramagnetic resonance (EPR) results.[24] This residue is located at the interface of two subunits in the trimeric form of the enzyme. Site–directed mutagenesis was carried out to prepare SLAC variants in which the tyrosine is replaced by phenylalanine (Y108F) or alanine (Y108A) in both the *wt* and the T1D (C288S) sequences.[26] All variants containing mutations in the wt sequence at position 108 were crystallized and analyzed by X–ray diffraction to a resolution of 2.7–2.8 Å.[26] The diffraction data confirm single amino acid

replacements at the desired position as well as intact active sites. No significant changes in the overall fold of the enzyme or near the active sites were observed (Figure 1). This facilitates a direct comparison of the enzyme kinetics and spectroscopic features of the mutants to those of the *wt* SLAC.[26]

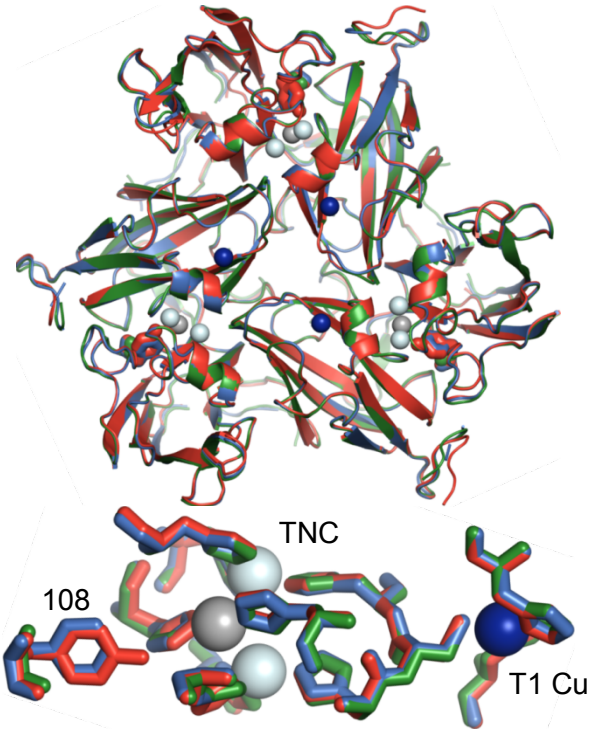

Figure 1: Ribbon representations of *wt* SLAC (red, PDB: 3CG8) overlaid with those of the mutants Y108F (blue, PDB: 4GXF) and Y108A (green, PDB: 4GY4). The bottom shows an expanded view of residues near the T1 Cu and TNC. The T3 Cu's are shown in light blue and the T2 Cu is colored in gray. Clearly the overall fold and active sites are intact in the mutants.

Steady–state kinetics experiments were performed using *N,N,N'N'*–tetramethyl–*p*–phenylenediamine (TMPD) as a substrate.[26] The enzymatic rate of reaction was monitored by following the formation of the oxidation product of TMPD at 610 nm at a given concentration of O_2. Alternatively, the rates of O_2 consumption during the reaction were measured using a Clark–type O_2 electrode.[26] TMPD is a one electron reductant, and the ratio of reaction rates monitored by optical spectroscopy versus those obtained by monitoring O_2

consumption was ~4 for any given concentration of substrates for the mutants studied. This implies complete reduction of O_2 to H_2O and shows that no H_2O_2 is released to solution. Addition of catalase to the reaction chamber, did not affect apparent O_2 uptake kinetics, nor did it show any increase in O_2 concentration, which strengthens this conclusion. The kinetic parameters obtained from the fits to the data are shown in Table I. The ratio of ${}^{app}k_{cat}$ obtained by the two methods is not exactly 4 owing to the fact that the solubility of O_2 is limited in buffer, and therefore rates at enzyme–saturating O_2 concentrations could not be measured.

Table 1: Turnover Number (k_{cat}) and Second–Order rate constant k_{cat}/K_M of *wt* and Mutant SLAC at 295 K in Phosphate Buffer at pH 6.[a]

	${}^{app}k_{cat}$ (s^{-1})		${}^{app}k_{cat}/K_M$ ($M^{-1}s^{-1}$) (x10^{-5})	
	O_2[b]	TMPD[c]	O_2[b]	TMPD[c]
wt–SLAC	90 ± 3	315 ± 9	2.8 ± 0.2	3.2 ± 0.4
Y108A	34 ± 1	128 ± 3	2.7 ± 0.2	3.8 ± 0.4
Y108F	35 ± 1	132 ± 4	2.6 ± 0.2	2.4 ± 0.3

[a]For Michaelis–Menten plots see SI.[26] Parameters based on concentration of single subunit of SLAC as determined from the 280nm absorption (*i.e.*, equal to three times the SLAC concentration). [b]monitoring decrease in O_2 concentration *vs* time. [c]monitoring increase in absorption as a result of TMPD oxidation *vs* time.

It is evident from the data in Table 1 that the mutation affects only the turnover number (k_{cat}) of the enzyme and not the second–order rate constants (k_{cat}/K_M). While one would expect such a result for TMPD, as the mutations are far away from the T1 Cu reaction site for the TMPD (Figure 1), it is not immediately obvious why the second–order rate constant for O_2 remains unaffected. After all, the mutations are close to the O_2 reaction site (*i.e.*, the TNC). For any given enzyme, k_{cat}/K_M encompasses the steps from substrate binding up to and including the first irreversible step, whereas k_{cat} signifies the steps related to turnover of the ES complex and/or product release.[27] From single–turnover experiments on SLAC, it is found that O_2 binding to the TNC is practically irreversible.[26] This is in agreement with the enzymatic mechanism proposed for laccases, where the binding of O_2 followed by its reduction to the peroxide intermediate (PI) at the TNC was found to be irreversible.[28] We conclude that

the rate-limiting step(s) must occur after the binding of O_2 and reduction to PI and may involve the decay of PI to the native intermediate (NI).[29] TMPD or another co-substrate may then reduce the NI, thereby completing the reaction cycle and regenerating fully reduced SLAC ready to bind and reduce oxygen (Scheme I). Since k_{cat} is affected by the mutations at position 108, the rate-limiting step(s) must involve Y108 in the case of *wt* SLAC.

Scheme 1: Proposed Pathway in the Reaction Mechanism of SLAC with a role for Y108 as postulated initially.[30] The scheme may need modification in the light of more recently obtained evidence [33].[a]

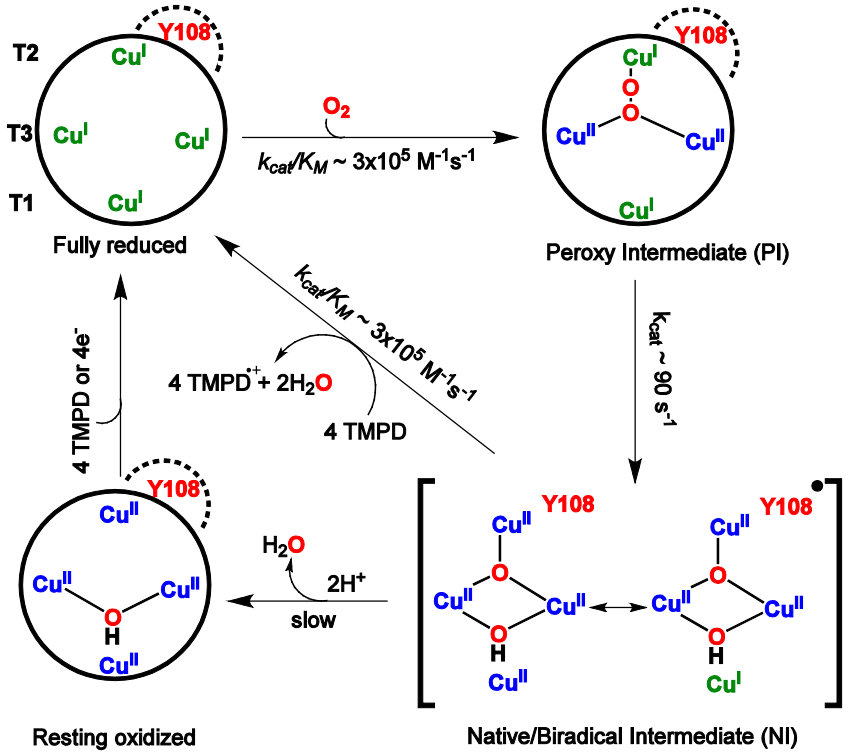

[a]Reduced copper sites are depicted in light green and oxidized ones in blue. Tyrosine is shown in red. The rate constants are those obtained for SLAC in this study. Work is going on to characterize the Native/Biradical Intermediate (NI) in more detail.

The results from transient absorption spectroscopy and EPR spectroscopy support the original hypothesis about the localization of the unpaired spins on Y108 and T2 Cu in the T1D SLAC.[24] Experiments analogous to those

performed earlier[24,26] with the T1D SLAC were now carried out with the double mutants, T1D–Y108F and T1D–Y108A, i.e., where both C288S and Y108A or Y108F mutations are present. Pre–steady–state kinetics experiments reveal that the absorption feature around 410 nm which was earlier attributed to the formation of a tyrosyl radical, is not observed in these variants. Instead, an intermediate resembling the PI[31] (absorption maxima around 340, 470 and 710 nm) is observed (Figure 2a). In conjunction with the results above, no biradical signal is observed in the EPR spectrum of T1D–Y108A mutant (Figure 2b). It is interesting to note that a new radical signal is observed in the T1D–Y108F mutant, which is distinct from the signal reported for T1D itself (not shown). However, the intensity of the new radical signal compared to that of the total spin is very low (<10%). While similar turnover numbers are observed for Y108A and Y108F variants, we conclude that this signal cannot be catalytically relevant and is formed only in the absence of Y108. High–field magnetic resonance spectroscopy studies are underway to determine if this signal may correspond to a phenylalanine or possibly a tryptophan (W284, see SI) radical.

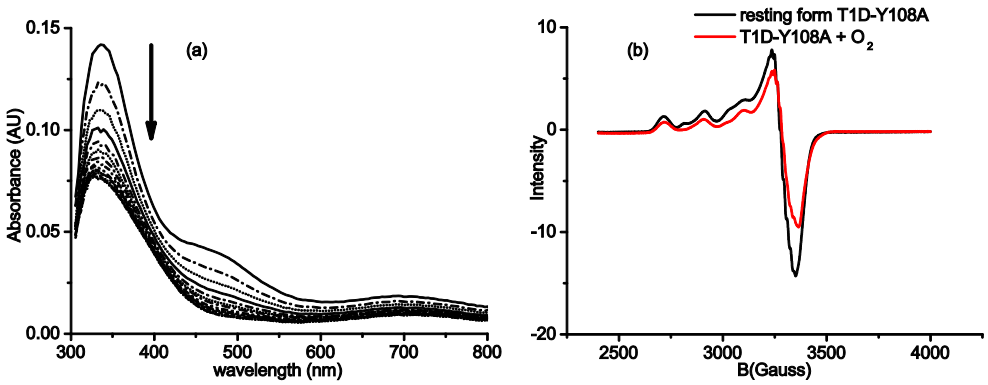

Figure 2: (a) Decay of the peroxide intermediate (PI) monitored by absorption spectroscopy following rapid mixing of reduced T1D–Y108A mutant (100 µM) with air–saturated phosphate buffer (pH 6.8) at 295 K. The PI is formed within 200 ms of mixing and then decays slowly with a half–life of 2.5 s. (b) X–band EPR spectrum of the resting form of T1D–Y108A mutant (black) overlaid with the spectrum of the same enzyme after it had been reduced, reoxidized, and frozen immediately (red). The spectra were recorded at 40 K (see also SI).

It is of interest here to contrast the sequence of O_2 reduction events as observed for SLAC (Scheme 1) with the sequence observed for the three–domain laccases. In *Rhus vernicifera* laccase (Lac), for instance, in which the T1Cu site has been inactivated by replacement of the T1Cu with a redox–innocent mercuric ion (T1Hg), complete reduction of the enzyme followed by reaction with O_2 results in the PI.[28] Similar behavior and rate constants are observed for another member of the three–domain MCOs, Fet3p, where the T1 site is inactivated by site–directed mutagenesis to prepare a T1D form of Fet3p.[32] Since in both cases there are only three electrons available in the reduced enzyme (i.e., at the T2 and the T3 sites), reduction of O_2 stops at the PI. In SLAC, on the other hand, under similar circumstances no PI is observed, but the optical and paramagnetic signatures of a Tyr radical appear instead. This is because the fourth electron, which is lacking in the T1D or T1Hg Lac, is now provided, apparently, by the Tyr moiety in the T1D SLAC, leading to the complete reduction of O_2 to H_2O. Consistent with this interpretation, we observe that only when the T1Cu site ***and*** Y108 have been deleted in SLAC does the spectroscopic evidence of PI be observed. We have not characterized the mode of peroxide binding at the TNC and other binding modes are possible than the one presented in Scheme 1. In addition, we can't exclude the possibility that under turnover conditions, two– or three–electron reduced SLAC can already start reacting with O_2.[33]

Multiple sequence alignment of SLAC with other multicopper proteins reveals that Y108 is conserved among the homologous two–domain MCOs[26] and also in human ceruloplasmin (hCp), for which a crystal structure has been published.[34] The appearance of a 410 nm intermediate (presumably oxidized tyrosine) during oxidation of fully reduced hCp was observed several years ago[35,36] but was not investigated further owing to the challenging mutagenesis of the recombinant protein and its purification in soluble form.[37] By analogy with SLAC, we now can assign, tentatively, this intermediate to a tyrosine radical. It is noteworthy that, among all known MCOs, only the six–domain ceruloplasmins and SLAC bind to the Cu sites with eight 2Nε–His coordination whereas the three–domain laccases and ascorbate oxidase contain seven 2Nε–His and one 1Nδ–His as a ligand, leading to a distinct asymmetry between the T3α (two 2Nε–His and one Nδ1–His) and T3β (three 2Nε–His) Cu's.[38] It has been suggested that this

structural difference between the T3α and T3β Cu's has important mechanistic consequences for O_2 binding and reduction in the three–domain laccases.[38] It will be of interest to see if the more symmetric coordination of the T3 site in SLAC (as in hCp) leads to different reaction kinetics than in the 3–domain laccases. Thus, SLAC and hCp share not only the conserved Y108 (Y107 in hCp) and the above same features of unique copper binding motifs but possibly also a similar enzyme mechanism.[26] We therefore propose SLAC to be suited as a model system to study the structure–function relationship of the more complicated hCp. We conclude that, not only from a structural viewpoint but also from a mechanistic point of view, our experiments appear to support the earlier postulated evolution of copper proteins, where the two–domain MCOs are proposed to be ancestors to the six–domain hCp.[15,39,40]

As for the evolutionary history of the three–domain laccases, it may be that the evolution of ascorbate oxidase and other three–domain MCOs such as the laccases took separate divergent paths or that, in the evolutionary process, subtle changes were incorporated in the primary coordination sphere of the TNC and also in the nearby protein environment by reorganizing the residues and the overall arrangement of the cupredoxin domains to provide a more efficient oxidase activity in laccases as compared to SLAC and hCp. In this connection, it must be noted that SLAC is secreted outside the cell and is supposed to perform its function there at relatively higher levels of oxygen (~5–8–fold) than inside the cell.[41] Thus, the 7–fold difference observed between the k_{cat}/K_M (and K_M) of O_2 between three–domain laccases and SLAC might reflect an evolutionary adaptation to the O_2 rich environment SLAC operates in. The lower k_{cat}/K_M of SLAC might be brought about by a reduced accessibility of the TNC connected with the access channel to the TNC in the trimeric form of SLAC.[42] Moreover, *S. coelicolor* is a soil and aqueous dwelling aerobe. It is conceivable that the concentration of reducing co–substrate is substantially less than that of oxygen. This may result in a slow loading of the enzyme with reducing equivalents, entailing the risk of producing long–lived forms of a three–electron loaded (PI + $1e^-$) intermediate which could lead to the generation of reactive oxygen species and consequent damage to the enzyme or the organism. In this case Y108 would be able to provide the fourth electron, thereby reducing the lifetime of a

deleterious three–electron reduced oxygen intermediate. This way, Y108 would act as a kinetic buffer of redox equivalents, thus preventing the generation of reactive oxygen species that might harm the enzyme and possibly also the bacterium. The danger posed at the same time by the presence of a reactive tyrosyl radical might be mitigated by the surrounding protein shell.

While the physiological significance of SLAC in the morphological development or metabolic system of *S. coelicolor* is not clear, along with the question of its natural substrates, it is evident that residue Y108 does form an integral part of the active site and is involved in the oxidase activity of this enzyme. If the natural substrate of SLAC has much higher turnover number for the *wt* SLAC, as known for the ferroxidase in yeast (Fet3p) and hCp,[43] the effect of mutation may be much more pronounced across the mutants. While we have noticed that SLAC catalyzes oxidative coupling of *o*–phenylenediamines and *o*–aminophenols to phenazines and phenoxazines, respectively, which are speculated to be extracellular secondary metabolites for signaling or self–defense of *Pseudomonas aeruginosa* and *S. antibioticus*,[44,45] their turnover numbers are too low to identify them as the natural substrates. The ability of SLAC to catalyze such reactions, along with a recombinant expression system, indeed holds new promises for the use of SLAC in industry for large–scale production of antibiotics for further studies or for human welfare. We are currently investigating other possible substrates and also attempting to identify the substrate binding pocket using crystallography, which may shed more light on the enzyme function and its similarities and dissimilarities relative to the other members of the family of MCOs.

2.3 Supplementary Information

Site–directed mutagenesis: Site–directed mutagenesis was carried out using the Quick Change site–directed mutagenesis kit (Stratagene). The primers used for respective mutations are given below where mutations are in bold and underlined.

Y108F

Forward primer: 5'–G CAC GGC CTG GAC **TTC** GAG ATC TCC AGC G–3'

Reverse primer: 5'–C GCT GGA GAT CTC **GAA** GTC CAG GCC GTG C–3'

Y108A

Forward primer: 5'–G CAC GGC CTG GAC **GCC** GAG ATC TCC AGC G–3'

Reverse primer: 5'–C GCT GGA GAT CTC **GGC** GTC CAG GCC GTG C–3'

Same set of primers were used to make mutations in the wt–SLAC or T1D–SLAC where the C288S mutant was used as a template. Desired mutations were confirmed by DNA sequencing (BaseClear).

The purification of the wt–SLAC and the mutants was carried out as reported previously.[10] The proteins were aliquoted and stored at –80 ^{0}C till further use. The absorption spectra of the *wt*–SLAC, Y108A and Y108F mutants are shown in Figure S1.

Crystallization and data collection: Crystallization experiments with SLAC were setup around conditions previously published.[16] SLAC crystals grew after 3 days in 35–45 % polyethylene glycol–550–monomethyl ether, 0.15–0.5 M NaCl and 0.1 M TRIS pH 8.5. Crystals were transferred to cryo–protectant containing 80 % mother liquor and 20 % glycerol, and frozen in liquid nitrogen. Single–crystal diffraction data were collected at the ESRF on beamline ID 14–4 (Grenoble) using an ADSC Q315 x–ray detector at a temperature of 100 K.

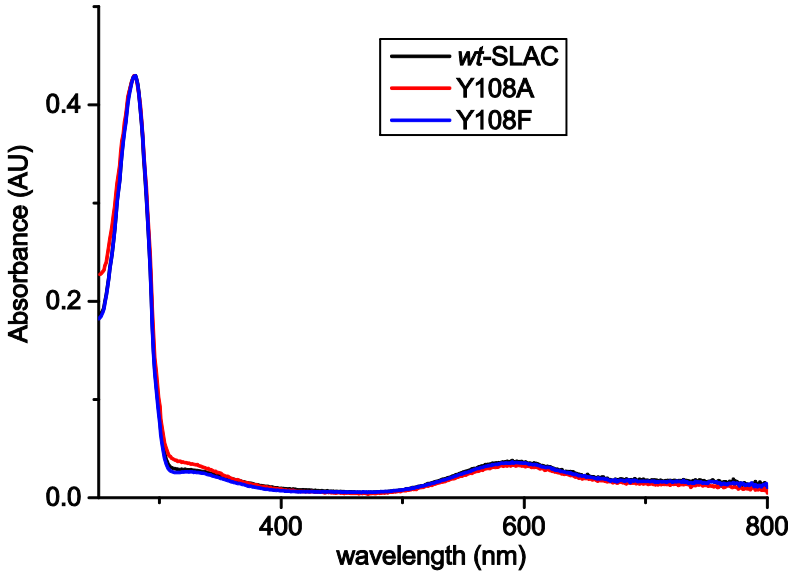

Figure S1: Absorption spectrum of the *wt*–SLAC overlaid with that of Y108A and Y108F. The spectra have been normalized at the 280nm absorption.

Diffraction data were indexed and integrated using Mosflm and imported into the CCP4 software package. SCALA was used for scaling the data. Crystals of SLAC variants belonged to the P43212 spacegroup and the cell dimensions are mentioned in table S1. Molrep was run for molecular replacement using 3CG8 as a homologous structure. Refmac was used to refine the structure. Terminal residues and mutations were built using Coot. The final structure parameters are summarized in Table S2.

Table S1. Data collection and processing statistics parameters for the SLAC variants studied (values in parenthesis correspond from highest resolution shell).

	Slac Y108F	Slac Y108A
Space Group	$P4_32_12$	$P4_32_12$
Unit Cell Parameters Å	$a = b = 176.66$ $c = 176.85$	$a = b = 178.44$ $c = 177.77$
Resolution Range Å	53.27 – 2.73 (2.88 – 2.73)	79.80 – 2.67 (2.81 – 2.67)
No of observations	370849 (46537)	1047174 (131331)
No of unique reflections	59361 (8756)	82018 (11803)
Data Completeness	80.5 (82.3)	100.0 (100.0)
Redundancy	6.2 (5.3)	12.8 (11.1)

Mosaicity (°)	0.45	0.65
Mean I/σ (I)	12.9 (3.5)	5.7 (0.9)
R_{pim}	0.043 (0.202)	0.099 (0.768)

Table S2. Structure parameters of SLAC variants.

	SLAC Y108F	SLAC Y108A
R_{work}	0.18204	0.21452
R_{free}	0.19858	0.22710
R_{all}	0.18238	0.21515
Mean *B*-factor (Å^2)	36.507	49.31
RMSD bond length from ideal (Å)	0.010	0.020
RMSD bond angles from ideal (°)	1.590	1.925
No of non hydrogen atoms	6888	6694
No of monomers in asymmetric units	3	3
No of water molecules	280	232
Other localized molecules	12 x Cu, 3 O , 8 PEGs	12 x Cu, 3 O , 8 PEGs
Solvent content (%)	84	84
Matthews Coefficient (Å^{3}DA^{-1})	7.52	7.78

EPR spectroscopy: Samples for EPR measurements were prepared as reported earlier.[24] Typically the enzyme concentration was ~1mM in 100mM phosphate buffer (pH 6.8). Spectra were recorded for the enzyme in the resting form. Alternatively, the enzyme was titrated with sodium dithionite to afford complete reduction of the copper centers and then reoxidized and immediately frozen in liquid N_2. The cw–EPR measurements were performed at X– band on a Bruker Elexsys E680 spectrometer at a temperature of 40K. All the spectra were acquired with a microwave power of 2 mW, a field modulation of 100 kHz, and a modulation amplitude of 0.5 mT. Spin quantification was performed against azurin or $CuSO_4$ as standard which reveals the content of paramagnetic Cu(II) in the resting form of the variants studied. The EPR spectrum of the resting form of *wt*–SLAC overlaid with those of Y108A and Y108F is shown in Figure S2.

Steady–state kinetics: Steady state kinetics measurements were performed in sodium phosphate buffer (200mM) at pH 6. The buffer concentration had no effect on the enzyme kinetics. A high buffer concentration was used owing to the

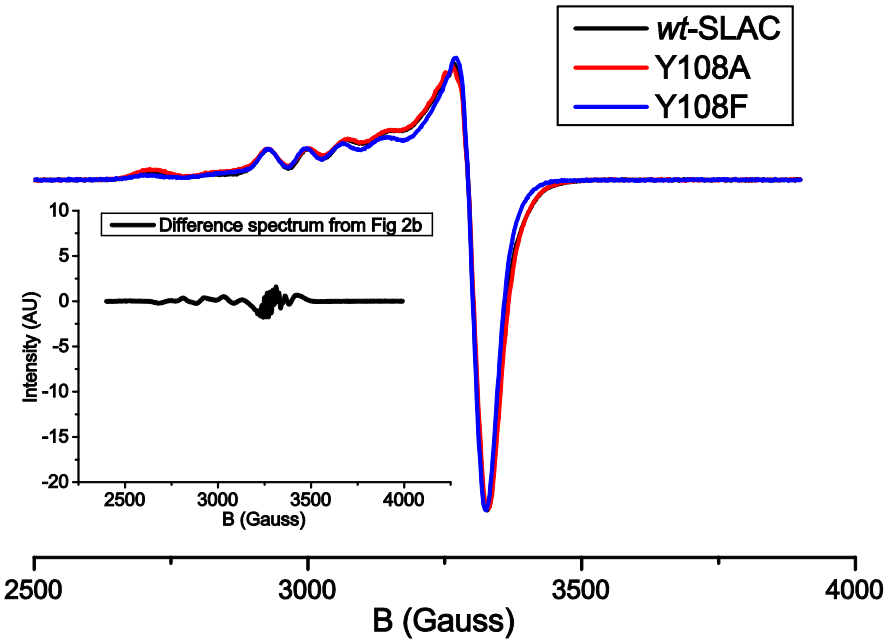

Figure S2: Normalized EPR spectra of the resting forms of *wt*–SLAC (black), Y108A (red) and Y108F (blue) overlayed on each other. The corresponding double integration reveals 2.0 ± 0.2 equivalents of Cu(II) per mol of monomer for *wt*–SLAC and Y108A and 1.7 ± 0.2 equivalents for Y108F mutant. The type–3 copper atoms are anti–ferromagnetically coupled and invisible, therefore, in the EPR spectrum. The inset shows the difference between the spectra reproduced in Figure 2b after normalization, which corresponds to less that 5% of total spin (~1.1 ± 0.2 equivalents of Cu(II) since T1 site is vacant).

higher concentration of the hydrochloride salts of the substrates used for the assays. The temperature was kept constant at 22 ^{0}C using a circulating water bath (Neslab). The measurements were made in two different ways: (1) by monitoring the absorption spectrum of the oxidized substrate with a UV–vis spectrometer (Varian) and (2) by monitoring O_2 consumption using a Clark–type O_2 electrode (Hansatech). Several organic and inorganic substrates were tested for activity and TMPD (N,N,N',N' tetramethyl–*p*–phenylenediamine) was chosen for measurements because of its high turnover and linear response with time. For solubility reasons, the dihydrochloride salt of this substrate was used.

TMPD oxidation was monitored at 610 nM (ϵ_{610} = 12,200 $M^{-1}cm^{-1}$). The stock solution of substrate was prepared fresh by dissolving the required amount in distilled water (MilliPore) up to a concentration of 250mM. The stock was diluted in desired buffer immediately prior to the measurement and the reaction was initiated by enzyme injection. Absorbance increase at 610 nM or O_2 consumption was monitored against time and the method of initial rates was used to analyze the data. In a typical measurement, the initial concentration of one of the substrates (O_2 or TMPD) was kept fixed while that of the other was varied to obtain data points at low rates and up to saturation (where possible). For O_2, the concentration is limited by its solubility (~1.3mM at O_2 saturation at room temperature) and so the data for higher concentrations could not be obtained. The rates for background oxidation of substrates or O_2 electrode drifts were subtracted before analyzing the data. The rates were fitted to a Michaelis–Menten type equation to obtain the kinetic parameters. As an example the plots are shown in Figure S3.

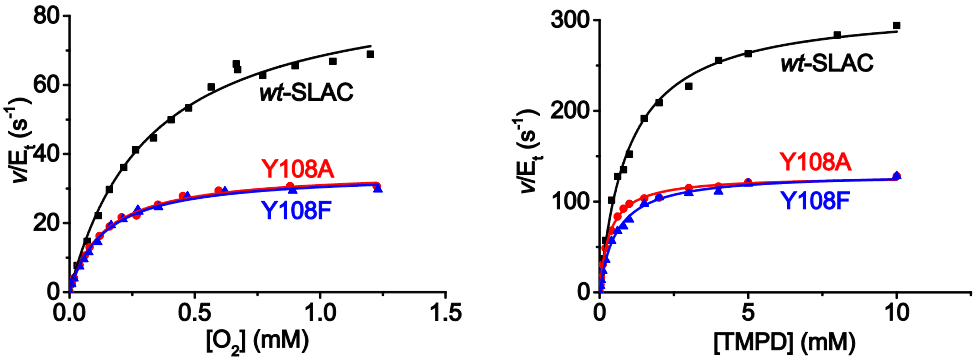

Figure S3: (a) Rate of O_2 consumption plotted against the respective O_2 concentration while keeping the initial TMPD concentration fixed at 10mM for each measurement. (b) Rate of TMPD oxidation plotted against the respective TMPD concentration while keeping the O_2 concentration fixed at maximum O_2 solubility (~ 1.3mM). Typical enzyme concentrations used in the assays were around 15–50 nM. Measurements were made at 295K in 200mM phosphate buffer (pH 6). The data were fitted to Michelis–Menten equation shown in bold lines. *wt*–SLAC shown in black, Y108A mutant in red and Y108F mutant in blue.

Transient kinetics: Transient kinetics was monitored using a stopped flow instrument (SX.18MV– Applied Photophysics). The instrument was used in a single mixing mode. It was made rigorously anaerobic by purging argon through all tubing and, where necessary, the argon flow was maintained throughout the measurement. One of the syringes was filled with buffer of known O_2 concentration while the other was filled with anaerobic buffer containing reduced enzyme. The enzyme concentration was typically 100 µM. Extinction coefficient of the ~340 nm band of the PI (Figure 2a) was estimated to be ~3000 $M^{-1}cm^{-1}$. The instrument dead time is ~2.5ms and 400 data points were recorded for each experiment. The spectra were recorded using a photo–diode array detector (300–1200nM). Data analysis was performed by global fitting of time traces using the software Pro–K. Reoxidation of completely reduced *wt*–SLAC or T1D SLAC was found to be irreversible under single turnover conditions as the y–axis intercept in Figure S4 is virtually zero ($k_{off} \approx 0$, see caption to Figure S4). Second order rate constants (k_{on}) similar to those presented in Table I were obtained.

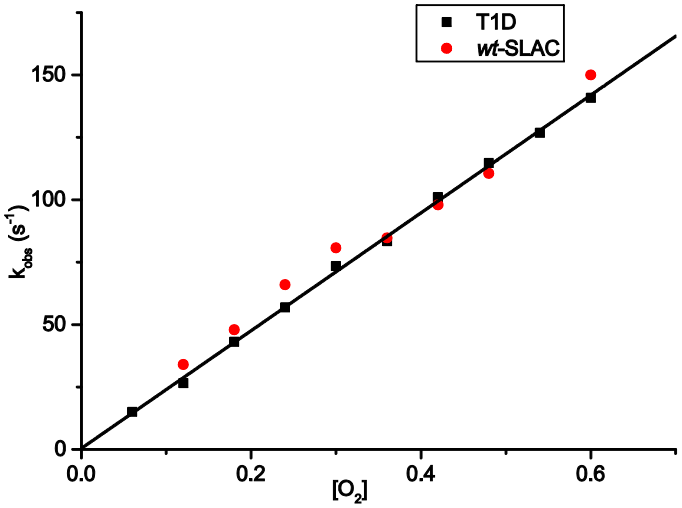

Figure S4: Rate of reoxidation of completely reduced *wt*–SLAC (red circles) or T1D (black squares) plotted against the respective O_2 concentration. The measurements were made following the fluorescence of tryptophan at 338 nm (excitation at 280nm) using the FRET principle as reported earlier.[42] The linear fit ($k_{obs} = k_{on}[O_2] + k_{off}$) yields a second order rate constant (k_{on}) of 2.3×10^5 $M^{-1}s^{-1}$ and a dissociation rate constant (k_{off}) of $<1s^{-1}$.

Relationship to Ceruloplasmin: Figure S5 represents the structural alignment of SLAC (3CG8) with human ceruloplasmin (2J5W). Cp is rendered in yellow, while the three domains of SLAC are represented in red, blue and green. The leftmost panel is a view perpendicular to the threefold symmetry axis of SLAC, the middle panel represents a view along this axis. The rightmost picture shows a close–up of the T1 site (dark blue for hCp ***and*** SLAC) and the TNC (light blue for hCp ***and*** SLAC). The hCp structure is shown again in yellow, while for SLAC the blue domain has been depicted. Moreover Tyr108 (SLAC) has been depicted in green and Tyr107 (hCp) in yellow. For completeness a conserved Trp has been depicted as well for SLAC (W284, blue) and hCp (W1019, yellow). The possible relevance of this residue for the function of the enzyme is under investigation. The alignment was performed using the Protein structure comparison service Fold at the European Bioinformatics Institute (http://www.ebi.ac.uk/msd–srv/ssm). The structural alignment of the quaternary structures of both proteins shows conserved domains and secondary structures including the highly conserved residues around the active site. It should be noted that hCp is a monomer and the TNC is located between the N and C terminus of the protein. SLAC is a trimer and the TNC are located at the N and C terminus of adjacent subunits.

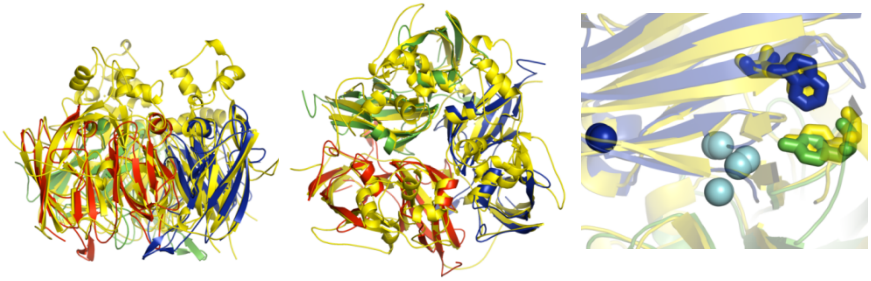

Figure S5: Overlay of human Ceruloplasmin (yellow) with SLAC (three chains shown in red, green and blue). Left: view perpendicular to the threefold symmetry axis of SLAC; middle: view along the same axis; right: close–up of the T1 site (dark blue for hCp ***and*** SLAC) and the TNC (light blue for hCp ***and*** SLAC) with hCp shown in yellow and the SLAC domain in blue. Tyr108 (SLAC) has been depicted in green and Tyr107 (hCp) in yellow. A conserved Trp (W284 (SLAC), blue; W1019 (hCp), yellow) has been depicted also.

Multiple sequence alignment of SLAC with all known 2–domain type–B MCOs: Sequence alignment of SLAC with the homologous type–B Multicopper proteins (following Nakamura's terminology[15]) is shown in Chart S1. The accession numbers are shown in the beginning and all of them are derived from various members of *Streptomycetes* genus. SLAC (gi 21225006) is highlighted on top. The residues coordinating to the Cu centers are highlighted in grey. The conserved tyrosines (corresponding to Y108 in SLAC) have been underlined. A conserved tryptophan which is shown in Figure S3 is also underlined. The sequence alignments were obtained using the NCBI BLAST tool (http://blast.ncbi.nlm.nih.gov/Blast.cgi).

Chart S1: Multiple sequence alignment of SLAC with other putative Multicopper proteins. Some of these have been recombinantly expressed and purified like EpoA (gi 15425710) from *Streptomyces griseus*. (see text above for further details)

```
21225006    ----------------M-----------------DR----RGFNRRVLLGGAAAA------ 18
294816028   -------------MASPGFRAPRQSARQRGEFTMDR----RSFGRRVLAGSAVAAG-GAA 42
291435857   ----------------M-----------------DR----RGFNRRVLLGGAAVA------ 18
254393501   --------------------------------MDR----RSFGRRVLAGSAVAAG-GAA 22
111559381   ----------------M-----------------DR----RGFNRRVLLGGAAVA------ 18
302557153   ----------------M-----------------DR----RGFNRRVLLGGAAVA------ 18
302555481   ----------------M-----------------DR----RSFNRRVLLGGAAVA------ 18
297203782   -------------MGAL-----------------DR----RGFNRRVLLGGAAVA------ 21
290955899   -------------MDAM-----------------DR----RGFNRRVLLGGAAAA------ 21
239992058   ------------------------------------------MLVGGAAVAATG-- 12
318060531   -------------MAST-----------------DEGSGGRRIGRRYLLGGAAAA------ 25
302522913   -------------MAST-----------------DEGSGGRRIGRRYLLGGAAAA------ 25
326775330   ----------------M-----------------DR----RTFSRRMLVGGAAAAATG-- 21
182434812   ----------------M-----------------DR----RTFSRRMLVGGAAAAATG-- 21
15425710    ----------------M-----------------DR----RTFSRRMLVGGAAAAATG-- 21
291455313   ------------------------------------------MAGGAVLATGG-- 11
302540243   -------------MP--------------------R----RGFSRRLLAGGAAAAAIGG- 22
295835579   ------------------------------------------------------------
320007304   ----------------M-----------------DR----RTFNRRMLVGGGVAAATG-- 21
297190627   -------------MPTT------------GEFDMDR----RSFNRRLLAGGAAAAATGVT 31
345011266   -------------MSDA------------PGIT-SR----RGLSRRLFTGGAAAAAVG-- 28
345003352   ----------------M-----------------DR----RTFNRRMLVGGGVAAATG-- 21
334337260   -------------MSGQ-------------RVAGDAA--KGGVSRRSVLTGTLAGLVAPA 32
354612709   -------------MTER-------------NASDDPP--GRGLSRRSMLVGTAAGVVTPV 32
354577634   -------------MTGE-------------QARL-PQ--SQKVSRRSMLVGAAAGVVAPV 31
257056126   -------------MIRK-------------YARTGAF--GKKVSRRSMLVGAAAGMAAPV 32
257056125   ------------------------------------------MLAGAAAGMATPV 13

21225006    --T--------------------SLSIA--------------PEVAGAAPAAKG------ 36
294816028   ----------------------LSLSPAAAAQAGGGALAGG--AALAANPP-------- 69
291435857   --T----------------------SLSLA--------------PEAVSATGPAK------ 35
254393501   ----------------------LSLSPAAAAQAGGGALAGG--AALAANPP-------- 49
111559381   --T----------------------SLSIA--------------PETAGAAGDAKG----- 36
302557153   --T----------------------SLSIA--------------PEAVSAARPAK------ 35
302555481   --T----------------------SLSVA--------------PEAISADGPAK------ 35
297203782   --T----------------------SLSLA--------------PEARSDAGPAQ------ 38
290955899   --T--------------------SLSVALETVAA--------PEAVSAAARAR------ 44
239992058   -VT--------------------SLSLGAVE-------------ASSAE---------- 27
```

```
318060531    --A--------------------GLGVVGAS----AT-----SGTAQAAVTAL------ 47
302522913    --A--------------------GLGVVGAS----AT-----SGTAQAAVTAP------ 47
326775330    -VT--------------------SLSLGAVE-------------ASSAE---------- 36
182434812    -VT--------------------SLSLGAVE-------------ASSAE---------- 36
15425710     -VT--------------------SLSLGAVE-------------ASSAE---------- 36
291455313    -LT----------------------SMS-------------------QSSAAAD-------- 23
302540243    ----------------------PLPLASPAASAASAA-------SATSATSASSASSAEG 53
295835579    --------------------------MVGAS----AT-----GGTAAAAVTAP------ 18
320007304    -VT--------------------SMSLGAVQ-------------ATSAE---------- 36
297190627    ----------------------SLSITSASNAA----------PAPAKGAP-------- 50
345011266    ----------------------PLALTSSAAAKAP----------KAPSGA---------- 47
345003352    -VT--------------------SMSLGAVQ-------------AAPAQAAVA------ 40
334337260    ----------------------AMSTMTAS-------------AAPGAPG-------- 47
354612709    ----------------------AVSSLGAA-------------AATADPGNGR----- 50
354577634    ----------------------AVSTLGAG-------------SAAAQ---GR----- 46
257056126    ----------------------VASTVGGT-------------TATAAPN-------- 47
257056125    ----------------------ITSAIGGT-------------PALAAPL-------- 28

21225006     ---------ITARTAPA--GGEVR--HLKMYAEKLADGQMGYGFEKGKASVPGPLIEVNE 83
294816028    -----R-------TAP--AGGRVR--HMRLCAERLPDGRMGYGPEKGKATVPGPPIELTE 113
291435857    -------------TAPA--GGEVK--RIKLYAERLGGGQMGYGLEKGKATIPGPLIELNE 78
254393501    -----R-------TAP--AGGRVR--HMRLCAERLPDGRMGYGPEKGKATVPGPPIELTE 93
111559381    ---------VTARTAPA--GGEVR--HIKMYAEKLPDGQMGYGLEKGKASVPGPLIELNE 83
302557153    -------------TAPA--GGEVR--RVKMYAERLDGGRMGYGFEKGKASVPGPLIELNE 78
302555481    -------------TAP--AGGEVK--RIKLYAEKLPDGQMGYGLEKGKASIPGPLIELNE 78
297203782    -------------AAP---GGEVR--RIKLYAERLADGQMGYGLEKGRATIPGPLIELNE 80
290955899    -------------TAP--AGGEVK--HVKLYAEKLADGQMGYGLEKGKASIPGPLIELNE 87
239992058    ---------KPPRTAPA--GGVTR--RLKMYAEKLPNGELGYGFEKGKASIPGPLIELNE 74
318060531    -------------TAPA--GGEVR--RITMYAERLANGQMGYGLEKGKASIPGPLIELNE 90
302522913    -------------TAPA--GGEVR--RITMYAERLANGQMGYGLEKGKASIPGPLIELNE 90
326775330    ---------NPPRTAPA--GGVVR--RLRMYAEKLPNGELGYGFEKGKASIPGPLIELNE 83
182434812    ---------NPPRTAPA--GGVVR--RLKMYAEKLPNGELGYGFEKGKASIPGPLIELNE 83
15425710     ---------NPPRTAPA--GGVVR--RLKMYAEKLPNGELGYGFEKGKASIPGPLIELNE 83
291455313    ---------TPPKTAPA--GGEVK--HLTMYCEKMADGMTGYGLEKGKPSIPGPLIELNE 70
302540243    AKRRVA-------TAA--AGGAVR--RIKMYAEKLPDGQMGYGLEKGKASIPGPLIELTE 102
295835579    -------------TAPA--GGEVR--RITMYAERLTNGQMGYGLEKGKASIPGPLIELNE 61
320007304    ---------NPAKTAPA--GGAVR--HLKLYAEKLADGQLGYGFEKGKASVPGPLIEITE 83
297190627    -----R-------TAQ--AGGQVR--HLKMYAEKRADGSMGYGLEKGKATVPGPLIELVE 94
345011266    ----VR-------TAT--AGGAVR--HLKLYAEKLPDGQMGYGLEKGKATIPGPLIELTE 92
345003352    ---------DPPKTAPA--GGVVR--HLTMYAEKLPDGSLGYGLEKGKASVPGPLIEINE 87
334337260    -----------APG----ASGRTR--RITMYAESLPGGQYGYGLAPGEATIPGPVLEMWE 90
354612709    -----------APGNAGRGDGRLR--RITMYAEKLPDGMIGYGLEPGGATVPGPVLEIWE 97
354577634    -----------GKGRPG-RTGETH--RVTVYAEELPGGLYGYGLEPGKATVPGPVFEIWE 92
257056126    -------------RAGDSQGEIR--RITMYAEELPGGMIGYGLEPGKATVPGPVLEMWE 91
257056125    -------------EANGFRGRPRPRRITLFAEELPGDMVGYGLAPGEATVPGPVLEMWE 74

21225006     GDTLHIEFTNTMDVRASLHVHGLDYEISSDGTAMNKSDVEPGGTRTYTWRTHKPGRRDDG 143
294816028    GDTLHIAFENTMDVPVSLHVHGVDYDIANDGTRLTRSHVEPGETRTYTWRTHLPARRPDG 173
291435857    GDTLHIEFENTMDVPVSLHVHGLDYEISSDGTKQSRSDVEPGGTRTYTWRTHVPGRRADG 138
254393501    GDTLHIAFENTMDVPVSLHVHGVDYDIANDGTRLTRSHVEPGETRTYTWRTHLPARRPDG 153
111559381    GDTLHIEFTNTMDVRASLHVHGLDYEISSDGTAMNKSDVEPGGTRTYTWRTHKPGRRADG 143
302557153    GDTLHIELENTMDVPASLHVHGLDYEISSDGTKQNNSHVEPGATRTYTWRTHKPGRRSDG 138
302555481    GDTLHVEFENTMDVAVSLHVHGLDYEITSDGTKLNRSHVEPGGTRTYTWRTHAPGRRKDG 138
297203782    GDTLHIEFENTMDVRASLHVHGLDYEVSSDGTTLNKSDVEPGGTRTYTWRTHAPGRRSDG 140
290955899    GDTLHIEFENTMDVTASLHVHGLDYETSSDGTKLNRSEVEPGGTRTYTWRTHAPGTRPDG 147
239992058    GDSVHIEFENLTDVDVSLHVHGVDYDIANDGTRMNKSHVEPGGTRTYTWRTHAPGRRKDG 134
318060531    GDTLHIDFENTMDVDASLHVHGLDYEITSDGTRMSGSHVPPGGHRTYTWRTHKPGKRADG 150
302522913    GDTLHIDFENAMDVDASLHVHGLDYEITSDGTRMSGSHVPPGGHRTYTWRTHKPGKRADG 150
326775330    GDTVHIEFENLTDVDASLHVHGVDYDIANDGTRMNKSHVEPGGTRTYTWRTHAPGRRKDG 143
182434812    GDTVHIEFENLTDVDASLHVHGVDYDIANDGTRMNKSHVEPGGTRTYTWRTHAPGRRKDG 143
15425710     GDTVHIEFKNLTDVDASLHVHGVDYDIANDGTRMNKSHVEPGGTRTYTWRTHAPGRRKDG 143
291455313    GDTLHIEFHNLLDVDASLHAHGVDYEISSDGTRQSNSHVEPGGSRTYTWRTHAPGRRKDG 130
302540243    GDTLHIEFENTMDVTASLHVHGLDYDTASDGTQLNRSAVEPGETRTYTWRTHAPGTRADG 162
295835579    GDTLHIDFENTMDVDASLHVHGLDYEISSDGTRMSGSHVPPGGHRTYTWRTHKPGKRADG 121
```

```
320007304    GDTLHIEFENTTDVDASLHVHGVDYDIASDGTRMNRSHVEPGGTRTYTWRTHAPGRRKDG 143
297190627    GDTLHIEFENLMDVPVSLHPHGVDYDISNDGTKMSRSHVEPGATRTYTWRTHAPGRRADG 154
345011266    GDTLHIEFENTMDVTASLHVHGLDYDVASDGTQLNRSAVEPGGTRTYTWRTHAPGKRADG 152
345003352    GDTLHIEFHNLTDADASLHVHGVDYDIASDGTRMNRSHVEPGGTRTYTWRTHAPGRRKDG 147
334337260    GETLEIELVNTTDRRLSIHPHGVNYTVDSDGSPLNASYNEPGETRTYVWSTQTQYQAGSG 150
354612709    GDTLEIELVNTTDKRLSIHPHGVDYSVDSDGAPLNGSFNEPGETRTYVWRTRAPSKGPGK 157
354577634    GDTLEIELVNNTDRRLSIHPHGVNYDVASDGSPLNDSFNEPGETRTYVWSTSFQSEGPGG 152
257056126    GDTLEIELVNNTDHRLSIHPHGVEYDTESDGSPLNDSFNNPGERRTYIWRSRAPYQAKDG 151
257056125    GETLEIQLVNNTDHRLSIHPHGVEYDTESDGSPLNDSFNAPGECRTYVWRSRTPYRAEDG 134

21225006     TWRPGSAGYWHYHDHVVGTEHGTGGIRNGLYGPVIVRRKGDVLPDATHTIVFNDMTINNR 203
294816028    TWRPGSAGYWHYHDHVVGTDHGTQGIRNGLYGPVVVRRAGDILPDRQFTIVFNDMTINNL 233
291435857    TWRAGSAGYWHYHDHVVGTEHGTGGIRNGLYGPVIVRRKGDVLPDRTHTIVFNDMTINNR 198
254393501    TWRPGSAGYWHYHDHVVGTDHGTQGIRNGLYGPVVVRRAGDILPDRQFTIVFNDMTINNL 213
111559381    TWRAGSAGYWHYHDHVVGTEHGTGGIRKGLYGPVIVRRKGDVLPDATHTIVFNDMLINNR 203
302557153    TWRAGSAGYWHYHDHVVGTVHGTGGIRNGLYGPVVVRRKDDVLPDATHTIVFNDMSINNR 198
302555481    TWRAGSAGYWHYHDHVVGTEHGTQGLQKGLYGPVIVRRKGDVLPDRTHTVVFNDMRINNR 198
297203782    TWRAGSAGYWHYHDHVVGTEHGTGGIRKGLYGPVIVRRKGDVLPDATHTIVFNDMLINNR 200
290955899    TWRPGSAGYWHYHDHAVGTAHGTGGIRKGLYGPVVVRRKGDVLPDKTVTIVFNDLRINNK 207
239992058    TWEPGSAGYWHYHDHVVGTDHGTGGIRKGLYGPVVVRRKGDILPDQTCTVVFNDMMINNK 194
318060531    TYRPGSAGYWHYHDHVVGTDHGTGGIRNGLYGGVVVRRKGDLLPDRTYTIVFNDMTINNL 210
302522913    TYRPGSAGYWHYHDHVVGTDHGTGGIRNGLYGGVVVRRKGDLLPDRTYTIVFNDMTINNL 210
326775330    TYEPGSAGYWHYHDHVVGTDHGTGGIRKGLYGPVVVRRKGDILPDQTCTVVFNDMMINNK 203
182434812    TYEPGSAGYWHYHDHVVGTDHGTGGIRKGLYGPVVVRRKGDILPDQTCTVVFNDMMINNK 203
15425710     TYEPGSAGYWHYHDHVVGTDHGTGGIRKGLYGPVVVRRKGDILPDQTCTVVFNDMMINNK 203
291455313    TWRPGSAGYWNYHDHVVGTDHGTGGLRQGLYGGLIVRRKGDILPDKTFQIVFNDMTVNNK 190
302540243    TWRPGSAGYWHYHDHAVGTPHGTGGLRKGLYGPVVVRRAGDVLPQKQFTIVFNDMTINNK 222
295835579    TYRPGSAGYWHYHDHVVGTDHGTGGIRNGLYGGVVVRRKGDPLPDRTYTIVFNDMTINNL 181
320007304    TWQAGSAGYWHYHDHVVGTDHGTGGIRKGLYGPLVVRRKGDVLPDKTITIVFNDMTINNK 203
297190627    TWRPGSAGYWHYHDHVVGTDHGTGGIRKGLYGPMVVRRKDDILPDKQFTIVFNDMTINNR 214
345011266    TWRPGSAGYWHYHDHAVGTPHGTGGLRKGLYGPVVVRRAGDILPDKQFTIVFNDMTINNK 212
345003352    TWQAGSAGYWHYHDHVVGTDHGTGGIRKGLYGPLVVRRKGDILPDRTITIVFNDMNINNK 207
334337260    LWMPGSAGYWHYHDHAMGTDHGTEGVRKGLYGALVVRRKGDVLPDRQFTVVFNDMTINNQ 210
354612709    LWMPGSAGYWHYHDHAMGTPHGTEGLRKGLYGALVVRRKGDVLPDRQFTVVFNDMTINNR 217
354577634    FWIPGSAGYWHYHDHALGSDHGTEGIAKGLYGALVVRREGDVVPDRQFTVVFNDMTINNK 212
257056126    TWRPGSAGYWHYHDHAMGTDHGTGGVLRGLYGALVVRRPGDILPDRQYTIVFNGMTINNR 211
257056125    AWMPGSAGYWHYHDHAMGTDHGTEGLTRGLYGALVVRRRGDILPDRQYTIVFNGTTINNR 194

21225006     KPHTGPDFEATVGDRVEIVMITHGEYYHTFHVVHGHRWADNRTGILTGPDDPSRVIDNKIT 263
294816028    PGHSGPDFRATVGDRVEIISITHGEYYHTFHLHGHRWADNRTGLLEGPGDVSRIIDNKIC 293
291435857    PAHTGPDFEATVGDRVEFVMITHGEYYHTFHLHGHRWADNRTGMLTGPDDPSQVIDNKIC 258
254393501    PGHSGPDFRATVGDRVEIISITHGEYYHTFHLHGHRWADNRTGLLEGPGDVSRIIDNKIC 273
111559381    APHTGPNFEATVGDRVEIVMITHGEYYHTFHMHGHRWADNRTGMLTGPDDPSQVIDNKIT 263
302557153    PAHTGPDFEATVGDRVEIVMITHGEYYHTFHMHGHRWADNRTGMLTGPDDPSQVIDNKIC 258
302555481    PPHSGPDFEATVGDRVEFVVITHGEFYHTFHMHGHRWADNRTGMLTGPDDPSQVIDNKIT 258
297203782    PAHSGPNFEATVGDRVEFVMITHGEYYHTFHMHGHRWADNRTGMLTGPDDPSQVVDNKIV 260
290955899    PAHTGPDFDATVGDRVEFVVITHGEYYHTFHMHGHRWADNRTGTLTGPDDPSQVIDNKIV 267
239992058    TAHNSVNFEATVGDRLEFVMITHGEYYHTFHIHGHRWADNRTGLLTGPDDPSRVIDNKIC 254
318060531    K--QGPDFEAVVGERVEIVMITHGEYYHTFHMHGHRWADNRTGLLTGPDDPSAVIDNKIV 268
302522913    K--QGPDFEAVVGERVEIVMITHGEYYHTFHMHGHRWADNRTGLLTGPDDPSAVIDNKIV 268
326775330    TAHNSVNFEATVGDRLEFVMITHGEYYHTFHIHGHRWADNRTGILTGPDDPSRVIDNKIC 263
182434812    TAHNSVNFEATVGDRLEFVMITHGEFYHTFHIHGHRWADNRTGILTGPDDPSRVIDNKIC 263
15425710     TAHNSVNFEATVGDRLEFVMITHGEFYHTFHIHGHRWADNRTGILTGPDDPSRVIGQQDL 263
291455313    PGHESPNFEATVGDRIEVLSITHGEFYHTFHMHGHRWADNRTGLLTGPDDPSPVIDNKIT 250
302540243    SGHDAPEFRATVGERVEIIMITHGEYYHTFHMHGHRWADNRTGILEGPDDPSRVIDNKIT 282
295835579    K--QGPDFEAVVGERVEIVMITHGEYYHTFHMHGHRWADNRTGLLTGPEDPSAVIDNKIV 239
320007304    AAHESPNFEVTVGDRVEVVMITHGEYYHTFHIHGHRWADNRTGLLTGPDDPSRVVDTKIC 263
297190627    PAADPPNFLATVGDRVEIIMITHGEYYHTFHMHGHRWADNRTGLLSGPEDVSRVIDNKIT 274
345011266    AGHEAPEFRATVGDRVEIIMITHGEYYHTFHMHGHRWADNRTGLLEGPDDVSRVIDNKIT 272
345003352    PADASPNFEATVGDRVEVVMITHGEYYHTFHIHGHRWADNRTGLLTGPDDPSRVVDTKIC 267
334337260    MAPNAPVLEANLGERVEFIAIGHGDMFHTFHLHAHRWADNRTGMLEGPNDSSQIIDNRDL 270
354612709    VAPDVPVLEANLGERVEFIAIGHGNNFHTFHLHAHRWADNRTGYLEGPNDPSRVIDNRDL 277
354577634    MAPDVPILEANLGERVEFIAIGHGNNFHTFHLHAHRWADNRTGYLQGPDDPSKVVDNRDL 272
257056126    VAPDAPIFEARLGERVEFIAIGHGDHFHTFHLHAHRWADNRTGLLSGPDDPTPIIDNKDL 271
257056125    VAPEAPIFEARLGERVEFIAISHGNSPHTFHLHGHRWADNRTGMLAGPDDPTPTIDNKDL 254
```

```
21225006     GPADSFGFQIIAGEGVGAGAWMYHCHVQSHSDMGMVGLFLVKKPDGTIP-GYEP--HEHG 320
294816028    GPADSFGFQILAGENVGAGAWMYHCHVQSHSDMGMVGLLLVAKPDGTIP-GYDP--HHPP 350
291435857    GPADSFGFQVIAGEGVGAGAWMYHCHVQSHSDMGMVGLFLVKKPDGTIP-GYDP--HRHH 315
254393501    GPADSFGFQILAGENVGAGAWMYHCHVQSHSDMGMVGLLLVAKPDGTIP-GYDP--HHPP 330
111559381    GPADSFGFQIIAGEGVGAGAWMYHCHVQSHSDMGMVGLFLVKKPDGTIP-GYDP--HEH- 319
302557153    GPADSFGFQIIAGEGVGAGAWMYHCHVQSHSDMGMVGLFLVKKPDGTIP-GYDP--HEHA 315
302555481    GPADSFGFQVIAGEGVGAGAWMYHCHVQSHSDMGMVGLFLVKKPDGTIP-GYDP--HE-- 313
297203782    GPADSFGFQVIAGEGVGAGAWMYHCHVQSHSDMGMVGLFLVKKTDGTIP-GYEP--HE-- 315
290955899    GPADSFGFQVIAGEGVGAGAWMYHCHVQSHSDMGMAGLFLVRKTDGTIP-GYEP--HKPH 324
239992058    GPADSFGLQIIAGERVGAGAWMYHCHVQSHSDMGMAGLLLIKKPDGTIP-GYEP--HHHT 311
318060531    GPADSFGFQVLAGEGVGAGAWMYHCHVQSHSDMGMAGMFLVAKEDGTVP-GHEG--HTMK 325
302522913    GPADSFGFQVLAGEGVGAGAWMYHCHVQSHSDMGMAGMFLVAKEDGTVP-GHEG--HTMK 325
326775330    GPADSFGLQIIAGERVGAGAWMYHCHVQSHSDMGMAGLLLIKKADGTIP-GYEP--HH-A 319
182434812    GPADSFGLQIIAGERVGAGAWMYHCHVQSHSDMGMAGLLLIKKADGTIP-GYEP--HH-A 319
15425710     RPRDSYGLQIIAGERVGAGAWMYHCHVQSHSDMGMAGLLLIKKADGTIP-GYEP--HH-A 319
291455313    GPADSFGFQFIAGEGVGAGAWMYHCHVQSHSDMGMAGLFLIAKADGTIP-GYDPDAPHHT 309
302540243    GPADSFGFQVIAGENTGAGAWMYHCHVQSHSDMGMAGLFLVAKPDGTIP-GYDP--HHLT 339
295835579    GPADSFGFQVVAGEGVGAGAWMYHCHVQSHSDMGMAGMFLVAKEDGTVP-GHEG--HGMK 296
320007304    GPADSFGFQIIAGEHVGAGAWMYHCHVQSHSDMGMAGLLLVAKADGTVP-GYDP--PHHA 320
297190627    GPADSFGFQVIAGEHVGPGAWMYHCHVQSHSDMGMAGLFLVAKEDGTIP-GYEP--HHPT 331
345011266    GPADSFGFQVIAGENVGPGAWMYHCHVQSHSDMGMAGLFLVAKADGTIP-GHDP--HQLS 329
345003352    GPADSFGFQIIAGEHVGAGAWMYHCHVQSHSDQGMAGLLLVAKPDGTVP-GYDP--PHHA 324
334337260    NPGESFGFQVIAGAGVGPGAWMYHCHVQFHSDAGMAGVFLVRNEDGSLPDGAQEALDRYR 330
354612709    NPGDSIGFQVLAGDGVGPGAWMYHCHVQFHSDGGMAGVFLVRNADGSMPEGAREALDRYH 337
354577634    NPGDSFGFQVIAGDGVGPGAWMFHCHVQSHSETGMSGIFLVRNADGSMPDGAQEAIDRYL 332
257056126    NPGSSFGFQVIAGEGVGPGAWMYHCHVQFHSDDGMAGIFLVRNEDGSLPPGAEEALERYR 331
257056125    NPGSSFGFQVIAGKGVGPGAWMYHCHMQVHSDDGMTGLFLVRNEDGSLPPGAEEALRRYH 314

21225006     GATAK--------SG-ESGEPTGGAA---------------AHEHEH------------- 343
294816028    GH-----------------------------------------AAR--------------- 355
291435857    HGAAS--------GKPEKAEKPAGSEKPAGS-----EKTEESEEHAH------------- 349
254393501    GH-----------------------------------------AAR--------------- 335
111559381    ---AH--------GG---GEPTADAP---------------AHQH--------------- 335
302557153    HGAAA-----------------------------------KEGQEHAH------------- 328
302555481    ----------------------HGEQ----------PP---AGGHEH------------- 325
297203782    ----------------------HSGQ--------------RAEHHH------------- 325
290955899    TAADP---GTAGTADGTTAGTTDGAG----------PT---GTSHHH------------- 355
239992058    AGATEKKAGEKAGEKTGGKAEKKSAEKTAAK-----DTGADAGEHQH------------- 353
318060531    KSG--------ATGKGTASGK---SA----------AG--EHAGHGG------------- 349
302522913    KSG--------ATGKGTASGK---SA----------AG--EHAGHGG------------- 349
326775330    AGGAEKKAGAKGAGANADKDAKGAA-----------------EHQH------------- 348
182434812    AGGTEKKAGAKGAGANADKAAKGAA-----------------EHQH------------- 348
15425710     AGGTEKKAGAKGAGANADKAAKGAA-----------------EHQH------------- 348
291455313    AP---KKSSKEAAEEKKAAEKKGEAQ--SGK-----SSQAESGDHAHH------------ 347
302540243    AG----------------------------------------RGS--------------- 344
295835579    KSGDSGTGGGAATGKGAAADKGVASG----------AG--AHAGHGG------------- 331
320007304    AG--------------------AA----------------KEHAH------------- 329
297190627    SE----------------------------------------EGHDH------------- 338
345011266    AH----------------------------------------HHG--------------- 334
345003352    AG--------------------AA----------------GEHAH------------- 333
334337260    DHQHGGHANH------------------------------------------------- 340
354612709    GHAGG------------------------------------------------------ 342
354577634    GHQGG----H------------------------------------------------- 338
257056126    NHG--------------------------------------------------------- 334
257056125    AHFS-------------------------------------------------------- 318
```

2.4 References

[1] Solomon, E. I.; Sundaram, U. M.; Machonkin, T. E. *Chem. Rev.* **1996**, *96*, 2563.

[2] Wherland, S.; Farver, O.; Pecht, I. *J. Biol. Inorg. Chem.* **2014**.

[3] Aasa, R.; Brändén, R.; Deinum, J.; Malmström, B. G.; Reinhammar, B.; Vänngård, T. *FEBS Lett.* **1976**, *61*, 115.

[4] Solomon, E. I.; Augustine, A. J.; Yoon, J. *Dalton Trans.* **2008**, 3921.

[5] Andréasson, L. E.; Brändén, R.; Malsmtröm, B. G.; Vänngård, T. *FEBS Lett.* **1973**, *32*, 187.

[6] Augustine, A. J.; Quintanar, L.; Stoj, C. S.; Kosman, D. J.; Solomon, E. I. *J. Am. Chem. Soc.* **2007**, *129*, 13118.

[7] Solomon, E. I.; Ginsbach, J. W.; Heppner, D. E.; Kieber-Emmons, M. T.; Kjaergaard, C. H.; Smeets, P. J.; Tian, L.; Woertink, J. S. *Faraday Discuss.* **2011**, *148*, 11.

[8] Kosman, D. J. *J. Biol. Inorg. Chem.* **2010**, *15*, 15.

[9] Farver, O.; Pecht, I. *Coord. Chem. Rev.* **2011**, *255*, 757.

[10] Machczynski, M. C.; Vijgenboom, E.; Samyn, B.; Canters, G. W. *Protein Sci.* **2004**, *13*, 2388.

[11] Messerschmidt, A.; Ladenstein, R.; Huber, R.; Bolognesi, M.; Avigliano, L.; Petruzzelli, R.; Rossi, A.; Finazzi-Agro, A. *J. Mol. Biol.* **1992**, *224*, 179.

[12] Taylor, A. B.; Stoj, C. S.; Ziegler, L.; Kosman, D. J.; Hart, P. J. *Proc. Natl. Acad. Sci. U. S. A.* **2005**, *102*, 15459.

[13] Roberts, S. A.; Weichsel, A.; Grass, G.; Thakali, K.; Hazzard, J. T.; Tollin, G.; Rensing, C.; Montfort, W. R. *Proc. Natl. Acad. Sci. U. S. A.* **2002**, *99*, 2766.

[14] Hakulinen, N.; Kiiskinen, L. L.; Kruus, K.; Saloheimo, M.; Paananen, A.; Koivula, A.; Rouvinen, J. *Nat. Struct. Biol.* **2002**, *9*, 601.

[15] Nakamura, K.; Go, N. *Cell. Mol. Life Sci.* **2005**, *62*, 2050.

[16] Skalova, T.; Dohnalek, J.; Ostergaard, L. H.; Ostergaard, P. R.; Kolenko, P.; Duskova, J.; Stepankova, A.; Hasek, J. *J. Mol. Biol.* **2009**, *385*, 1165.

[17] Skalova, T.; Duskova, J.; Hasek, J.; Stepankova, A.; Koval, T.; Ostergaard, L. H.; Dohnalek, J. *Acta Crystallogr., Sect. F: Struct. Biol. Cryst. Commun.* **2011**, *67*, 27.

[18] Komori, H.; Miyazaki, K.; Higuchi, Y. *FEBS Lett.* **2009**, *583*, 1189.

[19] Lawton, T. J.; Sayavedra-Soto, L. A.; Arp, D. J.; Rosenzweig, A. C. *J. Biol. Chem.* **2009**, *284*, 10174.

[20] Rodriguez Couto, S.; Toca Herrera, J. L. *Biotechnol. Adv.* **2006**, *24*, 500.

[21] Wheeldon, I. R.; Gallaway, J. W.; Barton, S. C.; Banta, S. *Proc. Natl. Acad. Sci. U. S. A.* **2008**, *105*, 15275.

[22] Bibb, M. J. *Curr. Opin. Microbiol.* **2005**, *8*, 208.

[23] Horinouchi, S. *Biosci. Biotechnol. Biochem.* **2007**, *71*, 283.

[24] Tepper, A. W. J. W.; Milikisyants, S.; Sottini, S.; Vijgenboom, E.; Groenen, E. J. J.; Canters, G. W. *J. Am. Chem. Soc.* **2009**, *131*, 11680.

[25] Stubbe, J. A.; van der Donk, W. A. *Chem. Rev.* **1998**, *98*, 2661.

[26] See Supporting Information.

[27] Northrop, D. B. *J. Chem. Educ.* **1998**, *75*, 1153.

[28] Cole, J. L.; Ballou, D. P.; Solomon, E. I. *J. Am. Chem. Soc.* **1991**, *113*, 8544.

[29] Lee, S. K.; George, S. D.; Antholine, W. E.; Hedman, B.; Hodgson, K. O.; Solomon, E. I. *J. Am. Chem. Soc.* **2002**, *124*, 6180.

[30] Gupta, A.; Nederlof, I.; Sottini, S.; Tepper, A. W.; Groenen, E. J.; Thomassen, E. A.; Canters, G. W. *J. Am. Chem. Soc.* **2012**, *134*, 18213.

[31] Shin, W.; Sundaram, U. M.; Cole, J. L.; Zhang, H. H.; Hedman, B.; Hodgson, K. O.; Solomon, E. I. *J. Am. Chem. Soc.* **1996**, *118*, 3202.

[32] Palmer, A. E.; Quintanar, L.; Severance, S.; Wang, T. P.; Kosman, D. J.; Solomon, E. I. *Biochemistry* **2002**, *41*, 6438.

[33] In recent studies presented in Chapters 3, we have obtained further evidence that T2 Cu is likely not involved in the peroxide binding a the TNC as shown in Scheme 1. Also, in Chapter 4, we fail to observe a long-lived on-state which suggests that fully reduced form of SLAC may not be part of the enzyme mechanism under turnover conditions. Thus, Scheme 1, as proposed earlier, may require further revisions in light of the new experiments.

[34] Bento, I.; Peixoto, C.; Zaitsev, V. N.; Lindley, P. F. *Acta Crystallogr., Sect. D: Biol. Crystallogr.* **2007**, *63*, 240.

[35] Manabe, T.; Manabe, N.; Hiromi, K.; Hatano, H. *FEBS Lett.* **1972**, *23*, 268.

[36] Manabe, T.; Hatano; Hiromi, K. *J. Biochem.* **1973**, *73*, 1169.

[37] Bielli, P.; Bellenchi, G. C.; Calabrese, L. *J. Biol. Chem.* **2001**, *276*, 2678.

[38] Augustine, A. J.; Kjaergaard, C.; Qayyum, M.; Ziegler, L.; Kosman, D. J.; Hodgson, K. O.; Hedman, B.; Solomon, E. I. *J. Am. Chem. Soc.* **2010**, *132*, 6057.

[39] Murphy, M. E. P.; Lindley, P. F.; Adman, E. T. *Protein Sci.* **1997**, *6*, 761.

[40] Dwulet, F. E.; Putnam, F. W. *Proc. Natl. Acad. Sci. U. S. A.* **1981**, *78*, 2805.

[41] Poyton, R. O. *Respir Physiol* **1999**, *115*, 119.

[42] Tepper, A. W. J. W.; Aartsma, T. J.; Canters, G. W. *Faraday Discuss.* **2011**, *148*, 161.

[43] Quintanar, L.; Stoj, C.; Taylor, A. B.; Hart, P. J.; Kosman, D. J.; Solomon, E. I. *Acc. Chem. Res.* **2007**, *40*, 445.

[44] Dietrich, L. E.; Teal, T. K.; Price-Whelan, A.; Newman, D. K. *Science* **2008**, *321*, 1203.

[45] Le Roes-Hill, M.; Goodwin, C.; Burton, S. *Trends Biotechnol.* **2009**, *27*, 248.

Chapter 3

Small laccase from *S. coelicolor* can turnover without Type 2 Cu but not without its Coordinating Histidine*

Abstract:

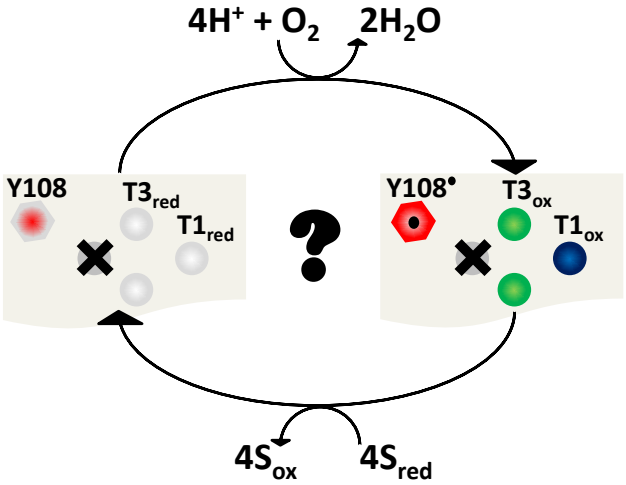

The type 2 Cu of the Small Laccase (SLAC) from *Streptomyces coelicolor* was removed from the protein under reducing conditions utilizing a Cu(I) chelator at neutral pH. The enzyme form thus produced still possesses about 33% activity relative to the wt protein. However, mutation of a coordinating (to type 2 Cu) His residue (H102) to a glycine, tyrosine, phenylalanine or glutamine causes enzyme activity to diminish by more than two orders of magnitude but doesn't lead to Cu depletion. Atomic absorption and EPR spectroscopy together with kinetics and inhibition studies suggest that T2 Cu is not involved in binding O_2 at the trinuclear Cu site and the enzyme is capable to function without this Cu. We hypothesize that during the evolution of Cu proteins, the type 3 Cu sites may have been recruited prior to the type 2 Cu sites in multicopper proteins. However, the question remains: how the protein containing only three Cu's (i.e. the T1 Cu and the T3 Cu pair) is capable of reducing O_2 to H_2O.

*In preparation: Gupta, A.; Nederlof, I.; Nami, F.; Groenen, E.J.J.; Canters, G.W.

3.1 Introduction

Biochemical conversion of O_2 to H_2O is an essential process from where respiratory beings derive the energy required for their vital processes. The reaction, requiring formally four electrons and four protons, is typically mediated by heme and/or Cu proteins. Multicopper oxidases (MCO's) constitute a family of enzymes containing four copper ions arranged within the protein matrix to catalyze this process. The reducing equivalents, from substrates, are accepted at the type 1 (T1) Cu site which transmits them through a conserved HisCysHis pathway to the trinuclear Cu cluster (TNC) where O_2 binds and gets reduced.[1] The TNC is composed of a normal or type 2 (T2) Cu and a binuclear type 3 (T3) Cu pair. It has been demonstrated from site–directed mutagenesis, spectroscopy, kinetics and theoretical approaches that the MCO's cannot catalyze the reduction of O_2 if the T2 Cu site is absent.[2] We demonstrate first clear evidence that small laccase (SLAC), from *S. coelicolor*, still exhibits catalytic activity after the T2 Cu site has been chemically removed. Further, the substitution of a T2 Cu coordinating His102 residue causes the activity to diminish by more than two orders of magnitude but doesn't lead to depletion of the T2 Cu.

The quest to identify polyphenol oxidase from lacquer trees as being a copper containing metallo–oxidase is more than a century old.[3] It is interesting to note that a clear demonstration of the Cu containing nature of these proteins comes from reconstitution experiments whereby completely inactive apo–protein was reconstituted with various metal ions and only cupric ion seemed to restore the activity of the protein.[4,5] Later on, MCO's were isolated from other sources including plants and fungi. Whereas the role of Cu in oxidase activity was established, the challenge remained to identify the contribution of individual Cu's to the spectroscopy and kinetics of these proteins. While the electron paramagnetic resonance (EPR) spectroscopic features and the mechanistic role of the blue or T1 Cu were well understood in terms of an electron transfer cofactor, the role of another paramagnetic Cu, the T2 Cu, was puzzling. It was shown that inorganic anions, which have strong Cu binding properties, inhibited the enzyme activity and also displayed spectroscopic evidence of binding to T2 Cu.[6] Further,

T2 Cu could be selectively removed from fungal laccase where the decrease of enzyme activity paralleled the extent of removal of T2 Cu.[7] These studies established clear evidence for a direct role of the T2 Cu in the fungal laccase enzyme mechanism. The ability to selectively remove the T2 Cu and to study the spectroscopy and kinetics of other MCO's triggered intense investigations and discussions. The method was further improved and was shown to work for ascorbate oxidase and other laccases.[8-15]

Apart from the T1 and T2 Cu's, there are two additional Cu ions in the MCO's which do not give rise to an EPR signal. This is because they are bridged by an oxygen atom which renders the Cu–pair diamagnetic properties by antiferromagnetic coupling. It provides a spectroscopic feature in absorption (λ_{max} ~ 330 nm) arising from a $O^{2-} \rightarrow$ Cu(II) charge transfer transition. The overall organization of Cu's in the protein became clearer when the crystal structure of ascorbate oxidase was solved.[16,17] The structure showed that the TNC is located ~13 Å away from the T1 Cu and that the organization of the two sites was in agreement with what was already anticipated from the spectroscopic studies. Despite the structural similarities of MCO's from various sources, there has been a strong debate about the mechanistic aspects of O_2 binding and reduction at the TNC.[18,19] X–ray diffraction experiments on ascorbate oxidase crystals soaked with H_2O_2 have demonstrated that the peroxide becomes terminally coordinated to one of the T3 Cu(II) ions.[20] A recent study on crystals of a blue laccase, from *Steccherinum ochraceum*, shows X–ray dose dependent reduction of the active site of the laccase as well as evidence of a peroxy group bound symmetrically between the two T3 Cu ions.[21] Yet another set of detailed spectroscopic and theoretical investigations on ferrous oxidase (Fet3p), from *Saccharomyces cerevisiae*, demonstrate that the O_2 binds between the T2 Cu and one of T3 Cu's called T3Cu–β.[2] Thus, the question about catalytically relevant intermediates present during the steady–state turnover of respective MCO's remains open. It won't be surprising to observe that different MCO's from different sources have unique catalytic mechanisms.

The advent of entire genome sequencing made it possible to identify gene fragments characteristic of MCO's in all domains of life and allowed researchers

to further investigate the similarities and differences among the members of this family of proteins.[22-24] Recently, a number of MCO's exhibiting structures different than those of the known MCO's, were identified, isolated and crystallized, seemingly filling in the voids in existing evolutionary theories of Cu proteins.[24-27] SLAC is one such protein which was identified as a homo–trimer of monomers, each monomer consisting of two cupredoxin domains unlike the three–domain monomeric laccases or ascorbate oxidase.[22,26] Careful mechanistic and spectroscopic studies enabled identification of the involvement of Tyr108 in the enzymatic reduction of O_2 at the TNC (see Chapter 2), a feature so far not seen for other laccases.[28] SLAC might be unique in this respect but this tyrosine appears to be conserved among all known sequences of the homologous putative two–domain multicopper proteins and also in human ceruloplasmin. Here we report another astonishing observation, viz. that SLAC doesn't lose its activity when the T2 Cu is chemically removed. This demands serious attention as it not only demonstrates the singular behavior of SLAC and possibly other members of the family, but also calls for a revised mechanism of O_2 binding and reduction to H_2O at the TNC.

3.2 Results and Discussion

SLAC was recombinantly expressed in *E. coli* and purified as reported earlier.[22] To selectively remove the T2 Cu from MCO's, majority of the methods reported in literature make use of prolonged dialysis of the protein in the presence of strong Cu(I)/Cu(II) chelators like bathocuprone disulfonate, dimethyl glyoxime and *N,N*–diethyldithiocarbamate.[7-10] Since the T2 Cu is coordinated by only two histidine residues, it is relatively labile and gets removed preferentially while the other Cu's remain bound to the protein. Several of these approaches were attempted to selectively remove the T2 Cu from SLAC without much success. In most of these experiments, the protein lost multiple Cu's and eventually got denatured. It became apparent that the Cu's in SLAC are much more weakly bound as compared to those of laccases and therefore somewhat mild conditions must be utilized to selectively remove the T2 Cu. The weak binding might arise from the fact that the TNC in SLAC is located at the interface of two SLAC monomers unlike the laccases where the TNC sits

between the N– and C–terminus of the same peptide chain.[26] The successful strategy of Cu removal was derived from a modification of the method by Malkin *et al.*[7] Briefly, 10mM of sodium bicinchoninate (BCA) was added to ~100uM SLAC in 200mM sodium phosphate buffer at pH 7.2. Thereafter, sodium ascorbate (Asc) was added to a final concentration of 100mM. Immediately upon addition of ascorbate the solution turned purple owing to the formation of $Cu(I)(BCA)_2$ complex (Figure 1a). The absorption of the complex was monitored at 560 nm (ϵ_{560} = 8000 $M^{-1}cm^{-1}$) for 30–60 mins till it reached a plateau. From the absorption, with the knowledge of protein concentration and extinction coefficient of the $Cu(I)(BCA)_2$ conplex, it was clear that one equivalent of Cu had formed a complex with BCA. The solution was then passed through a desalting column or dialysed against 100mM NaPi buffer at pH 7.2 to remove the excess ascorbate and the $Cu(I)(BCA)_2$ complex. The protein thus prepared (T2D SLAC) was checked for its Cu content by atomic absorption spectroscopy (AAS) and EPR. AAS revealed presence of only 3.0 Cu's per SLAC monomer, which was as expected (Table 1). The EPR spectrum showed no signs of the broad hyperfine lines in the low field region due to T2 Cu indicating that this Cu has been selectively removed from the protein (Figure 1b). The protein was checked for its activity as reported earlier and still possessed almost one–third of the wt–SLAC activity (Table 1).

A number of features are worth pointing out. First, the Cu was easily removed at neutral pH unlike previous experiments where Cu depletion was observed at pH <4.5 under mild denaturing conditions.[7] Second, the protein solution after desalting was blue in color and possessed almost identical absorption in the 600 nm region as before T2 Cu depletion and slightly diminished absorption around 330 nm (Figure 1c). There has been an intense debate about the redox state and spectroscopic properties of the T3 Cu site following T2 Cu removal from *Rhus* laccase which was largely dependent on the method employed for Cu depletion.[11-13,15,29-31] It has been suggested that there may exist multiple isotypes of T2D laccase, depending on the method of preparation, which might be responsible for the differences in observations.[32] Third, all the T2 Cu depleted MCO preparations in the past have yielded inactive protein indicating a direct role of the T2 Cu in O_2 reduction.[7-10] However, SLAC only partially loses

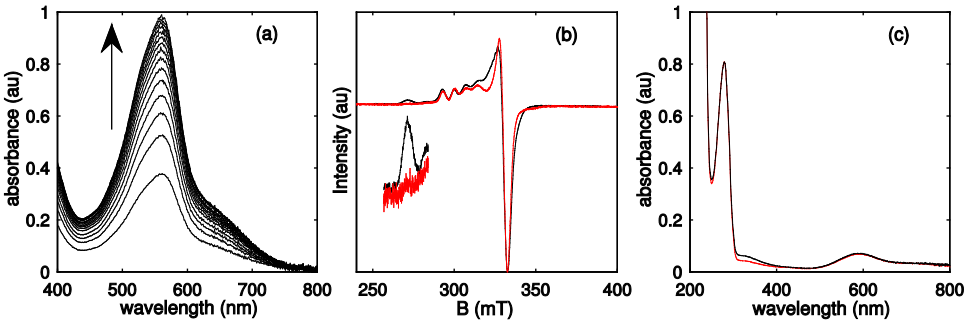

Figure 1: (a) Absorption of the $Cu(I)(BCA)_2$ complex increases and reaches saturation when wt SLAC (100 µM) is treated with BCA (10 mM) and Asc (100 mM) in sodium phosphate buffer (200mM) at pH 7.2. Normalized (b) EPR and (c) absorption spectrum of the wt SLAC (black) overlaid with the spectrum of the protein from where T2 Cu had been chemically removed (red) by the method used in (a). The inset in (b) shows the zoomed in portion of the spectra where the absence of the T2 Cu signal in the T2 Cu depleted SLAC spectrum is clearly visible.

Table 1: Catalytic rate of enzyme turnover (v/E_T) and copper quantification (ratio of Cu concentration vs the protein concentration) using atomic absorption spectroscopy. The turnover rate was measured at 5 mM DMPD in 200 mM air saturated (~270 µM O_2) sodium phosphate buffer (pH 6) at 295 K.

	v/E_T (s^{-1})*	[Cu]/[protein]
wt SLAC	135 ± 5	3.9
T2D SLAC	45 ± 2	3.0
H102G	<1	3.8
H102Y	<1	3.6
H102F	<1	4.1
H102Q	<1	3.7
T2D Y108A	30 ± 2	2.9

* v denotes the catalytic rate and E_T is the total enzyme concentration. Thus, v/E_T denotes the normalized unimolecular rate constant.

activity after the removal of the T2 Cu, clearly showing that the enzyme is capable of functioning without this Cu. Moreover, it was found that azide or fluoride, which strongly inhibits activity of other MCO's by coordinating to T2

Cu,[6] did not inhibit SLAC activity, nor did the azide cause any change in the EPR spectrum of SLAC (Figure S2). On the contrary, azide boosted the SLAC activity by about 25%. Cyanide, another laccase inhibitor, showed strong inhibition of SLAC activity but it is suggested to bind to the T3 Cu site instead of the T2 Cu.[33] Taking all the above observations into account, we conclude that the O_2 binding, at least in SLAC, occurs at the T3 Cu site and the T2 Cu may only be partly involved either in binding or reducing O_2 to H_2O.

We further performed stopped–flow experiments as reported earlier (see Chapter 2) where fully reduced protein was reacted against air/O_2 saturated buffer (Figure 2a).[28] Again, these experiments indicate that fully reduced T2D SLAC is capable of reacting with O_2 unlike the T2D MCO's studied previously. We could also observe the formation of the peroxide intermediate (PI) which is formed by two electron reduction of O_2 bound to the TNC. This intermediate decayed with concomitant increase of the absorption at 590 nm, characteristic of the oxidized T1 Cu, and 410 nm, characteristic of Y108$^{\bullet}$, consistent with the mechanism reported earlier.[28] However, it is worth mentioning that the yield of the tyrosyl radical as judged from the absorption of the 410 nm ($\epsilon_{410} \approx 3250\ M^{-1}cm^{-1}$) band is very small which is puzzling. It appears that the protein abstracts the fourth electron from another site which doesn't show up in the absorption spectrum. Such an observation is consistent with the previous observations where the type–1 depleted Y108A mutant showed formation of PI followed by its rapid decay (see Chapter 2).[28] This is a subject of further study.

To further strengthen these findings, SLAC variants were prepared where one of the two coordinating histidine residues of the T2 Cu, H102, was replaced by a glycine (H102G), glutamine (H102Q), tyrosine (H102Y), or phenylalanine (H102F).[34] All these variants showed activity diminished by more than two orders of magnitude. AAS revealed presence of ~3.6–4.1 Cu's per SLAC monomer (Table 1) and the EPR spectrum showed the presence of features characteristic of T2 Cu in all these mutants (Figure 2b). This was surprising as such mutations in other MCO's in the past have been shown to yield protein containing only three Cu's per molecule as there is only one histidine residue available to bind to the T2 Cu.[2,35] Addition of EDTA didn't help remove this Cu

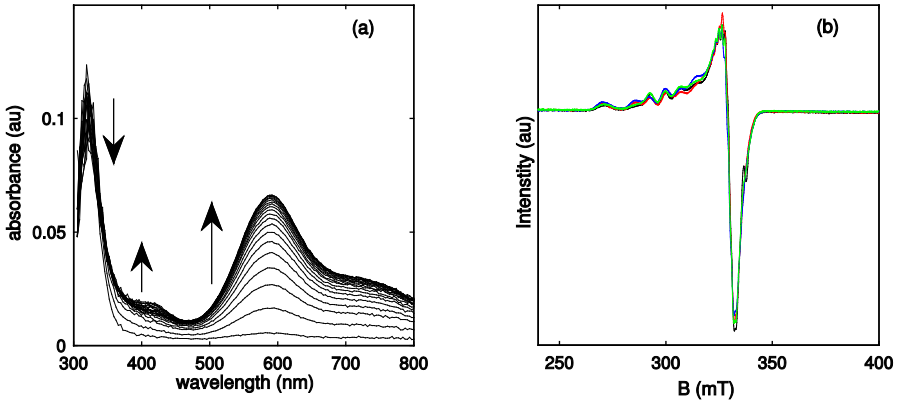

Figure 2: (a) Reaction of fully reduced T2D SLAC with air saturated buffer monitored using stopped–flow. The absorption around 320 nm (PI absorption) changes only slightly while the absorption around 600 nm (T1 Cu absorption) and 410 nm (tyrosyl radical absorption) starts to appear. The measurement was made in 100 mM sodium phosphate buffer (pH 6.8) at ~22 °C. (b) X–band cw–EPR spectra of H102G (black), H102Y (red), H102F (blue) and H102Q (green) variants overlaid on top of each other. The spectra of the variants are nearly identical to each other and to that of wt SLAC (Figure S2). The spectra were recorded in 100 mM sodium phosphate buffer (pH 6.8) at 40 K.

which suggests that this is not adventitiously bound Cu. Further, all attempts to remove the T2 Cu from these mutants by the method reported above failed as it always led to removal of all the Cu's and protein denaturation. It appears that neither the H102 residue nor the T2 Cu individually affect the enzyme stability but together provide strong foundation to the tertiary structure of the enzyme.

The above experiments immediately trigger an interesting thought: Though the chemical depletion of the T2 Cu had only a moderate effect on SLAC activity, the His102 mutation abolished the enzyme activity even when the T2 Cu was present in these mutants. This clearly suggests a role of His102 in the O_2 reduction by SLAC. It might be possible that His102 mediates proton transfer to the O_2 bound at the T3 Cu site, a role which is thought to be played by aspartate and glutamate residues in the three domain MCO's.[18,36] We observed that the presence of imidazole in the activity assay of H102G variant caused a significant burst in the activity (~10 fold) which lasted for only few seconds. Further

experiments are underway to precisely define a role for His102 in the SLAC mechanism.

In a previous study (Chapter 2), the involvement of a tyrosine residue (Y108) in the enzyme mechanism of SLAC was discovered, where it acts as a purported redox buffer and provides an electron during O_2 reduction. Thus, one explanation for the above observations could be that after removal of the T2 Cu, the enzyme is utilizing Y108 to fulfil its role and thus, is still able to turnover. If this was true then we should have observed, using optical and EPR spectroscopy, the quantitative formation of a tyrosyl radical in the single turnover measurements as described above. Moreover, if this hypothesis is correct then the removal of T2 Cu from the Y108A mutant of SLAC, where tyrosine at position 108 is replaced by alanine, should yield completely inactive protein. Indeed, this preparation was significantly less active as compared to wt–SLAC but still possessed significant activity (Table 1) which demands further investigation. Taken together, the experiments now seem to suggest that although Y108 residue is the site of radical on the longer time scale, it is not the immediate electron donor to the O_2 and there must be another redox active residue which is crucial for enzyme activity. Regardless, this is the first example of an MCO which is capable of turnover with only three Cu's per monomer.

SLAC is active as a homotrimer in solution and thus consists of three T1 Cu sites and three TNC's. The T1 Cu sites, as revealed from the crystal structure are only ~18 Å apart. It is conceivable that these T1 Cu sites communicate with each other by exchanging electrons when required. Such a mechanism has been proposed for ceruloplasmin which contains three T1 Cu sites but only one TNC.[37] We're planning to investigate whether this is true or not from dual color single molecule experiments. Though less likely, another possibility to explain the above results would be direct reduction of partially reduced oxygen species by reducing substrate. Although it is clear that the first and the second electron reduction of the TNC in MCO's take place via T1 Cu, there are no clear experiments which prove that subsequent reductions can't take place directly by the substrate as the redox potential of the T3 Cu's and the T1 Cu are more or less identical. Once the TNC is in a more reduced state, smaller reorganization

energy would be required for further electron transfer steps which – accompanied by the strong oxidizing capability of partially reduced O_2 species – may make the direct reduction by substrate favorable.[38] A last possibility will be that upon binding of O_2 to the two electrons reduced T3 Cu site, the two electrons are transferred to the O_2 forming the PI, which remains bound to the T3 Cu's and awaits entry of two more electrons through the T1 Cu before getting fully reduced to H_2O. If this pathway is being followed, we must be able to observe formation of PI upon treatment of the SLAC with H_2O_2. No such evidence was obtained from the experiments and thus this mechanism is unlikely to be the right one. Further experiments are required to single out which one of the above mentioned pathways are likely to occur in the reduction of O_2 by SLAC containing only three Cu's per monomer.

These new findings also seem to have implications for the proposed evolution of Cu proteins. It seems that incorporation of the T2 Cu site in the MCO's must have occurred after the incorporation of the T3 Cu sites, which are sufficient to catalyze the reduction of O_2 to H_2O. Thus, the scheme as drawn by Nakamura and Go about the evolutionary relationships of multicopper proteins may require revision or further experimental data to include/exclude the new findings reported in this work.[25] Indeed the warning put forward by Keilin and Mann in their paper in 1939 seems to fit here: "…These results also serve as a warning against generalizations… and against the tendency of ascribing to one enzyme the properties of another enzyme in the same class, contrary to all the available evidence."[4] With more and more genes being identified from different organisms, it remains to be seen how the evolutionary theory and the previously proposed mechanisms will fit into one consensus.

3.3 Supplementary Information

Site–directed mutagenesis: Site–directed mutagenesis was carried out using the Quick Change site–directed mutagenesis kit (Stratagene). The primers used for respective mutations are given below where mutations are in bold and underlined. Desired mutations were confirmed by DNA sequencing (BaseClear).

H102G

Forward primer: 5'– GTG CGG GCC AGC CTG **GGC** GTG CAC GGC CTG GAC –3'

Reverse primer: 5'– GTC CAG GCC GTG CAC **GCC** CAG GCT GGC CCG CAC –3'

H102Y

Forward primer: 5'– GTG CGG GCC AGC CTG **TAC** GTG CAC GGC CTG GAC –3'

Reverse primer: 5'– GTC CAG GCC GTG CAC **GTA** CAG GCT GGC CCG CAC –3'

H102F

Forward primer: 5'– GTG CGG GCC AGC CTG **TTC** GTG CAC GGC CTG GAC –3'

Reverse primer: 5'– GTC CAG GCC GTG CAC **GAA** CAG GCT GGC CCG CAC –3'

H102Q

Forward primer: 5'– GTG CGG GCC AGC CTG **CAA** GTG CAC GGC CTG GAC –3'

Reverse primer: 5'– GTC CAG GCC GTG CAC **TTG** CAG GCT GGC CCG CAC –3'

The purification of the wt–SLAC and the mutants was carried out as reported previously.[22] The proteins were aliquoted and stored at –80 ^{0}C till further use. The absorption spectra of the H102G, H102Y, H102F and H102Q variants are shown in Figure S1.

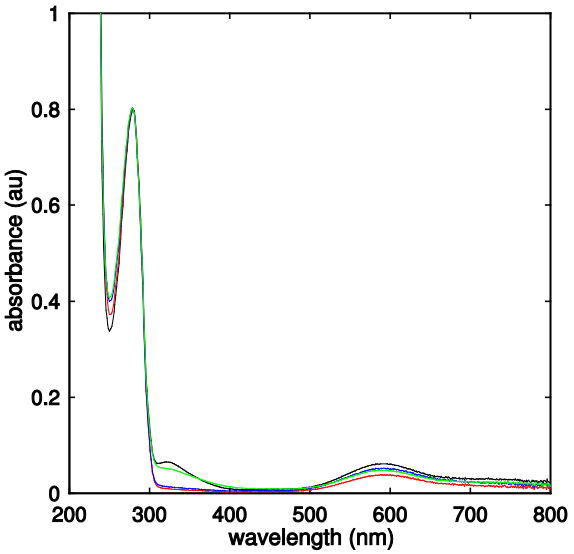

Figure S1: Absorption spectra of the H102G (black), H102Y (red), H102F (blue) and H102Q (green). The spectra have been normalized at the 280nm absorption.

EPR spectroscopy: Samples for EPR measurements were prepared as reported earlier (see Chapter 2). The EPR spectrum of the wt SLAC (~500 µM) in the presence of 10 equivalents of sodium azide (~5 mM) is shown in Figure S2.

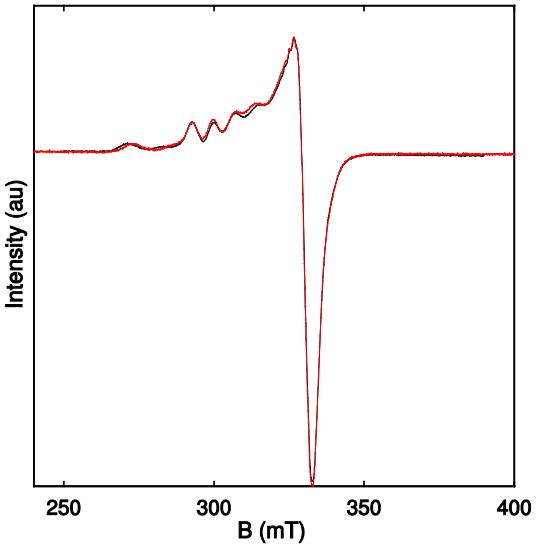

Figure S2: Normalized EPR spectrum of the wt SLAC (black) overlaid with that of the protein incubated with 10 equivalents of sodium azide (red). Clearly, the two spectra are superimposable and thus, rule out azide binding to the T2 Cu.

Steady–state kinetics: Steady state kinetics measurements were performed as reported earlier (see Chapter 2). However, in the current experiments, the rates were measured at a single concentration of TMPD, i.e. at 5 mM under air saturation.

Transient kinetics: Transient kinetics was monitored using a stopped flow instrument (SX.18MV– Applied Photophysics) as reported earlier (see Chapter 2).

3.4 References

[1] Solomon, E. I.; Sundaram, U. M.; Machonkin, T. E. *Chem. Rev.* **1996**, *96*, 2563.

[2] Augustine, A. J.; Kjaergaard, C.; Qayyum, M.; Ziegler, L.; Kosman, D. J.; Hodgson, K. O.; Hedman, B.; Solomon, E. I. *J. Am. Chem. Soc.* **2010**, *132*, 6057.

[3] Yoshida, H. *J. Chem. Soc. Trans.* **1883**, *43*, 472.

[4] Keilin, D.; Mann, T. *Nature* **1939**, *143*, 23.

[5] Tissieres, A. *Nature* **1948**, *162*, 340.

[6] Malkin, R.; Malmstrom, R. G.; Vanngard, T. *FEBS Lett.* **1968**, *1*, 50.

[7] Malkin, R.; Malmstrom, B. G.; Vanngard, T. *Eur. J. Biochem.* **1969**, *7*, 253.

[8] Graziani, M. T.; Morpurgo, L.; Rotilio, G.; Mondovi, B. *FEBS Lett.* **1976**, *70*, 87.

[9] Avigliano, L.; Desideri, A.; Urbanelli, S.; Mondovi, B.; Marchesini, A. *FEBS Lett.* **1979**, *100*, 318.

[10] Morpurgo, L.; Savini, I.; Mondovi, B.; Avigliano, L. *J. Inorg. Biochem.* **1987**, *29*, 25.

[11] Reinhammar, B.; Oda, Y. *J. Inorg. Biochem.* **1979**, *11*, 115.

[12] Morpurgo, L.; Graziani, M. T.; Finazzi-Agro, A.; Rotilio, G.; Mondovi, B. *Biochem. J.* **1980**, *187*, 361.

[13] Morpurgo, L.; Graziani, M. T.; Desideri, A.; Rotilio, G. *Biochem. J.* **1980**, *187*, 367.

[14] Hanna, P. M.; McMillin, D. R.; Pasenkiewicz-Gierula, M.; Antholine, W. E.; Reinhammar, B. *Biochem. J.* **1988**, *253*, 561.

[15] Frank, P.; Farver, O.; Pecht, I. *J. Biol. Chem.* **1983**, *258*, 11112.

[16] Messerschmidt, A.; Rossi, A.; Ladenstein, R.; Huber, R.; Bolognesi, M.; Gatti, G.; Marchesini, A.; Petruzzelli, R.; Finazzi-Agro, A. *J. Mol. Biol.* **1989**, *206*, 513.

[17] Messerschmidt, A.; Ladenstein, R.; Huber, R.; Bolognesi, M.; Avigliano, L.; Petruzzelli, R.; Rossi, A.; Finazzi-Agro, A. *J. Mol. Biol.* **1992**, *224*, 179.

[18] Solomon, E. I.; Ginsbach, J. W.; Heppner, D. E.; Kieber-Emmons, M. T.; Kjaergaard, C. H.; Smeets, P. J.; Tian, L.; Woertink, J. S. *Faraday Discuss.* **2011**, *148*, 11.

[19] Farver, O.; Pecht, I. *Coord. Chem. Rev.* **2011**, *255*, 757.

[20] Messerschmidt, A.; Luecke, H.; Huber, R. *J. Mol. Biol.* **1993**, *230*, 997.

[21] Ferraroni, M.; Matera, I.; Chernykh, A.; Kolomytseva, M.; Golovleva, L. A.; Scozzafava, A.; Briganti, F. *J. Inorg. Biochem.* **2012**, *111*, 203.

[22] Machczynski, M. C.; Vijgenboom, E.; Samyn, B.; Canters, G. W. *Protein Sci.* **2004**, *13*, 2388.

[23] Endo, K.; Hayashi, Y.; Hibi, T.; Hosono, K.; Beppu, T.; Ueda, K. *J. Biochem.* **2003**, *133*, 671.

[24] Komori, H.; Miyazaki, K.; Higuchi, Y. *FEBS Lett.* **2009**, *583*, 1189.

[25] Nakamura, K.; Go, N. *Cell. Mol. Life Sci.* **2005**, *62*, 2050.

[26] Skalova, T.; Dohnalek, J.; Ostergaard, L. H.; Ostergaard, P. R.; Kolenko, P.; Duskova, J.; Stepankova, A.; Hasek, J. *J. Mol. Biol.* **2009**, *385*, 1165.

[27] Lawton, T. J.; Sayavedra-Soto, L. A.; Arp, D. J.; Rosenzweig, A. C. *J. Biol. Chem.* **2009**, *284*, 10174.

[28] Gupta, A.; Nederlof, I.; Sottini, S.; Tepper, A. W.; Groenen, E. J.; Thomassen, E. A.; Canters, G. W. *J. Am. Chem. Soc.* **2012**, *134*, 18213.

[29] LuBien, C. D.; Winkler, M. E.; Thamann, T. J.; Scott, R. A.; Co, M. S.; Hodgson, K. O.; Solomon, E. I. *J. Am. Chem. Soc.* **1981**, *103*, 7014.

[30] Hahn, J. E.; Co, M. S.; Spira, D. J.; Hodgson, K. O.; Solomon, E. I. *Biochem. Biophys. Res. Commun.* **1983**, *112*, 737.

[31] Penner-Hahn, J. E.; Hedman, B.; Hodgson, K. O.; Spira, D. J.; Solomon, E. I. *Biochem. Biophys. Res. Commun.* **1984**, *119*, 567.

[32] Frank, P.; Pecht, I. *J. Phys. Chem.* **1986**, *90*, 3809.

[33] Meyer, T. E.; Marchesini, A.; Cusanovich, M. A.; Tollin, G. *Biochemistry* **1991**, *30*, 4619.

[34] See Supplementary Information.

[35] Blackburn, N. J.; Ralle, M.; Hassett, R.; Kosman, D. J. *Biochemistry* **2000**, *39*, 2316.

[36] Augustine, A. J.; Quintanar, L.; Stoj, C. S.; Kosman, D. J.; Solomon, E. I. *J. Am. Chem. Soc.* **2007**, *129*, 13118.

[37] Bielli, P.; Bellenchi, G. C.; Calabrese, L. *J. Biol. Chem.* **2001**, *276*, 2678.

[38] Farver, O.; Tepper, A. W.; Wherland, S.; Canters, G. W.; Pecht, I. *J. Am. Chem. Soc.* **2009**, *131*, 18226.

Chapter 4

One at a Time: Intramolecular Electron–Transfer Kinetics in Small Laccase observed during turnover*

Abstract:

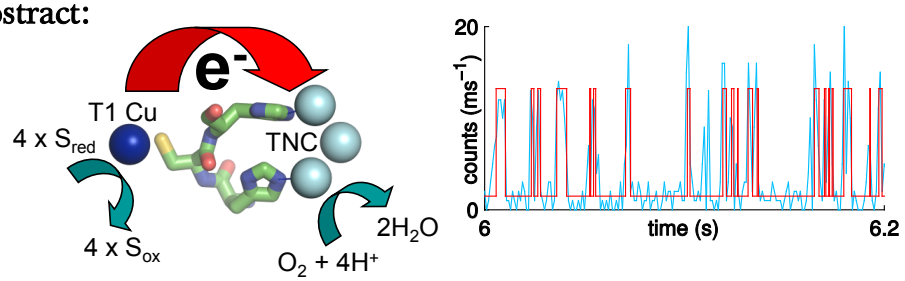

Single–molecule enzymology provides an unprecedented level of detail about enzyme mechanisms, which have been very difficult to probe in bulk. One such aspect is intramolecular electron transfer (ET) which is a recurring theme in the research on oxidoreductases containing multiple redox–active sites. We measure the intramolecular ET rates between the copper centers of the small laccase (SLAC) from *Streptomyces coelicolor* at room temperature and pH 7.4, one molecule at a time, during turnover. The forward and backward rates across many molecules follow a log–normal distribution with means of 460 s^{-1} and 85 s^{-1}, respectively, corresponding to activation energies of 347 and 390 meV for the forward and backward rates. The driving force and the reorganization energy amount to 0.043 eV and 1.5 eV, respectively. The spread in rates corresponds to a spread of ~30 meV in the activation energy. The second–order rate constant for reduction of the T1 site amounts to 2.9×10^4 $M^{-1}s^{-1}$. The mean of the distribution of forward ET rates is higher than the turnover rate from ensemble steady–state measurements and, thus, is not rate limiting.

*Adapted from: Gupta, A.; Aartsma, T.J.; Canters, G.W. *J. Am. Chem. Soc.* **2014**, *136*, 2707.

4.1 Introduction

Efficient and controlled electron transfer (ET) is essential for the proper course of metabolic processes like energy conversion and storage. Traditionally, ET rates in proteins are measured under single–turnover conditions using techniques like pulse radiolysis or flash photolysis, and the results are sometimes not in agreement with the results of steady–state kinetics measurements.[1-3] Study of enzyme kinetics at the single–molecule (SM) level allows direct access to real–time events under steady–state conditions.[4] SM techniques and the underlying theoretical framework have evolved rapidly and greatly advanced our knowledge of enzyme mechanisms over the past decade.[5-7] The redox kinetics of flavin–containing cholesterol oxidase[8] and pentaerythritol tetranitrate reductase,[9] Cu–containing nitrite reductases,[10-12] and the conformational dynamics of dihydrofolate reductase,[13] for instance, have been studied profitably by SM techniques. In this chapter, we report the first SM measurements of the ET rate between the copper centers of a multicopper oxidase (MCO), *i.e.*, small laccase (SLAC) from *Streptomyces coelicolor*.

MCOs catalyze the four–electron reduction of O_2 to H_2O concomitant with oxidation of substrate molecules. Laccases belong to the family of MCOs which have been commercialized by industry owing to their ability to oxidize a wide variety of substrates. Their enzymatic machinery consists of a type 1 (T1) Cu which accepts reducing equivalents from substrate molecules and transfers them across ~13 Å via a conserved HisCysHis motif to the trinuclear Cu cluster (TNC), where O_2 is converted to H_2O.[14,15] The TNC is traditionally considered to be composed of a binuclear type 3 (T3) Cu pair and a normal type 2 (T2) Cu. A crucial step in the catalytic process is the transfer of an electron from the T1 Cu to the TNC, one at a time, four times to complete a turnover. Several reports exist in the literature focusing on measuring the ET rates anaerobically using pulse radiolysis and flash photolysis under single–turnover conditions.[2,3,16-18] The pioneering studies of Farver, Pecht and coworkers, for instance, greatly advanced our understanding of how the electrons move and equilibrate between different redox centers and the consequences of these dynamics on the enzyme mechanism. However, close evaluation of these studies reveals that the measured

ET rates are sometimes an order of magnitude or more lower than the turnover rates.[2,16] Although measurements under single–turnover conditions can provide valuable information about the enzyme mechanism, the observed intermediates are not necessarily similar to the intermediates occurring during steady–state turnover. Thus, there is a continuous demand for new methods to measure the ET rates during turnover.

Recently, a new principle was introduced: fluorescence–based detection of protein redox state(s) (FluRedox),[19] which allows monitoring the redox state changes of oxido–reductases during turnover at a high temporal resolution and at the SM level.[10-12] Not only does this method allow the study of hidden aspects of enzyme kinetics/dynamics (which are often masked by the rate–determining step in a bulk measurement), it also allows the study of the heterogeneity in a population of molecules. We make use of this principle to study the ET in SLAC.

SLAC is a homotrimer in which each monomer consists of two cupredoxin domains (Figure 1a) unlike the more common MCOs, which are three– or six–domain monomeric proteins.[20-22] However, it has a similar active–site morphology consisting of T1 and TNC sites and catalyzes the same reaction as other MCOs. It has been proposed that such trimeric proteins are evolutionary precursors to ascorbate oxidase, the 3–domain laccases and the 6–domain ceruloplasmin.[23] Recently, it was shown that SLAC may also differ from the common laccases in its mechanism of O_2 reduction, wherein a redox–active tyrosine residue (Y108) may have a participatory role.[24,25] SLAC has been structurally characterized[21,22,25] and, together with a recombinant expression system, provides excellent opportunities to study the ET in this enzyme in great detail.

4.2 Results and Discussion

To selectively label SLAC, K204C and R203C variants were prepared which contain a surface–exposed cysteine available for conjugation with thiol–reactive dyes and linkers.[26] When oxidized, the enzyme exhibits absorption bands at 330 and 590 nm, the latter characteristic of the T1 Cu site. The 590 nm absorption

overlaps with the emission of the Atto647N dye; thus, when using SLAC labeled with this dye, the fluorescence of the dye is quenched by means of Förster resonance energy transfer (FRET) from the fluorophore to the T1 Cu chromophore. The 590 nm absorption band is absent when the enzyme is reduced in which case the fluorescence is recovered. Thus, the emission from the enzyme–dye conjugate can serve as a highly sensitive probe of the redox state of the T1 Cu. Such fluorescence switching of the labeled variants was verified in bulk when the enzyme was cycled between oxidized and reduced states (Figure S3). Both the R203C and K204C variants showed similar fluorescence switching but further experiments focused on the K204C variant. The enzyme was conjugated with thiol–reactive biotin–PEG linkers to make it suitable for surface immobilization.[26] A cartoon depicting the labeling strategy is shown in Figure 1a.

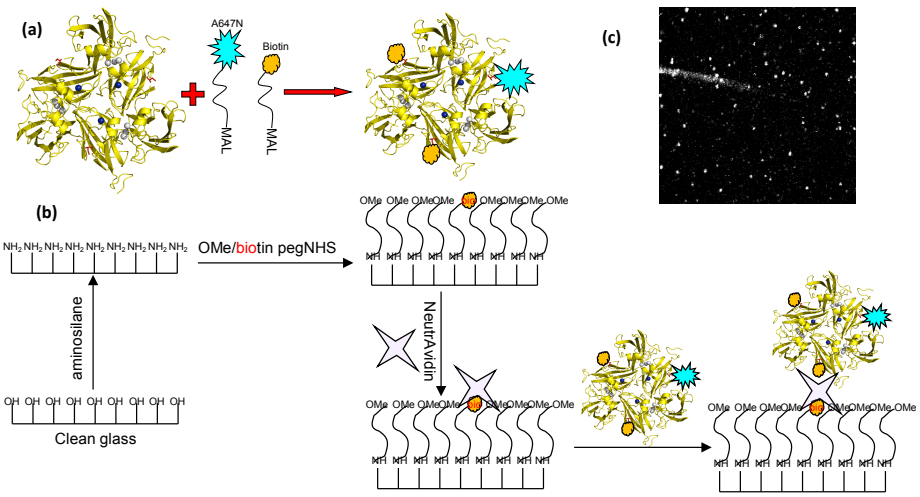

Figure 1: (a) K204C variant of SLAC conjugated with Atto647N–maleimide and biotin–PEG–maleimide. The conditions are chosen so that the dye–to–protein labeling ratio does not exceed 5 % to ensure most enzyme molecules carry only one or no fluorescence label. T1 Cu is depicted in blue, TNC in grey and Cys204 in red. (b) Functionalization of glass coverslips with aminosilane and PEG linkers and immobilization of SLAC conjugates using the NeutrAvidin–biotin interaction. (c) A 40x40 μm^2 image taken under a confocal fluorescence microscope of the sample prepared in (b). The bright spots are individual SLAC molecules. For details about conjugation, immobilization, and confocal setup, see Supplementary Information.

SLAC molecules must be immobilized on a transparent solid support before any measurements can be made on a confocal microscope. A number of methods are described in the literature for immobilization of proteins on a surface.[27-29] It was an additional interest for us to immobilize SLAC in a site–specific manner. To achieve this, the glass coverslips were functionalized as shown in Figure 1b.[26] Briefly, clean coverslips were first functionalized with 3–(2–aminoethyl)aminopropyl trimethoxysilane to create an amine–terminated hydrophilic surface. This functionalized surface was further treated with polyethylene glycol (PEG) linkers containing an amine–reactive end (NHS ester) and a biotin or methoxy group at the other terminus. It was demonstrated previously that the PEG linkers minimize non–specific adsorption of the protein on the surface.[30-32] The ratio of biotin–terminated PEG to methoxy–terminated PEG on the surface was kept below 0.1%. The SLAC conjugates prepared earlier were then tethered to the surface via biotin–NeutrAvidin interactions (Figure 1b). This labeling and immobilization strategy helps ensure that the label/linkers attach to the protein at a specific site and minimize any heterogeneity in the sample preparation. A typical confocal image of immobilized SLAC molecules on a coverslip prepared by the above method is shown in Figure 1c.

When the laser is focused on one of the molecules, the variation in fluorescence count rate with time can be observed. In the absence of substrate, the fluorescence intensity is low and, apart from statistical noise, no fluorescence fluctuations are observed, indicating that the enzyme is in a stable oxidized state (Figure S4). In the presence of excess reductant under aerobic conditions and with the TNC selectively inhibited by incubation with cyanide, a high fluorescence intensity is observed and no fluctuations are observed, either (Figure S4), indicating that the T1 site is in a stably reduced state. The two experiments demonstrate that ET between the excited label and the T1 Cu in either the reduced or the oxidized form does not occur at a measurable rate. However, under aerobic conditions and in the presence of *N,N*–dimethyl–p–phenylenediamine (DMPD) as a mediator and ascorbate as a substrate, the enzyme starts to turn over, and discrete fluctuations in the emission count rates are observed.[26] A typical measurement is shown in Figures 2a,b. We ascribe these fluctuations to ET from the T1 Cu to the TNC (high to low fluorescence)

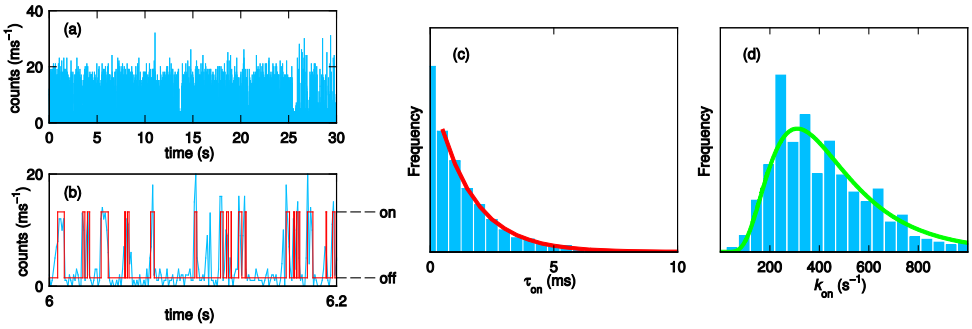

Figure 2: (a) Typical binned time trace (1 ms bin time) of a turning over single SLAC molecule. The molecule shows fluctuations between the high and low emission rates as the redox state of T1 Cu changes, which can be seen from a small portion of the trace as shown in (b). The red trace in (b) is bin–free and was obtained from the changepoint analysis. (c) The dwell time (τ_{on}) distribution of the molecule in the on–state from the trace shown in (a).The number of "on" intervals present in this trace amounted to 2767. The red line is the monoexponential fit to the normalized data with a decay constant k_{on} = 660 s^{-1}. (d) Distribution of k_{on} obtained from ~720 molecules of SLAC. The green line is the fit corresponding to a log–normal distribution with a mean value of 450 s^{-1}. The measurements reported in panels (a)–(c) were made in 20 mM MOPS buffer (pH 7.4) and at 20 $^{\circ}$C with DMPD and ascorbate concentrations of 5 and 10 mM, respectively. The data reported in panel (d) represent measurements that were performed at concentrations of DMPD varying from 0.02 to 5 mM.

and from the substrate or the TNC to the T1 Cu (low to high fluorescence).

Data were collected in a photon–by–photon manner. Since only the arrival times are recorded, it is common to bin the data to visualize the count rate fluctuations. Such binning generally limits the time resolution of the experimental analysis. Thus, we made use of a bin–free method, a so–called changepoint analysis, which utilizes Bayesian statistics to analyze the raw data and to determine the time points when the molecule switches from one state to another.[33] It is evident from Figure 2b that the red trace obtained by such an analysis overlaps well with the binned trace. Thereafter, the dwell times in the on–state were binned, and a histogram of these dwell times was obtained (Figure 2c).[26] As can be seen from the fit in Figure 2c, the distribution of dwell times in the on–state follows a single–exponential decay and directly provides a rate constant (~660 s^{-1} in this

example) which we equate to the rate of ET from T1 to TNC, denoted by $k_{T1\rightarrow TNC} \equiv k_{on}$.[6] We measured time trajectories of ~720 molecules where the DMPD concentration was varied between 0.02 and 5 mM and obtained ET rate constants in the manner discussed above. It appears that the logarithm of the rate constants can be well fitted by a Gaussian distribution (Figure S7). Thus, the rate constants follow a log–normal distribution with an arithmetic mean of $k_{T1\rightarrow TNC} = 460\ s^{-1}$, corresponding to a normal distribution of activation energies.[34] The distribution of ET rates appears quite broad and demonstrates the heterogeneity that exists from one molecule to another (*vide infra*). While in bulk experiments the catalytic reaction rate depends on substrate concentration, it is gratifying to note that the k_{on} distributions are concentration independent (Figure S8a,b), which confirms that we are dealing with an intramolecular process.

In a similar way, the off–times were analyzed. Since they appear dependent on the DMPD concentration, they could not be combined into a single data set for analysis as had been done for the on–time analysis (see above). The data sets obtained at 50 µM and 5 mM DMPD were large enough to allow a preliminary analysis, which resulted in $k_{TNC\rightarrow T1} = 85\ s^{-1}$ and a second order rate constant $k_s = 2.9\text{x}10^4\ M^{-1}s^{-1}$.[26] From the ratio of the two internal ET rate constants and associated variances, a driving force of 43 meV can be derived. The bimolecular rate constant is smaller than the rate constant measured in the bulk ($1.3\text{x}10^5\ M^{-1}s^{-1}$; Figure S2). We ascribe the difference to how the enzyme is present: free in solution *vs.* labeled and immobilized on a solid support.

A number of features are worth pointing out. First, the waiting time distributions can be fit by monoexponential decays (see Figure 2c, for example). Apparently, on the time scale of the experiment (0.5–120 s) the distribution of ET rates (Figure 2d) is static. Second, since four ET steps are needed to complete the enzyme cycle, the differences between the *k*'s for the different steps must be small (<20% of the mean). This is in line with relatively small changes in driving force for the T1–TNC ET step as the TNC fills up with electrons.[35] Third, the internal ET rate is larger than the turnover rate measured under substrate saturating conditions in the bulk (Figure S2). This means that the frequent transitions between on– and off–states that we observe are due, in large measure, to jumps

of electrons back and forth between the TNC and the T1 site. Moreover, since no long on–times (of the duration of the enzyme turnover time) were observed, a long–lived four–electron–reduced state is not part, apparently, of the enzyme cycle. It is conceivable that, after loading the TNC with two or three electrons, charge compensation is necessary through the uptake of protons and/or through dehydroxylation involving a rearrangement of the water and H–bonding network around the TNC before any further electrons can enter the T1 site. Another possibility is that a reversible conformational change temporarily switches off the T1 site, as suggested for the homologous Cu–containing nitrite reductase.[36] A more extensive exploration of this finding must await further experiments.

The distribution in rates may be connected with intrinsic and extrinsic causes. Enzyme immobilization on solid surfaces may lead to (partial) loss of activity. In the present study, we investigate only enzyme molecules that were still active after immobilization. The distribution of forward ET rates in Figure 2d is ascribed, thus, to intrinsic causes and is related to the thermodynamics of the catalytic process. In view of the average distance between the T1 Cu and the TNC (~13 Å) and the distance dependence of the electronic coupling (H_{DA}) between the donor (T1 Cu) and the acceptor (TNC) ($H_{DA} = k_0 \exp\{-\beta (r - r_0)\}$) we can calculate (with $\beta = 1$ Å^{-1}) an activationless ($\Delta G^0 = -\lambda$) ET rate constant $k^0 = 3.7 \times 10^8$ s^{-1}.[26] Using semiclassical Marcus theory and mean and variance of the k_{on} distribution obtained from Figure 2d, an estimate of 0.347 eV for the activation energy ($\Delta G^{\ddagger}$) can be calculated. Using a value of 43 meV for the driving force a value for the reorganization energy $\lambda = 1.5$ eV is obtained which is in line with the reorganization energy of other metalloenzymes including laccases.[26,1,37-39] The spread in the activation energy, corresponding to the k_{on} distribution, amounts to ± 28 meV, which would be equivalent to a spread in the driving force of ± 56 meV or a spread in λ of ± 110 meV.

A similar analysis can be performed for the back ET rates. The rates obtained at [DMPD] = 50 µM can be used for this purpose since the contribution of the bimolecular reaction to the observed rates is negligibly small in this case.[26] We find an activation energy of 390 meV with a spread of ± 25 meV, which leads to

a value for the reorganization energy of $\lambda = 1.5$ eV. As expected, the spread in activation energies for the forward and backward ET is the same within the experimental uncertainty.

Gray and Winkler argued that, with the available experimental and theoretical methods, it is difficult to obtain values of λ to a precision that is better than $\pm$ 100 meV.[37] It is surprising to realize that such a small uncertainty is compatible with the distribution in ET rates that is observed in the present SM measurements. Thus, the distribution that initially appears quite broad relates to a rather narrow distribution of $\Delta G^{\ddagger}$ ($\pm$ 28 meV). A similar observation was reported earlier for copper proteins.[40,41]

In pulse radiolysis experiments on SLAC under anaerobic conditions, it was reported that the ET rate increases as the TNC acquires electrons, one at a time.[17] Moreover, the smallest and the largest ET rates that could be measured in those experiments amounted to ~ 15 and 186 s^{-1}, respectively. However, within the time resolution of the current measurements under turnover or aerobic conditions, we do not observe such a variation of ET rates, as the dwell time distribution fits to a single exponential (*vide supra*). Moreover, in the ensemble steady–state measurements at pH 6, enzymatic rates in excess of 300 s^{-1} were measured, which is faster than the ET rate that could be obtained from the pulse radiolysis experiments.[25] It has been shown for ascorbate oxidase that the presence of oxygen enhances the ET rate by structural perturbation of the TNC.[2,3] Very recently, it was demonstrated with stopped–flow measurements on *Rhus vernicifera* laccase that the so–called native intermediate (or freshly cycled enzyme) is capable of transferring electrons (from T1 Cu to TNC) at a much higher rate than the resting enzyme.[39] Although the "cycled" form of SLAC was used in the pulse radiolysis experiments, the experimental setup may not allow the experiment to proceed quickly enough so as to prevent the (partial) decay of the native intermediate to the resting form of SLAC. This might explain the difference between the pulse radiolysis and the current experiments. Nevertheless, the above points clearly emphasize the fact that a more reliable way to measure such a rate would be to do it during the enzyme turnover.

We are in the process of performing more experiments to analyze the correlation with the bulk measurements. The method reported here may be applicable to study ET in virtually any redox enzyme with a suitable fluorophore, provided that the enzyme exhibits distinctly different absorption spectra in the reduced and oxidized states.

4.3 Supplementary Information

Site–directed mutagenesis: In order to be able to attach a label or a linker to the protein surface a cysteine was introduced into the sequence of the protein. Notice that the native enzyme does not contain any cysteines except for Cys288 which is one of the ligands of the type 1 Cu and which is not accessible for external reactive groups. Site–directed mutagenesis was carried out using the Quick Change site–directed mutagenesis kit (Stratagene). The primers used for respective mutations are given below where mutations are in bold and underlined.

R203C

Forward primer: 5'– G ACC ATC AAC AAC **TGC** AAG CCG CAC ACC G –3'

Reverse primer: 5'– C GGT GTG CGG CTT **GCA** GTT GTT GAT GGT C –3'

K204C

Forward primer: 5'– G ACC ATC AAC AAC CGC **TGT** CCG CAC ACC GGC CCC GAC –3'

Reverse primer: 5'– GTC GGG GCC GGT GTG CGG **ACA** GCG GTT GTT GAT GGT C –3'

Desired mutations were confirmed by DNA sequencing (BaseClear). The position/distance of the residue for mutation was chosen so that the fluorophore can be expected not to undergo any redox chemistry or photoinduced electron transfer with the T1 Cu but at the same time is within the Förster radius to enable highly selective sensing of the desired T1 Cu.

The purification of the mutants was carried out as reported previously.[20] The proteins were aliquoted and stored at –80 ^{0}C till further use. The absorption spectra of the *wt*–SLAC, K204C and R203C variants are shown in Figure S1.

Steady–state kinetics: Bulk steady state kinetics measurements were performed as reported earlier with a slight modification.[25] Instead of TMPD (*N,N,N',N'*

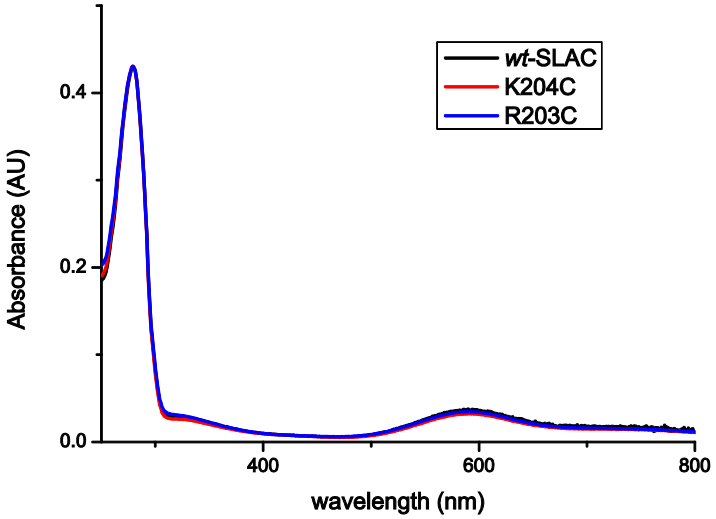

Figure S1: Absorption spectra of the oxidized *wt*–SLAC overlaid with those of K204C and R203C in 20mM sodium phosphate buffer (pH 7.4) at ambient temperature. The spectra have been normalized at the 280nm absorption.

tetramethyl–*p*–phenylenediamine), DMPD (*N,N* dimethyl–*p*–phenylenediamine) was used as substrate in the presence of 10mM ascorbate. Variations in the concentration of ascorbate had no effect on enzyme activity as the reaction with ascorbate is too slow to reduce T1 Cu directly. The presence of ascorbate had an unintended advantage in that it kept the solution colorless which aided in establishing the fluorescence assays. Typical plots of the catalytic rates vs substrate concentration are shown in Figure S2.

Labeling SLAC mutants: The engineered thiols were activated by incubating the enzyme with 5–10 equivalents of TCEP (*tris*(2–carboxyethyl)phosphine) or DTT (dithiothreitol). The following steps were performed as quickly as possible as the thiols have a tendency to get oxidized in the presence of air. Excess reductant was removed by gel filtration (HiTrap Desalting column, GE). At the same time the buffer was exchanged to 20mM Sodium phosphate (pH 7.4) if the sample was not already in this buffer. About 0.25 equivalents of Atto647N–maleimide were added to the protein solution and the reaction was allowed to proceed on ice for 1–2 minutes. Immediately afterwards, a large excess of biotin–PEG–maleimide (MW 3400, LaysanBio) linker was added to quench the excess

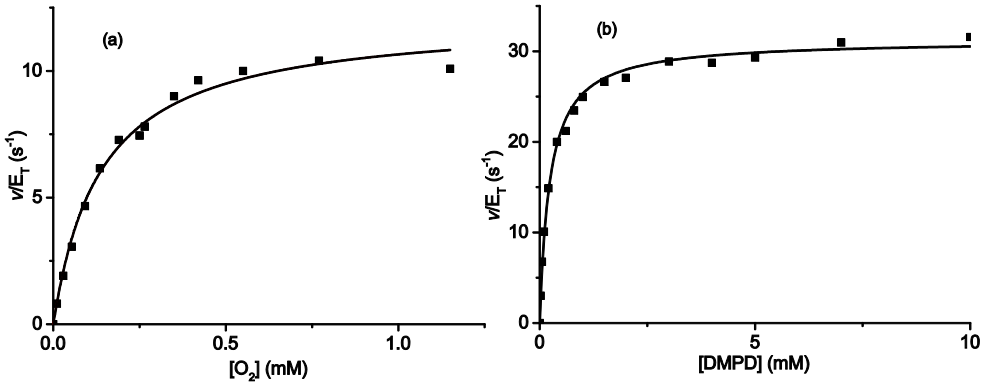

Figure S2: (a) Plot of O_2 consumption rates plotted against the respective O_2 concentration while keeping the initial DMPD and ascorbate concentrations fixed at 5 mM and 10mM, respectively, for each measurement. The solid line is a fit of the data to the Michaelis-Menten equation which yields $v_{max} = 12\ s^{-1}$ and K_M (O_2) = 130 µM. (b) Plot of DMPD oxidation rate plotted against the respective DMPD concentration at air saturation (i.e. around 260 µM O_2). No ascorbate was used in this measurement. The solid line is a fit of the data to the Michaelis-Menten equation which yields $v_{max} = 31\ s^{-1}$, K_M (DMPD) = 235 µM and $k_S = 1.3 \times 10^5\ M^{-1}s^{-1}$. The measurements were made in 200mM sodium phosphate (pH 7.4) at 22 ^{0}C.

of thiols on the protein. This serves a dual purpose: the protein may not dimerize or aggregate by forming inter–protein disulfide bonds and a biotin group is present at the end of the linker, which can be used in combination with Avidin to immobilize the protein on the surface. The reaction was further allowed to proceed in the dark on ice for 30 minutes. The excess of dye and linkers was removed by gel filtration and the degree of labeling was estimated from the absorption spectrum of the protein. It was necessary to ensure that the degree of labeling with the fluorophore be kept very low (in our case we kept it at less than 5%) so that most molecules will carry only one fluorophore or no fluorophore at all. The protein conjugates were not purified further to separate labeled from unlabeled protein as the unlabeled protein would not be visible in the fluorescence microscope anyway and would not affect our results. Since an excess of biotin–PEG linker was used, the majority of the proteins will carry two or three linkers. Again, no attempts were made to separate the various species. The samples were aliquoted and stored at –80 ^{0}C till further use.

Fluorescence switching in bulk: To establish that the fluorescence of the dye–conjugated protein is sensitive to the redox state of the protein, steady–state fluorescence measurements were made in bulk. Upon excitation with 645 nm light, the fluorescence intensity was found to switch between high and low states when the enzyme was reduced and oxidized successively. An example of this switching is shown in Figure S3. We checked that the fluorophore itself or the unconjugated fluorophore in the presence of protein doesn't show such a switching, confirming that the FRET occurs only when the fluorophore is conjugated with the molecule. The switching ratio of the fluorescence was found to be ~85%. This is in agreement with a theoretical value of 84% calculated on the basis of the Förster formalism[42] with R= 24 Å and the orientational factor k = 0.67.

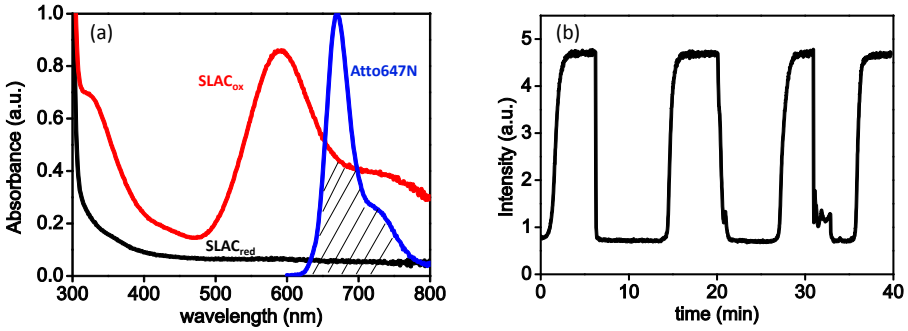

Figure S3: (a) Absorption spectrum of SLAC in the oxidized (red) and the reduced form (black). The emission spectrum of the fluorophore Atto 647N (blue) overlaps with absorption of the protein (hatched area) which is characteristic of the T1 Cu. (b) Fluorescence response of the K204C variant labeled with Atto647N when cycled between the reduced (high intensity, no FRET) and the oxidized (low intensity, high FRET) state using ascorbate for reduction under anaerobic condition and air for oxidation. This process can be repeated many times as shown above. Fluorophore only doesn't show any switching in these conditions.

Functionalization of coverslips: 0.17mm thickness (#1.5H) glass coverslips (Marienfield) were used for all immobilizations. The coverslips were first rinsed with acetone and water and then treated for 1 minute with 5% Hydrofluoric acid (HF) inside a fume hood.[43] (**Caution: HF is an extremely dangerous chemical and proper training is required before handling it.**) Immediately afterwards, they were rinsed several times with milliQ water and then treated with

$H_2O/NH_4OH/H_2O_2$ (5:1:1) bath at 70 ^{0}C. The coverslips were then rinsed several times with water and finally with ethanol. They were then flamed and used immediately for the next step or stored inside a desiccator until further use. The coverslips thus prepared contain active silanol groups which can readily react with silanes providing capability to functionalize the surface. The coverslips were then treated for 30 minutes with 1% solution of 3–(2–aminoethyl)aminopropyl trimethoxysilane in methanol containing 5% glacial acetic acid and afterwards washed extensively with methanol. Thereafter, they were dried with a gentle flow of clean nitrogen and then left in the desiccator overnight. The following day coverslips were treated with a 5 mg/ml solution of methoxy–peg–NHS (MW 2000, Laysan Bio) and biotin–peg–NHS (MW 3400, Laysan Bio) (NHS: N–hydroxysuccinimide) in 50mM sodium phosphate buffer at pH 8. The ratio of methoxy to biotin peg was kept at or below 1000:1 to ensure only few biotin functionalities are present on the surface. The treatment continued for 8–10 hours or overnight and then the coverslips were washed extensively with water and dried with a gentle flow of clean nitrogen. The coverslips thus functionalized were used immediately for protein immobilization or kept desiccated at –20 ^{0}C until required.

Protein Immobilization: The functionalized coverslips were placed in a sample holder and incubated with 20mM MOPS buffer (pH 7.4) for 5–10 minutes. The buffer was then removed and a drop of NeutrAvidin (0.1mg/ml, Pierce) was applied to the coverslip. After 1 minute the coverslip was washed with excess buffer to remove unbound NeutrAvidin. The dye–protein conjugate (10–30 pM) was then applied to the surface to obtain the desired density of molecules and allowed to stand for 1 min. The unbound protein was then removed by washing with excess buffer taking care not to withdraw the entire buffer from the top of the coverslip as it was found that enzyme denatured at the air interface. The sample thus prepared was imaged on a confocal microscope to locate single molecules of the protein.

Confocal Microscope: Single molecule fluorescence measurements were performed on a home built confocal microscope. A pulsed laser emitting at 639 nm was controlled by PDL 800–B (PicoQuant) laser driver at 40MHz repetition

rate. The beam was passed through a narrow band clean–up filter (LD01–640/8–25, Semrock) and coupled into a single mode optical fiber (OZ Optics). The beam was collimated to the desired diameter with an aspheric lens of suitable focal length near the fiber end and reflected via a dichroic mirror (ZT640RDC, Chroma) to an infinity corrected high numerical aperture (NA) oil immersion objective (1.4 NA, 100X oil, Zeiss). The sample to be imaged was mounted on a scanning stage controlled by nanopositioning piezo elements (P517.3CD, Physik Instrumente). The emission was collected through the same objective and filtered through an emission filter (ET655LP, Chroma) to clean up the reflected and scattered light that passes through the dichroic. The emission was then focused onto a 75 µm pinhole to filter the background and then on the active area of a single photon counting module (SPCM–AQR–14, Perkin Elmer). Data acquisition was performed by a photon counting PC–board (TimeHarp 200, PicoQuant) in the time–tagged–time–resolved mode. The hardware and data acquisition were controlled by using the software SymPhoTime (PicoQuant).

Data collection: The sample to be scanned was mounted on a scanning stage and was brought into the focal plane of the objective. The images of typically (40 x 40) $(\mu m)^2$ were recorded as x–y scans to locate single isolated SLAC molecules.To collect data from a single molecule, the laser was parked at one of the spots and measurement was made for 30 seconds to 5 minutes. One drawback of this method is that due to their limted photostability many fluorophores bleach within a few seconds. Thus, only the time traces containing more than 20 transitions between the upper and lower states were included for further analysis. A number of tests were performed to make sure that the observed fluctuations in the fluorescence intensity were not due to photophysics of the dye or to ET between the Cu and the dye. Firstly, in the absence of substrate, a stable signal corresponding to the low fluorescence state is observed and we did not encounter any dye photophysics (Figure S4a) under aerobic conditions (removal of the oxygen resulted in pronounced blinking of the dye in the presence as well as in the absence of reductant). This also ruled out that ET from the excited dye to the T1 Cu(II) center was responsible for the observed fluorescence intensity fluctuations. Secondly, under aerobic conditions a stable high fluorescence signal was observed in the presence of substrate and potassium

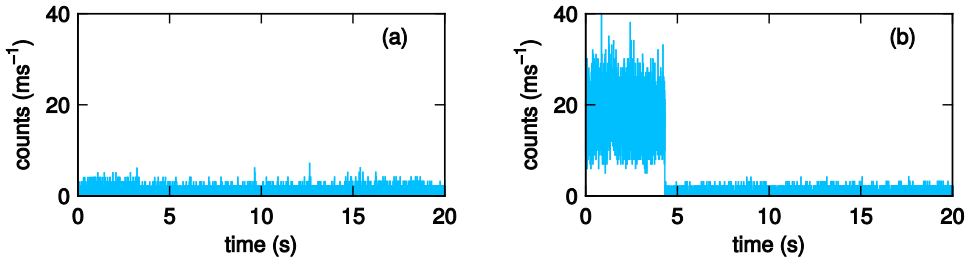

Figure S4: Binned time traces observed under aerobic conditions of (a) SLAC molecule in the oxidized state in the absence of DMPD and ascorbate. (b) SLAC molecule in the reduced state in the presence of DMPD (5mM), ascorbate (10mM) and KCN (1mM).

cyanide (KCN). KCN selectively and irreversibly inhibits the reaction of the enzyme with O_2 at the TNC so that the enzyme can not turn over[44] and the T1 Cu stays reduced leading to a high fluorescence signal (Figure S4b). This result ruled out that ET from the reduced T1 Cu(I) center to the excited dye was responsible for the observed fluorescence intensity fluctuations. It is conceivable that KCN affects the activity of the T1 site and that in the absence of KCN still ET from the Cu(I) to the dye label may occur. We verified from the bulk kinetics assays that the enzyme is completely inhibited by 1mM KCN. In a related experiment we observed that addition of 1 mM KCN to an aerobic solution of ~80 µM of SLAC diminished the 330 nm absorption band typical of the oxidized T3 Cu pair in the TNC while the 600 nm absorption due to the oxidized T1 site was not affected (Figure S5). Addition of 500µM ascorbate and ~5µM DMPD quickly and completely abolished the 300 nm and 600 nm absorptions, indicating complete reduction of the protein, which is otherwise not possible in the presence of O_2 (Figure S5). Finally, the T1 Cu absorption at 600 nm was recovered by addition of ~1mM $K_3[Fe(CN)_6]$ (Figure S5). We conclude that KCN selectively inhibits the O_2 binding at TNC while the T1 site can still reversibly be reduced and oxidized, which is consistent with previous studies.[44] To make sure that the dye doesn't show any critical behavior in the presence of substrate, NeutrAvidin, which cannot turnover, was labeled with the same dye and the fluorescence was also checked in the presence of substrate. Alternatively, Atto647N–biotin which consists of a biotin moiety linked to the fluorophore was used on the NeutrAvidin functionalized coverslips. In both cases no fluctuations

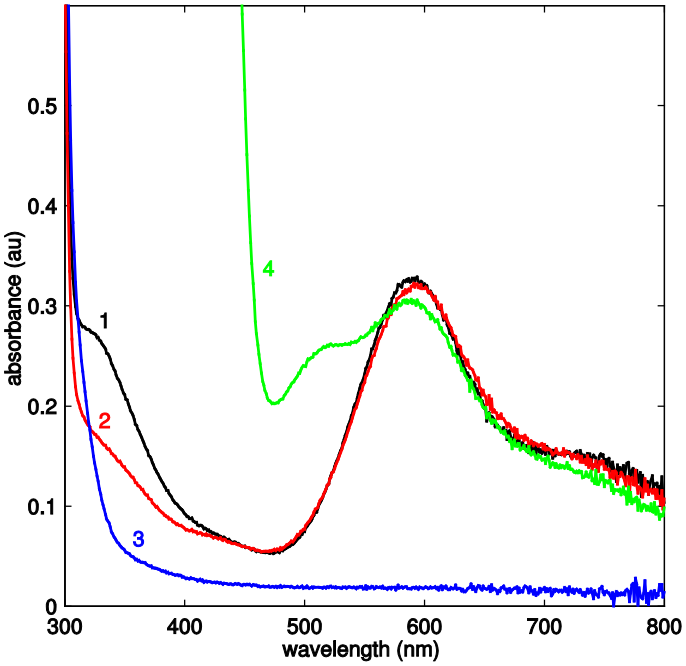

Figure S5: (1) Absorption spectra of resting SLAC in air saturated 200mM sodium phosphate buffer (pH 7.4) at ambient temperature; (2) 1 mM KCN added to 1; (3) 500 µM ascorbate and 5 µM DMPD added to 2; and (4) 1 mM $K_3[Fe(CN)_6]$ added to 3.

in fluorescence were observed under aerobic conditions and in the presence of reductant and the traces similar to those shown in Figure S4b were observed. Only when the substrate is present in the solution above the immobilized SLAC, time traces like the ones shown in Fig 2a (main manuscript) were observed.

Data analysis: Data analysis was performed using MATLAB and C in three steps. In the first step the traces containing count rates less than 300 Hz were discarded and the remaining ones were binned and inspected one by one. Binning was performed only to visualize the data. Then the markers were set up to mark the portion of the time trace which contained useful information and to separate it from the remainder where, for example, the fluorophore had bleached. This was necessary for the second step when the raw time traces were submitted to the changepoint algorithm kindly provided by Prof. Haw Yang (Princeton University, USA). The algorithm is bin–free and uses a recursive binary segmentation of a trajectory (containing only photon arrival times) and

uses several statistical tests to determine the maximum number of changepoints where the count rate changes with a certain confidence interval. We can choose in the beginning the confidence intervals on the type–I (false positive) and the type–II (false negative) errors. We chose the values that suited best the description of our data while still preserving information about the fast dynamics. Complete details about the algorithm have been published elsewhere.[33] The estimated error rate in the changepoint determination amounts to 1% or less.[45] The spurious dynamics that are not associated with the activity of enzyme are taken care of during the next step of the analysis. Basically, by applying this algorithm, we have filtered the poissonian noise from the data and assigned intensity levels, and this results in traces as shown in Fig 2b red trace (main manuscript). In the next step, dwell times of the molecule in the on or off state were obtained and binned in the form of a histogram. The data could be well fitted with a single exponential. The first time bin contains the most uncertainty and was not used when fitting the data. Analysis of dwell times in the on state provided the decay rate of the on state (k_{on}) which is equal to the electron transfer rate constant ($k_{T1\rightarrow TNC}$) from T1 Cu to TNC. Similar analysis of the dwell times in the off state provided the decay rate of the off state (k_{off}) which equals the sum of the rate of electron transfer from TNC to T1 Cu ($k_{TNC\rightarrow T1}$) and the rate of reduction by DMPD: $k_{off} = k_{TNC\rightarrow T1} + k_S[DMPD]$ in which k_S is the second order rate constant for the reduction of the T1 Cu by DMPD (see also Figure S6).

The rate constants were combined in histograms whereby each individual k value was weighed by the inverse of its variance as obtained from the exponential fit of the dwell times. Thus, the time traces which contained a low number of transitions due to photobleaching received less weight because of low statistics. The logarithms of the rate constants appear to represent a bell shaped curve corresponding to a normal distribution of the free energy of activation (Figure S7).

The rates of forward electron transfer, thus, follow a lognormal distribution (see Figure 2d, main manuscript). Although histograms were plotted to visualize the distribution, the fitting was performed on the unbinned data. To demonstrate

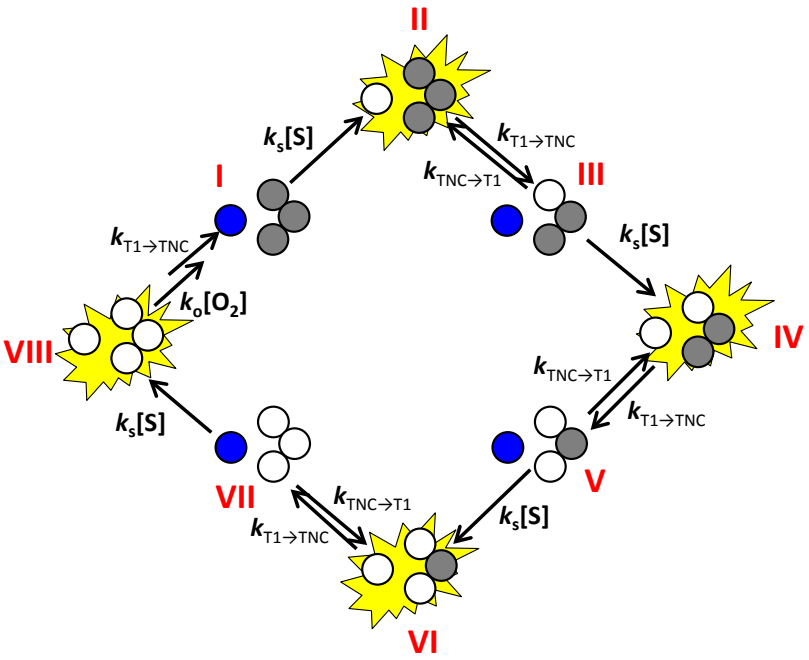

Figure S6: Cartoon representation of the enzyme cycle highlighting the sequential electron transfer steps. Oxidized T1 Cu is depicted in dark blue and the oxidized Cu's in the TNC in grey. Reduced Cu sites are depicted colorless. The fluorescence emission state of the molecule is shown as a bright yellow star, i.e. when the T1 Cu is reduced. Oxygen binding is supposed to occur, in this scheme, in state VIII but may also occur earlier, for instance in state V, VI or VII.

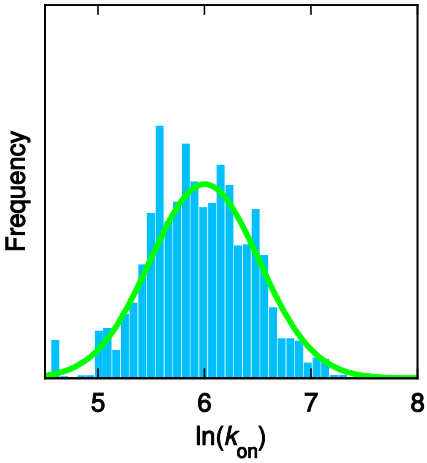

Figure S7: Distribution of log k_{on} values corresponding to the data shown in Figure 2d of main manuscript. The green line is the fit to the corresponding normal distribution.

that the distribution of k_{on} is independent of the substrate concentration, the distribution of rates measured at 50 µM and 5mM DMPD concentration are shown in Figure S8(a, b). It is evident that the mean and the distribution are essentially identical at the two concentrations even though the catalytic reaction rates at these concentrations are very different. Similarly, the distribution of k_{off} at these two concentrations are shown in Figure S8(c, d). It can be clearly noticed that the k_{off} distribution is dependent on substrate concentration as expected. We utilized these data to estimate the rate of back electron transfer (from TNC to T1 Cu) and the second order rate constant for the reduction of T1 Cu by DMPD.

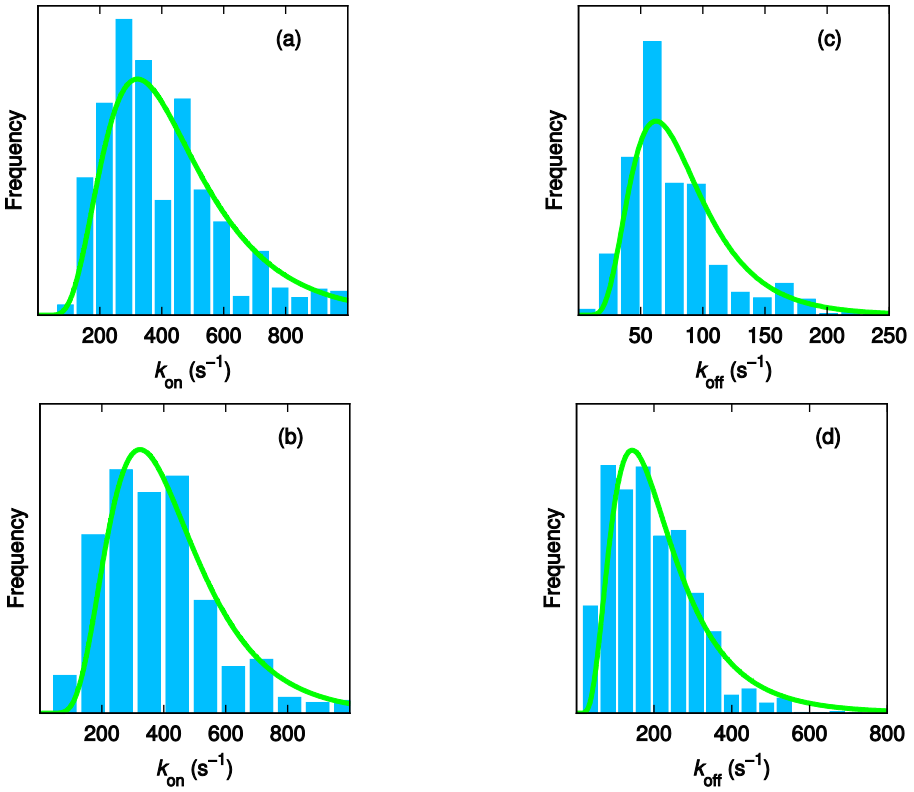

Figure S8: The distribution of ET rates across many molecules at different substrate concentrations. Distribution of (a) k_{on} across 176 individual molecules at 50 µM DMPD and (b) across 196 individual molecules at 5 mM DMPD concentration. (c) and (d) represent the distribution of k_{off} for the same molecules as shown in (a) and (b). Notice the different horizontal scales in (c) and (d). Ascorbate concentration = 10mM. The green lines are fits to the data corresponding to a lognormal distribution although, strictly speaking, (c) and (d) are the sum of two lognormal distributions.

Calculation of the reorganization energy (λ_{TOT}): The semiclassical expression of Marcus theory was used which is given by:[46]

$$k_{et} = \sqrt{\frac{4\pi^2}{h^2 \lambda RT}} H_{DA}^2 exp\left\{-\frac{(\Delta G^0 + \lambda)^2}{4\lambda RT}\right\}$$

Where λ is the reorganization energy, H_{DA} is the electronic coupling matrix element between the donor and the acceptor and $-\Delta G^0$ is the driving force.
The activationless ET rate (k^0) was calculated by using the following expression in context of the Marcus theory.

$$k^0 = 10^{13} exp\{-\beta(r - r_0)\}$$

where β is the distance dependence of the decay of H_{AB} having a value of 1 $Å^{-1}$,[37] r is the distance between the donor and the acceptor and r_0 is the distance where the k^0 reaches a value of 10^{13} (2.8 Å).

Thus, the simplified form of the Marcus equation can be written as

$$k_{et} = k^0 exp\left\{-\frac{\Delta G^{\ddagger}}{RT}\right\}$$

which provides the activation energy (ΔG^*) and the associated uncertainty, with

$$\Delta G^{\ddagger} = \frac{(\Delta G^0 + \lambda)^2}{4\lambda}$$

from where the reorganization energy and the associated uncertainty were estimated.

4.4 References

[1] Farver, O.; Pecht, I. *Coord. Chem. Rev.* **2011**, *255*, 757.

[2] Farver, O.; Wherland, S.; Pecht, I. *J. Biol. Chem.* **1994**, *269*, 22933.

[3] Tollin, G.; Meyer, T. E.; Cusanovich, M. A.; Curir, P.; Marchesini, A. *Biochim. Biophys. Acta* **1993**, *1183*, 309.

[4] Special Issue on Single-Molecule Spectroscopy. Acc. Chem. Res. 2005, 38, 503.

[5] English, B. P.; Min, W.; van Oijen, A. M.; Lee, K. T.; Luo, G.; Sun, H.; Cherayil, B. J.; Kou, S. C.; Xie, X. S. *Nat. Chem. Biol.* **2006**, *2*, 87.

[6] Smiley, R. D.; Hammes, G. G. *Chem. Rev.* **2006**, *106*, 3080.

[7] van Oijen, A. M.; Loparo, J. J. *Annu Rev Biophys* **2010**, *39*, 429.

[8] Lu, H. P.; Xun, L.; Xie, X. S. *Science* **1998**, *282*, 1877.

[9] Pudney, C. R.; Lane, R. S.; Fielding, A. J.; Magennis, S. W.; Hay, S.; Scrutton, N. S. *J. Am. Chem. Soc.* **2013**, *135*, 3855.

[10] Kuznetsova, S.; Zauner, G.; Aartsma, T. J.; Engelkamp, H.; Hatzakis, N.; Rowan, A. E.; Nolte, R. J.; Christianen, P. C.; Canters, G. W. *Proc. Natl. Acad. Sci. U. S. A.* **2008**, *105*, 3250.

[11] Goldsmith, R. H.; Tabares, L. C.; Kostrz, D.; Dennison, C.; Aartsma, T. J.; Canters, G. W.; Moerner, W. E. *Proc. Natl. Acad. Sci. U. S. A.* **2011**, *108*, 17269.

[12] Tabares, L. C.; Kostrz, D.; Elmalk, A.; Andreoni, A.; Dennison, C.; Aartsma, T. J.; Canters, G. W. *Chem. Eur. J.* **2011**, *17*, 12015.

[13] Zhang, Z.; Rajagopalan, P. T.; Selzer, T.; Benkovic, S. J.; Hammes, G. G. *Proc. Natl. Acad. Sci. U. S. A.* **2004**, *101*, 2764.

[14] Solomon, E. I.; Sundaram, U. M.; Machonkin, T. E. *Chem. Rev.* **1996**, *96*, 2563.

[15] Solomon, E. I.; Augustine, A. J.; Yoon, J. *Dalton Trans.* **2008**, 3921.

[16] Farver, O.; Wherland, S.; Koroleva, O.; Loginov, D. S.; Pecht, I. *FEBS J.* **2011**, *278*, 3463.

[17] Farver, O.; Tepper, A. W.; Wherland, S.; Canters, G. W.; Pecht, I. *J. Am. Chem. Soc.* **2009**, *131*, 18226.

[18] Wherland, S.; Farver, O.; Pecht, I. *ChemPhysChem* **2005**, *6*, 805.

[19] Kuznetsova, S.; Zauner, G.; Schmauder, R.; Mayboroda, O. A.; Deelder, A. M.; Aartsma, T. J.; Canters, G. W. *Anal. Biochem.* **2006**, *350*, 52.

[20] Machczynski, M. C.; Vijgenboom, E.; Samyn, B.; Canters, G. W. *Protein Sci.* **2004**, *13*, 2388.

[21] Skalova, T.; Dohnalek, J.; Ostergaard, L. H.; Ostergaard, P. R.; Kolenko, P.; Duskova, J.; Stepankova, A.; Hasek, J. *J. Mol. Biol.* **2009**, *385*, 1165.

[22] Skalova, T.; Duskova, J.; Hasek, J.; Stepankova, A.; Koval, T.; Ostergaard, L. H.; Dohnalek, J. *Acta Crystallogr., Sect. F: Struct. Biol. Cryst. Commun.* **2011**, *67*, 27.

[23] Nakamura, K.; Go, N. *Cell. Mol. Life Sci.* **2005**, *62*, 2050.

[24] Tepper, A. W. J. W.; Milikisyants, S.; Sottini, S.; Vijgenboom, E.; Groenen, E. J. J.; Canters, G. W. *J. Am. Chem. Soc.* **2009**, *131*, 11680.

[25] Gupta, A.; Nederlof, I.; Sottini, S.; Tepper, A. W.; Groenen, E. J.; Thomassen, E. A.; Canters, G. W. *J. Am. Chem. Soc.* **2012**, *134*, 18213.

[26] See Supporting Information

[27] Wong, L. S.; Khan, F.; Micklefield, J. *Chem. Rev.* **2009**, *109*, 4025.

[28] Heering, H.; Canters, G. *Engineering the Bioelectronic Interface: Applications to Analyte Biosensing and Protein Detection; Davis, JJ, Ed* **2010**, 120.

[29] Durán, N.; Rosa, M. A.; D'Annibale, A.; Gianfreda, L. *Enzyme Microb. Technol.* **2002**, *31*, 907.

[30] Prime, K. L.; Whitesides, G. M. *Science* **1991**, *252*, 1164.

[31] Ha, T.; Rasnik, I.; Cheng, W.; Babcock, H. P.; Gauss, G. H.; Lohman, T. M.; Chu, S. *Nature* **2002**, *419*, 638.

[32] Rasnik, I.; Myong, S.; Cheng, W.; Lohman, T. M.; Ha, T. *J. Mol. Biol.* **2004**, *336*, 395.

[33] Watkins, L. P.; Yang, H. *J. Phys. Chem. B* **2005**, *109*, 617.

[34] McKinney, S. A.; Joo, C.; Ha, T. *Biophys. J.* **2006**, *91*, 1941.

[35] Tepper, A. W. J. W.; Aartsma, T. J.; Canters, G. W. *Faraday Discuss.* **2011**, *148*, 161.

[36] Strange, R. W.; Murphy, L. M.; Dodd, F. E.; Abraham, Z. H.; Eady, R. R.; Smith, B. E.; Hasnain, S. S. *J. Mol. Biol.* **1999**, *287*, 1001.

[37] Gray, H. B.; Winkler, J. R. *Q. Rev. Biophys.* **2003**, *36*, 341.

[38] Voityuk, A. A. *J. Phys. Chem. B* **2011**, *115*, 12202.

[39] Heppner, D. E.; Kjaergaard, C. H.; Solomon, E. I. *J. Am. Chem. Soc.* **2013**, *135*, 12212.

[40] Salverda, J. M.; Patil, A. V.; Mizzon, G.; Kuznetsova, S.; Zauner, G.; Akkilic, N.; Canters, G. W.; Davis, J. J.; Heering, H. A.; Aartsma, T. J. *Angew Chem Int Ed Engl* **2010**, *49*, 5776.

[41] Davis, J. J.; Burgess, H.; Zauner, G.; Kuznetsova, S.; Salverda, J.; Aartsma, T.; Canters, G. W. *J. Phys. Chem. B* **2006**, *110*, 20649.

[42] Lakowicz, J. R. *Principles of Fluorescence Spectroscopy*; Springer, 2007.

[43] Betzig, E.; Patterson, G. H.; Sougrat, R.; Lindwasser, O. W.; Olenych, S.; Bonifacino, J. S.; Davidson, M. W.; Lippincott-Schwartz, J.; Hess, H. F. *Science* **2006**, *313*, 1642.

[44] Meyer, T. E.; Marchesini, A.; Cusanovich, M. A.; Tollin, G. *Biochemistry* **1991**, *30*, 4619.

[45] Terentyeva, T. G.; Engelkamp, H.; Rowan, A. E.; Komatsuzaki, T.; Hofkens, J.; Li, C. B.; Blank, K. *ACS Nano* **2012**, *6*, 346.

[46] Marcus, R. A.; Sutin, N. *Biochim. Biophys. Acta* **1985**, *811*, 265.

Chapter 5

General Conclusions and Outlook

This chapter provides general conclusions relating to the work presented in this thesis. Currently ongoing experiments and promising future directions are also discussed in brief. For conclusions related to a specific chapter, the reader is referred to the Ist page of either chapter which contains a graphical abstract of the study concerned.

The research presented in this thesis was aimed to investigate the catalytic mechanism of a newly discovered protein: small laccase (SLAC) from *Streptomyces coelicolor*. SLAC, like other multicopper oxidases (MCO's), catalyzes the four electron reduction of O_2 to H_2O for which the electrons are donated by a reducing co–substrate. MCO's are found in all life forms and have diverse roles. However, this category of enzymes is gaining increasing attention by the energy industry. This is because the enzyme, when immobilized on a conducting electrode, can function as a (bio)cathode in a fuel cell. To be able to exploit full potential of such biochemical electrodes, it is important to understand their mechanism of operation. In the case of studying SLAC, there is an additional interest, i.e., to understand its evolutionary relationship with other multicopper proteins as postulated by phylogenetic analysis.

Chapter 2 of this thesis focuses on understanding the mechanism of O_2 reduction at the SLAC trinuclear Cu cluster (TNC). It was demonstrated, using a variety of spectroscopic and kinetics measures, that a tyrosine residue (Y108) may have a participatory role in the reduction of O_2 at the TNC. In addition, this tyrosine residue appears to be conserved among the sequences of the homologous two–domain multicopper oxidases and also seems to have structural homology with human ceruloplasmin. It is postulated that the role of Y108 may become crucial when there is an imbalance of oxidizing and reducing equivalents in the environment surrounding the protein. Although, kinetics and spectroscopic data strongly suggest a role for Y108 during steady–state turnover, we have not yet established its presence under these conditions. Further, the characterization of the biradical species that was observed upon reaction of type 1 depleted (T1D) SLAC is still lacking. Finally, Y108A variant doesn't show formation of transient paramagnetic species but Y108F does. Is this an oxidized phenylalanine or another nearby residue (W284) that we are observing? A number of the above questions may be answered by trapping the intermediates on a short time–scale using rapid–freeze–quench and study them with multifrequency EPR. These experiments are currently being performed by Ms. Faezeh Nami, in the group of Prof. Edgar J. J. Groenen and Prof. Gerard W. Canters. Although the mutations at position Y108 had a clear effect on enzyme kinetics, the effect was small. It would be interesting to study the pH dependence of the steady–state and pre–

steady–state kinetics to establish conditions where the role of Y108 residue in the enzyme mechanism can be concluded with certainty.

Chapter 3 of this thesis was partly a follow up of the study presented in Chapter 2. The main question to be answered was: Does the enzyme (SLAC) really need a stock of 5 redox active components (4 Cu's and Y108) at any given time and if not, then which ones are actually essential? It could be concluded, from Cu depletion and kinetics experiments, that the presence of type 2 (T2) Cu is not essential for the enzyme activity. Moreover, the H102G/Y/F/Q mutations led to a more than 2 orders of magnitude drop in enzyme activity but did not lead to T2 Cu depletion. Though preliminary, the experiments in this chapter seem to suggest that SLAC is capable of turning over with as little as three Cu's in its active site, which is so far not observed for any of the MCO's studied. The question to be answered is: How is it possible and why might nature have recruited a fourth Cu site (the T2 Cu)? The latter might be reformulated and asked as: Whether, in the evolution of multicopper blue proteins, the T2 Cu site evolved first or the T3 Cu site? Future investigations may focus on understanding the steady–state kinetics of the T2 Cu depleted (T2D) SLAC to realize whether the effect on turnover rate is related to the binding of O_2 (K_M of O_2) at the TNC. Further, stopped–flow and rapid–freeze–quench EPR experiments may be utilized to identify the early intermediates in the reaction of fully reduced T2D SLAC or H102G/F variants with O_2. We are currently collaborating with Dr. Igor Nederlof to solve the crystal structure of the T2D SLAC and the H102G/Y/F/Q variants to confirm whether the removal of Cu or the mutation of a Cu coordinating residue disturbs the active site or overall fold of the enzyme which may explain the difference in activity. It will be interesting to see whether the T2D SLAC can be reconstituted back with Cu(II) and/or other transition metal ions like Zn(II), Hg(II) or Co(II) and observe the effect of such enzyme forms on their activity and spectroscopy.

Chapter 4 of this thesis focused on studying the electron transfer (ET) processes between the T1 and TNC of SLAC. A special interest was to measure the intramolecular ET during steady–state turnover and to do so we studied the enzyme kinetics at the single molecule level. We could, for the first time, measure

the forward (T1→TNC) and backward (TNC→T1) electron transfer rate constants (*k*'s) for a molecule under steady–state turnover conditions. It was demonstrated that there exists a heterogeneity/disorder across *k*'s measured for many molecules of the population and we were able to obtain the mean and spread of this distribution. The broad and asymmetric *k* distribution actually corresponds to a narrow and symmetric distribution of activation energy which was elaborated further in terms of reorganization energy and driving force. A reasonable and straightforward follow–up of the study would be to measure the ET rate constants with different reducing substrates and at varying O_2 concentrations. In addition, the protein may be labeled with a different fluorophore to measure the ET kinetics. Since we are measuring an intramolecular process, any of the extrinsic changes mentioned above should yield similar results. A more stringent approach would be to utilize a second label (say tryptophan fluorescence) or another extrinsically attached fluorophore to monitor the redox changes at the TNC and then obtain a cross correlation from the two color measurements.

Summary

Multicopper oxidases (MCO's) are present in all life forms including plant, fungi and humans. The most well studied members of the MCO family are the laccases (Lc's) and ascorbate oxidase (AO). Although the biological role of most of these proteins is unknown, they invariably catalyze oxidation of substrate molecules ranging from phenols to aromatic amines to low–valent metal ions. The electrons gathered from the substrates are transferred to oxygen which is converted to water. Each enzymatic turnover requires four reducing equivalents in the form of four $1e^-$ donors, one molecule of O_2 and, of course, four protons.

In this thesis, we have studied the structure–function relationship of a newly discovered member of the family of MCO's: small laccase (SLAC) derived from *Streptomyces coelicolor*. The journey starting from the discovery of the unique characteristics of this protein and the new results obtained in this thesis are summarized in the following paragraphs.

In 2004, Michael Machczynski discovered that the growth media of *S. coelicolor* exhibited phenoloxidase activity (Protein Sci. 2004, 13, 2388). Disruption of the gene encoding SLAC in the bacterium abolished this activity. To study this protein in more detail, the corresponding gene was cloned into a pET vector suited for high level overexpression in *E. coli*. Recombinant SLAC, thus produced, contained a full load of four Cu ions and possessed laccase activity but contained only 343 amino acids contrary to the larger molecular weights of known Lc's and AO. Later, the crystal structure of SLAC revealed that this protein exists as a homotrimer, where each monomer consists of only two cupredoxin domains (unlike three domains for Lc's and AO). This new discovery was quickly adapted into the existing phylogenetic analysis which had predicted the presence of such multimeric Cu proteins. The evolutionary theory had suggested that the Lc's and AO might have evolved from trimeric two–domain MCO's. The obvious and immediate question that followed was: The structural similarities of these different MCO species are obvious but do they also follow the same enzyme mechanisms?

The first investigation into this question was made by Armand Tepper. He showed that the reaction of fully reduced type 1–depleted SLAC with O_2 resulted in the formation of a biradical intermediate which has not been observed for other Lc's (J. Am. Chem. Soc. 2009, 131, 11680). Instead, a similar reaction of type 1–depleted laccases, results in the formation of a long lived peroxide intermediate. Based on transient kinetics and spectroscopic measurements, it was proposed that the two spins in the biradical intermediate reside on two cofactors in the vicinity of each other: the type 2 (T2) Cu and a tyrosine, possibly Y108. While, it was clear that the reactivity of SLAC with O_2 is different from other Lc's, this observation demanded further investigation of the enzyme mechanism. The challenge was to identify the position of the organic radical, i.e. if the unpaired spin is localized at the Y108 or not, and to understand its involvement in enzyme catalysis, if any.

Chapter 2 details the efforts that I have undertaken to identify the position of the organic radical within SLAC. Mutants were prepared where the tyrosine residue at position 108 was replaced with an alanine (Y108A) or a phenylalanine (Y108F) residue in both the wild–type and the type 1–deplted SLAC. To support the comparisons in the enzyme activity or spectroscopy between the native enzyme and the variants, the crystal structures of the new variants were uncovered. These revealed that the active site and overall fold of the variants was essentially identical to that of the native enzyme. The steady–state kinetics measurements revealed that both Y108A and Y108F variants were less active than the wild–type SLAC, a finding that is compatible with a possible role of Y108 residue in the enzyme mechanism. Further, reaction of fully reduced T1D–Y108A SLAC with O_2 did not result in the formation of any biradical intermediate. Instead, a new kind of intermediate was observed resembling the peroxide intermediate, where O_2 has been reduced at the TNC by two electron equivalents. Thus, it was confirmed that Y108 gets oxidized and forms a radical. Y108 was also found to be conserved across all known homologous MCO's and also with human ceruloplasmin. We propose that Y108 gets oxidized to prevent formation of reactive oxygen species under the circumstances when there is an imbalance of reducing and oxidizing equivalents in the milieu. However, this raised an immediate question: Does SLAC really need a stock of five redox active

components (four Cu's and Y108) at any given point of time to carry out four electron reduction of O_2 to H_2O? If not, then which ones are actually essential?

Chapter 3 contains preliminary data that partly answers this question. The type 2 (T2) Cu of the SLAC was selectively removed. The removal of T2 Cu was confirmed by Electron Paramagnetic Resonance (EPR) and Atomic Absorption Spectroscopy (AAS). T2 Cu depleted (T2D) ascorbate oxidase and laccases have been found to be completely devoid of catalytic activity. However, T2D SLAC still possessed almost 1/3rd of the activity of the native enzyme. One hypothesis could be that Y108 replaces the role of T2 Cu when this Cu has been removed. To confirm this hypothesis, we took another route to prepare T2D SLAC. We made mutations to replace one of the T2 Cu coordinating histidine residues (H102) with a glycine (H102G), tyrosine (H102Y), phenylalanine (H102F) or glutamine (H102Q). To our surprise, EPR and AAS revealed that these variants may still possess the T2 Cu. Moreover, the activity of the variants was more than 2 orders of magnitude lower than the activity of the native enzyme. Thus, we could conclude that H102 is crucial for enzyme activity. Further experiments are required to understand how the H102 residue modulates enzyme activity and to answer the question: Can a redox active amino acid really replace the role of a Cu site?

Chapter 4 of this thesis takes a slightly different stand from the previous two chapters. In this chapter, instead of looking at the reactivity of the protein with O_2, we attempted to understand the communication between the T1 Cu and the trinuclear Cu cluster (TNC) sites of SLAC. The main goal was to study the electron transfer (ET) kinetics between the two Cu centers during steady–state turnover. We made use of a single molecule approach to monitor the ET kinetics. A method recently introduced by Sofya Kuznetsova (Anal. Biochem. 2006, 350, 52) was used here which allows fluorescence readout of the redox state of the protein cofactor, T1 Cu in the present case. Thus, by monitoring the fluctuations in the fluorescence count rate from a single molecule that is turning over, the lifetime or rate constant of the decay of the redox state of the T1 Cu (corresponding to the fluorescence intensity) could be obtained. SLAC variants were prepared to allow site specific labeling and immobilization of protein on

transparent glass surface. The fluorescence–count–rate fluctuations of single turning–over SLAC molecules were recorded on a home–built confocal microscope. From these data, we extracted ET rate constants from T1 to TNC (and back) and binned them in a histogram. The forward and backward ET rates across many molecules follow a log–normal distribution with means of 460 and 85 s^{-1}, respectively, corresponding to activation energies of 347 and 390 meV for the forward and backward ET rates. In the context of Marcus theory, the driving force and reorganization energy were calculated from above data and amount to 0.043 eV and 1.5 eV, respectively. The distribution of electron transfer rates shows more than one order of magnitude spread of these rate constants across many molecules which corresponds to a small 30 meV spread in activation energy or 0.1 eV in reorganization energy. Thus, the single–molecule strategy used here not only allows monitoring the internal dynamics of enzymes under steady–state, it is much more informative than the ensemble measurements where the heterogeneity in the sample (extrinsic or intrinsic) can be observed.

Chapter 5 provides general conclusions to the work presented in this thesis. In addition, it also provides promising directions for future research to gain more insight into the SLAC mechanism and advance our knowledge of the mechanism of MCO's in general.

Samenvatting

Multi–copper oxidases (MCO's) zijn in alle levende organismen aanwezig zoals planten, schimmels en de mens. De meest bestudeerde vertegenwoordigers van deze 'MCO–familie' zijn de laccases (LC's) en ascorbaat oxidase (AO). Hoewel de biologische functie van het grootste deel van deze eiwitten niet precies bekend is, weten we wel dat ze oxidatie–reductie reacties katalyseren zoals de oxidatie van fenolen tot aromatische aminen en de oxidatie van metaalionen in een lage oxidatietoestand naar metaalionen met een hogere oxidatietoestand (bv. van Fe(II) naar Fe(III) of van Cu(I) naar Cu(II)). Bij de oxidatie–reacties komen electronen vrij die worden overgedragen aan zuurstof (O_2), dat tot water (H_2O) wordt gereduceerd. Voor elke enzymatische turnover zijn vier donormoleculen nodig die elk één electron aanleveren, één zuurstofmolecuul (O_2) dat de electronen opneemt, en vier protonen.

Dit proefschrift beschrijft het onderzoek naar de relatie tussen de structuur en de functie van een recent ontdekt lid van de MCO–familie: 'small laccase' (SLAC) afkomstig van *Streptomyces coelicolor*. Het relaas van de reis die met de ontdekking van dit eiwit begint en daarna de eigenschappen van dit eiwit in kaart brengt, wordt hieronder samengevat.

Dr. Michael Machczynski ontdekte in 2004 dat de groeimedia van *S. coelicolor* een nog niet eerder beschreven fenoloxidase activiteit vertoonden (Protein Sci. 2004, 13, 2388). De uitschakeling van het gen dat in de bacterie voor SLAC codeert, bleek deze activiteit te stoppen. Ter verdere bestudering van dit SLAC eiwit werd het desbetreffende gen gekloneerd in een pET vector in *E.coli* zodat het eiwit tot hoge expressie gebracht kon worden. Het zo verkregen (recombinante) eiwit bleek vier Cu–ionen per eiwitmolecuul te bevatten en ook laccase–activiteit te vertonen. Het eiwit bleek opgebouwd te zijn uit slechts 343 aminozuren in tegenstelling tot de grotere laccases (LC's) en ascorbaatoxidase (AO). Vervolgonderzoek van de drie–dimensionale structuur van het eiwit (uitgevoerd m.b.v. Röntgendiffractie) toonde aan dat dit eiwit opgebouwd is als een homotrimeer, en dat elke monomeer uit twee zgn. cupredoxine domeinen bestaat (in tegenstelling tot de drie domeinen van de LC's en AO). Deze

ontdekking leidde tot een aanpassing van de evolutionaire stamboom van de MCO's op basis waarvan vroeger het voorkomen van zgn 'two–domain MCO's' was voorspeld maar nog nooit was bevestigd. De voor de hand liggende vraag was nu: de structurele gelijkenissen tussen deze verschillende MCO–soorten ('two–domain' vs. three–domain' MCO's) zijn evident maar werken deze enzymen ook volgens hetzelfde mechanisme?

De eerste in onze groep die dit onderzocht was Dr. Armand Tepper. Hij toonde aan dat zich een 'biradicaal intermediair' vormt wanneer volledig gereduceerd SLAC, ontdaan van één van zijn koper atomen (zgn. T1D SLAC, waarin het type–1 Cu niet meer aanwezig is) reageert met zuurstof (J. Am. Chem. Soc. 2009, 131, 11680). Een dergelijk biradicaal was nog niet eerder waargenomen bij de laccases (LC's). Wel leidt bij de T1D–laccases de reactie met zuurstof tot de vorming van een langlevend peroxide intermediair. Op basis van kinetische en spectroscopische metingen werd geconcludeerd dat de twee spins in het biradicaal van SLAC zich bevinden op twee naast elkaar liggende cofactoren: type–2 (T2) koper en mogelijk een tyrosine, vermoedelijk Y108. Hoewel het duidelijk was dat de reactiviteit van SLAC met O_2 verschilt van die van de andere laccases, vergt deze waarneming nader onderzoek naar het mechanisme van het enzym. De uitdaging was om de locatie van de spins te bepalen d.w.z. dat er nagegaan moest worden of één van de ongepaarde spins op Y108 zit of niet en of dit residu (Y108) een rol speelt bij de enzymkatalyse.

Hoofdstuk 2 beschrijft het onderzoek dat is uitgevoerd om de aard en locatie van het organische radicaal (Y108$^{\bullet}$) te identificeren. Mutanten werden gemaakt waarbij het tyrosine–residu op positie 108 was vervangen door een alanine (Y108A) of een fenylalanine (Y108F) in zowel het oorspronkelijke ('*wild type*') als T1D SLAC. Om de enzymactiviteit en de spectroscopische eigenschappen van het wild–type enzym en de varianten goed te kunnen analyseren, werden de kristalstructuren van de nieuwe varianten bepaald. Die toonden aan dat de structuur van het actieve centrum en de gehele 3–dimensionale structuur van de varianten grotendeels identiek zijn aan die van het wild–type enzym. De gemeten 'steady–state' kinetiek toonde aan dat zowel de Y108A– als de Y108F–variant minder actief waren dan wild–type SLAC (in overeenstemming met een

mogelijke rol van het Y108 residu in het enzymmechanisme). De reactie van volledig gereduceerd T1D–Y108A SLAC met O_2 leidde niet tot de vorming van een biradicaal. Integendeel, een nieuw soort intermediair dat op het peroxide intermediair lijkt werd waargenomen. Dit peroxide onstaat uit O_2 door opname van 2 electronen. Dit vormde de bevestiging dat Y108 geoxideerd word in het wild–type enzym en daarmee verandert in een radicaal. Ook werd aangetoond dat dit tyrosine aanwezig is in alle bekende 'two–domain' MCO–homologen en ook in menselijk ceruloplasmine. Wij veronderstellen dat Y108 geoxideerd wordt om te voorkomen dat er vorming van reactieve zuurstofproducten optreedt onder omstandigheden waarbij in het milieu de reducerende en oxiderende equivalenten niet in balans zijn. Dit roept nochtans onmiddellijk een nieuwe vraag op: heeft SLAC werkelijk vijf redoxactieve componenten nodig (vier Cu's en Y108) om op elk willekeurig moment vier elektronen aan O_2 over te kunnen dragen om H_2O te vormen? Als dat niet het geval is, welke van deze componenten zijn dan onmisbaar?

Hoofdstuk 3 bevat voorlopige gegevens die de bovengenoemde vraag gedeeltelijk beantwoorden. Het type–2 (T2) Cu van SLAC werd selectief verwijderd. De verwijdering van type–2 Cu werd m.b.v. Elektron Paramagnetische Resonantie (EPR) en Atomaire Absorptie Spectroscopie (AAS) bevestigd. Uit werk van anderen was al gebleken dat ascorbaat oxidase en laccases, ontdaan van type–2 Cu (T2D), hun katalytische activiteit verliezen. Maar T2D–SLAC bezit nog bijna 1/3 van de activiteit van het wild–type enzym. De veronderstelling was dat Y108 de functie van het type–2 Cu overneemt wanneer dit Cu wordt verwijderd. Om deze aanname te bevestigen, hebben wij bij de bereiding van T2D SLAC een alternatieve procedure gevolgd. Door middel van mutaties werd één van de type–2 Cu coördinerende histidines (H102) door een glycine (H102G), tyrosine (H102Y), fenylalanine (H102F) of glutamine (H102Q) vervangen. Opmerkelijk genoeg toonden EPR en AAS aan dat het T2 Cu in deze varianten nog steeds aanwezig was. Maar de activiteit van de varianten was meer dan 2 ordes van grootte lager dan de activiteit van het wild–type enzym. Hieruit konden we concluderen dat H102 cruciaal is voor de enzymactiviteit. Nadere experimenten zijn nodig om inzicht te krijgen in de wijze waarop H102 de enzymactiviteit reguleert en om een antwoord te krijgen op de

vraag: kan een redox–actief aminozuur werkelijk de rol van een Cu co–factor overnemen?

Hoofdstuk 4 van dit proefschrift is complementair aan de vorige twee hoofdstukken. In hoofdstuk 4 hebben we niet gekeken naar de reactiviteit van het eiwit met O_2, maar in plaats daarvan hebben we geprobeerd inzicht te krijgen in hoe de uitwisseling van electronen tussen het T1 Cu en het trinucleaire Cu–cluster (TNC) van SLAC verloopt. Het belangrijkste doel hiervan was om onderzoek te doen naar de kinetiek van de elektronenoverdracht (ET) tussen de twee Cu–centra tijdens steady–state turnover. Daarvoor hebben wij gebruik gemaakt van single–molecule technieken. Een methode die onlangs door Sofya Kuznetsova werd geïntroduceerd (Anal. Biochemie. 2006, 350, 52 werden), is toegepast om aan de hand van de fluorescentie van een covalent aangebracht fluorescerend label de redox toestand van het T1 Cu af te lezen. Door het meten van de fluctuaties in de fluorescentie–intensiteit van één enkel molecuul, kon de levensduur van een bepaalde redox toestand van het T1 Cu worden afgeleid en daarmee de snelheid van de electronoverdracht. SLAC varianten werden geconstrueerd om plaatsspecifiek een label te kunnen aanbrengen en om immobilisatie van het eiwit op een transparant glasoppervlak mogelijk te maken. De intensiteitsfluctuaties van individuele SLAC–moleculen werden geregistreerd met behulp van een confocale microscoop. Uit deze gegevens werden de elektron–overdracht snelheden van T1 naar TNC (en omgekeerd) afgeleid en vervolgens uitgezet in een histogram. De verdeling van de snelheden blijkt een normale log–distributie met gemiddelden van 460 en 85 s^{-1} te vertonen, corresponderend met activeringsenergieën van resp. 347 en 390 meV voor de voorwaartse en achterwaartse elektron-overdracht. M.b.v. van Marcus theorie werden een “driving force” en een “reorganisatie–energie” berekend van respectievelijk 0.043eV en 1.5eV. De elektron–overdracht snelheden distributie toont een spreiding van meer dan één orde van grootte overeenkomend met een kleine 30 meV spreiding in de activeringsenergie, of met 0.1 eV in de reorganisatieenergie. De hier gevolgde aanpak om individuele moleculen te bestuderen heeft dus niet alleen het volgen van de interne dynamica van enzymen onder steady–state condities mogelijk gemaakt, maar hij is bovendien

veel informatiever gebleken dan metingen die op macroscopische schaal worden uitgevoerd (bv. aan oplossingen).

Hoofdstuk 5 geeft de algemene conclusies weer van het werk dat in dit proefschrift is gepresenteerd. Verder bevat het suggesties voor onderzoek dat meer inzicht kan geven in het enzymatische mechanisme van SLAC en van het mechanisme van MCO's in het algemeen.

List of Publications

Gupta, A.; Aartsma, T.J.; Canters, G.W. "One at a Time: Intramolecular Electron–Transfer Kinetics in Small Laccase Observed during Turnover" *J. Am. Chem. Soc.* **2014**, *136*, 2707.

Hiruma, Y.; Gupta, A.; Kloosterman, A; Olijve, C.; Ölmez, B.; Hass, M.A.S.; Ubbink, M. "Hot spot residues in the cytochrome P450cam–putidaredoxin binding interface" *ChemBioChem* **2014**, *15*, 80. (*Featured on the journal cover*)

Gupta, A.; Nederlof, I.; Sottini, S.; Tepper, A.W.J.W.; Groenen, E.J.J.; Thomassen, E.A.J; Canters, G.W. "Involvement of Tyr108 in the Enzyme Mechanism of the Small Laccase from *Streptomyces coelicolor*" *J. Am. Chem. Soc.* **2012**, *134*, 18213.

Gupta, A.; Mukherjee, A.; Matsui, Kenji; Roth, J.P. "Evidence for Protein Radical–Mediated Nuclear Tunneling in Fatty Acid α–Oxygenase" *J. Am. Chem. Soc.* **2008**, *130*, 11274.

Joseph, R.; Gupta, A.; Rao, C. P. "Photophysical properties of the interaction of lower rim 1,3–bis(aminoethoxy)–calix[4]arene derivative with Pb^{2+}, Hg^{2+} and Cd^{2+} ions: Recognition of Hg^{2+} *J. Photochem. Photiobiol. A* **2007**, *188*, 325.

Joseph, R.; Gupta, A.; Ali, A.; Rao, C. P. "Fluorescence and absorption studies on the selective recognition of iodide by lower rim 1,3–bis(aminoethoxy)–*p*–*t*–butyl–calix[4]arene derivative" *Ind. J. Chem.* **2007**, *46A*, 1095.

Curriculum Vitae

Ankur Gupta was born in Agra, India, on July 14, 1983. He did his schooling in Kendriya Vidyalaya No. 1 in Jaipur and then in 2001 he moved to Mumbai for his undergraduate studies at the Indian Institute of Technology Bombay. After completing his integrated MSc in Chemistry in 2006, he attended the Johns Hopkins University (Baltimore, U.S.A.) to study Biochemistry and obtained his MA in Chemistry. There, in the group of Dr. Justine P. Roth, he studied tyrosyl radical mediated nuclear tunneling in a heme containing enzyme, Rice–α–oxygenase.

In 2009, he came to Netherlands to start his PhD research in the group of Prof. Gerard W. Canters and Prof. Thijs J. Aartsma at Leiden University. During his PhD research, he studied the mechanism of electron transfer and oxygen reduction by the multicopper oxidase SLAC. The results obtained are presented in this thesis. He presented his research at a number of national and international conferences including the NWO Biophysics and Protein Chemistry meetings in Veldhoven (2009–2013), the International Conference of Biological Inorganic Chemistry (ICBIC)–15 in Vancouver (2011), ICBIC–16 in Grenoble (2013) and the Gordon Research Conference – Metals in Biology in Ventura (2014).

Acknowledgements

In the end, I would like to acknowledge everyone who helped in the research presented in this thesis. First of all, I would like to thank Dr. Armand Tepper who helped me getting started when I joined the lab. Thanks to Dr. Igor Nederlof, Dr. Silvia Sottini and Dr. Ellen Thomassen for their help with the work presented in this thesis.

I am very thankful to Prof. Edgar Groenen and Ms. Faezeh Nami for helpful discussions during our meetings and for their support with the EPR spectroscopy facilities. Thanks to Dr. Navraj Pannu and Ms. Dieuwertje Augustijn for their help with the collection and solving of the crystallography data on SLAC variants over the past few months. I acknowledge Prof. Haw Yang (Princeton University) who provided the changepoint algorithm, which was crucial to analyze the single–molecule time trajectories.

I would like to thank Ms. Trudie Brouwer and Mr. Arjan Oudshoorn for letting me use the Oxygraph system for O_2 kinetics measurements. It would have been very difficult to work without the support of our excellent and talented staff in the Department of Fine Mechanics who could convert a vague idea into a robust practical solution, so easily. Thanks to the Electronics Department, especially Ing. Arno van Amersfoort, for help with developing the changepoint algorithm and on various occasions to test the TCSPC instrumentation.

I would also like to thank past and present members of the Protchem and Biophysics groups, especially Dr. Alessio Andreoni, Dr. Leandro Tabares and Dr. Abdalmohsen Elmalk, for useful discussions. Special thanks to Ing. Anneloes Blok who was always there to help whenever I got stuck with my experiments. The person I can't thank enough is Ing. Lionel Ndamba who helped me learning the lab practices when I joined the lab. I would like to thank him for useful scientific and non–scientific discussions, for the Dutch translation of the summary, for quietly listening to my comments and complaints and also for his gracious help with the preparation and purification of the SLAC variants that were used for the work reported in Chapter 3 of this thesis.

Last, but not the least, I would like to thank my parents, grandparents and my wife, Swati, for their encouragement and continued support throughout this long journey, and for believing in me.